2014

Coronavirus Proteases as Therapeutic Targets: Development of Biosensors to Detect Inhibition of Protease Activity and Separation of the Multiple Functions of Coronavirus Papain-Like Proteases

Andrew Kilianski
Loyola University Chicago

LOYOLA UNIVERSITY CHICAGO

CORONAVIRUS PROTEASES AS THERAPEUTIC TARGETS: DEVELOPMENT OF BIOSENSORS TO DETECT INHIBITION OF PROTEASE ACTIVITY AND SEPARATION OF THE MULTIPLE FUNCTIONS OF CORONAVIRUS PAPAIN-LIKE PROTEASES

A DISSERTATION SUBMITTED TO

THE FACULTY OF THE GRADUATE SCHOOL

IN CANDIDACY FOR THE DEGREE OF

DOCTOR OF PHILOSOPHY

PROGRAM IN MICROBIOLOGY AND IMMUNOLOGY

BY

ANDY KILIANSKI

AUGUST 2014

ACKNOWLEGEMENTS

I would like to thank all of the people who have made this work possible during my time at Loyola. The Department of Microbiology and Immunology was an excellent atmosphere to conduct research in, and Dr. Katherine Knight has done a wonderful job in not only leading the department, but mentoring young graduate students through the program. My committee of Thomas Gallagher, Chris Wiethoff, Ed Campbell, and Harel Dahari were very constructive during committee meetings and were always accessible for questions and advice. The Baker lab has played an enormous role in my success as a graduate student. Anna Mielech, Xufang Deng, Brian Nichols, and Bridget Banach were helpful colleagues but also great friends. Without the guidance and support of Dr. Susan Baker I would have never been so productive and grown so much as a scientist and person. She is truly an expert in the field and her introductions and contacts will continue to be invaluable beyond my career at Loyola. Finally, I would like to dedicate my dissertation to my amazingly supportive wife Mary and my two beautiful daughters Grace and Violet. They are constant sources of inspiration and are always there for me, regardless of what is happening in the lab. Mary has been especially supportive and tolerant of me throughout grad school. I would also like to thank my parents, Tom and Carol, who have always fostered my scientific spirit. My family has allowed for me to pursue my dream of becoming a successful scientist and a good son, husband, and father.

TABLE OF CONTENTS

LIST OF TABLES

LIST OF FIGURES

ABSTRACT

Coronaviruses are important human pathogens and have the potential to severely impact public health on an international scale. The emergence of SARS-CoV and MERS-CoV highlight the need for research to identify antivirals and vaccines against coronaviruses. To develop therapeutics against current and potentially emergent coronaviruses, I utilized two approaches targeting the proteases encoded within all coronaviruses. The papain-like protease and 3C-like protease of coronaviruses are responsible for cleaving viral polyproteins early during infection, and this step is required for viral replication. To quantitatively assess the inhibition by small-molecule compounds on MERS-CoV protease activity, I developed a luciferase-based biosensor to monitor protease cleavage within cells. Using this assay, I demonstrated that an inhibitor that is efficacious against SARS-CoV had activity against the 3C-like protease of MERS-CoV. In the second approach, I investigated the multifunctional papain-like protease of SARS-CoV, which has been implicated in pathogenesis by acting as a deubiquitinating (DUB) enzyme and blocking host immune responses. To determine if PLpro DUB activity is responsible for innate immune antagonism, I mutated residues predicted to interact with ubiquitin and discovered that when this interaction was interrupted, PLpro was unable to antagonize innate immune pathways. Engineering these mutations into SARS-COV may generate an attenuated virus that could stimulate a protective immune response in the absence of disease.

CHAPTER I

INTRODUCTION

CORONAVIRUSES: SIGNIFICANT HUMAN PATHOGENS

Coronaviruses are enveloped, positive strand RNA viruses that cause mild to severe disease in humans, livestock such as pigs, cattle, and poultry, and domesticated pets. Coronaviruses are members of the order *Nidovirales* and are the largest known RNA viruses, with some coronaviral genomes extending over 30kb in length. They were originally identified as infectious agents of disease in chickens (infectious bronchitis virus, IBV) and later identified in mice and pigs (mouse hepatitis virus, MHV and transmissible gastroenteritis virus, TGEV) (Siddell, Wege, & Ter Meulen, 1983). The name "coronavirus" comes from the morphology of the viral particles under electron microscopy. The viral spike glycoproteins which mediate cell entry gave a characteristic rays-of-the-sun or crown appearance, hence "corona." The first human coronavirus was isolated from the upper respiratory tract of an infected medical student in 1967 and was named human coronavirus 229E (HCoV-229E) (Hamre, Kindig, & Mann, 1967). Coronaviruses are grouped into the genus *alphacoronavirus*, *betacoronavirus*, *gammacoronavirus*, or *deltacoronavirus* based on amino acid sequence similarity from conserved coronavirus domains and coronaviruses infecting humans remain limited to the *alphacoronavirus* and *betacoronavirus* genus. Until recently, human coronaviruses have

been demonstrated to cause common cold symptoms in healthy adults and croup and pneumonia in children and the elderly.

In the last twelve years, two major outbreaks of highly pathogenic coronaviruses capable of zoonotic transmission have alerted the coronavirus field and public health officials to the dangers of coronaviruses within animal reservoirs. Severe Acute Respiratory Syndrome (SARS) was first detected in the Guangdong province of China in late 2002. It spread from China to neighboring Hong Kong via human to human transmission and eventually spread to pandemic proportions with a reported mortality of 10% (Tsang et al., 2003). Rapid work within the scientific community identified the causative agent to be a coronavirus (SARS-CoV) and determined that the virus emerged from Chinese horseshoe bats, who harbor SARS-like coronaviruses endemically, and was transmitted to an intermediate host, civet cats, before obtaining the mutations necessary to transmit to humans (Lau et al., 2005; Perlman & Netland, 2009; Poon et al., 2005). Coronaviruses have since been detected in many bat species both abroad but also within the United States (Dominguez, O'Shea, Oko, & Holmes, 2007; Woo, Lau, Huang, & Yuen, 2009). The endemic nature of coronaviruses within bats creates the potential for re-emergence of a SARS-like coronavirus or other coronaviruses capable of animal to human and human to human transmission (Stockman et al., 2008).

These dangers were realized with the identification of a novel coronavirus with unknown origins from a man who died of pneumonia in the Middle East in late 2012 (Zaki, van Boheemen, Bestebroer, Osterhaus, & Fouchier, 2012). Since the identification

of Middle East respiratory syndrome coronavirus (MERS-CoV), there have been 178 laboratory confirmed cases and 76 deaths, with a case/fatality rate of over 40% ((WHO), 2014). Currently it is unclear if there are additional asymptomatic cases of infection with MERS-CoV within the human population. MERS is reminiscent of the outbreak of Severe Acute Respiratory Syndrome (SARS) in the Guangdong province in China in 2002-2003. MERS-CoV is capable of infecting bat and human cells directly; and both the bat and human receptor, dipeptidyl peptidase or CD26, are capable of supporting viral entry (Muller et al., 2012; Raj et al., 2013). Recently, a 181 bp fragment of the RNA-dependent RNA polymerase gene that was genetically identical to MERS-CoV was detected in one Egyptian Tomb bat and dromedary camels were found to have neutralizing antibodies against MERS-CoV, perhaps linking an endemic source of the virus and an intermediate host (Memish ZA Olival KJ, Fagbo SF, Kapoor V, Epstein JH, et al., 2013; Perera et al., 2013; Reusken et al., 2013). Camels have also been found to carry MERS-CoV, however the epidemiology of viral emergence and the chain of transmission remains to be solved (Alagaili et al., 2014).

Since the outbreak of SARS-CoV, there have been extensive efforts on antiviral drug development, but no FDA approved antiviral drugs or vaccines exist against any human coronaviruses (reviewed in (Barnard & Kumaki, 2011)). However, much has been learned from studies evaluating the pathogenesis and diseases caused by SARS-CoV that can be applied to new emergent coronaviruses. The goals of the first part of my research were to design a cell-based assay that could be used for the rapid evaluation of potential small compound inhibitors against MERS-CoV papain-like and 3C-like

protease. I then wanted to expand this assay to build a platform for broad spectrum inhibitor identification against alpha and beta coronavirus PLPs. The following sections will introduce druggable targets within the coronavirus life cycle and the work that has been done to generate potential antivirals using cell-based assays for SARS-CoV and MERS-CoV.

The goal of my second research direction was to examine the role of the multiple functions of the papain-like protease, PLpro, of SARS-CoV. This multifunctional enzyme is important for viral replication but is also predicted to block host innate immune responses and alter host proteins within infected cells. Below, I will introduce the concept of viral protease multifunctionality and the hypothesized role for these accessory functions during viral infections. These multifunctional enzymes are conserved within coronaviruses but also exist in viral families outside of the coronaviruses. Building an understanding of how these enzymes work will be critical in my attempts to separate out these functions to examine their individual contributions to PLpro function and SARS-CoV replication and pathogenesis.

DRUGGABLE TARGETS OF CORONAVIRUSES

The coronavirus genome encodes many druggable targets, and these targets are highlighted in their role in the replication cycle life cycle (Figure 1). Human dipeptidyl peptidase IV (DDP4, CD26) has been discovered as the receptor for MERS-CoV (Raj et al., 2013), the receptor-binding domain (RBD) of the spike protein has been identified

and structurally characterized (Y Chen et al., 2013; Du et al., 2013; Mou et al., 2013) and the crystal structure of the complex between DPP4 and the RBD has been determined reviewed in (F. Li, 2013; Lu et al., 2013; N. Wang et al., 2013). The interactions between viral glycoproteins and receptors have been targeted in other viruses, including SARS-CoV. Coronaviruses can enter cells through receptor mediated endocytosis or by membrane fusion with the plasma membrane. Endocytosis of the receptor-virus complex can occur, and upon acidification of the endosome, the host protease cathepsin L is activated and can cleave the viral spike protein to initiate viral fusion. The coronaviral spike can also be activated by extracellular proteases (trypsin) or proteases present on the cell surface (type II transmembrane serine protease or TMPRSS2), and this cleavage allows coronaviruses to enter cells in an cathepsin-independent manner (Glowacka et al., 2011; Matsuyama et al., 2010; Shulla et al., 2011; Simmons, Zmora, Gierer, Heurich, & Pohlmann, 2013)

Upon viral entry and fusion of the viral and host cell membranes, the positive sense RNA genome, which is 5' methyl-capped and poly-adenylated, is translated in the cytoplasm. This translation yields two large polyproteins, pp1a and pp1b, which are then cleaved into 16 non-structural proteins by the papain-like protease, encoded within nsp3, and the 3C-like protease, encoded by nsp5. The proteases are drug targets, as the proteolysis of the non-structural proteins is required for replication of the virus. Further, the papain-like protease of SARS-CoV and other coronaviruses has been shown to antagonize host innate immune responses, so inhibiting the papain-like protease will stop

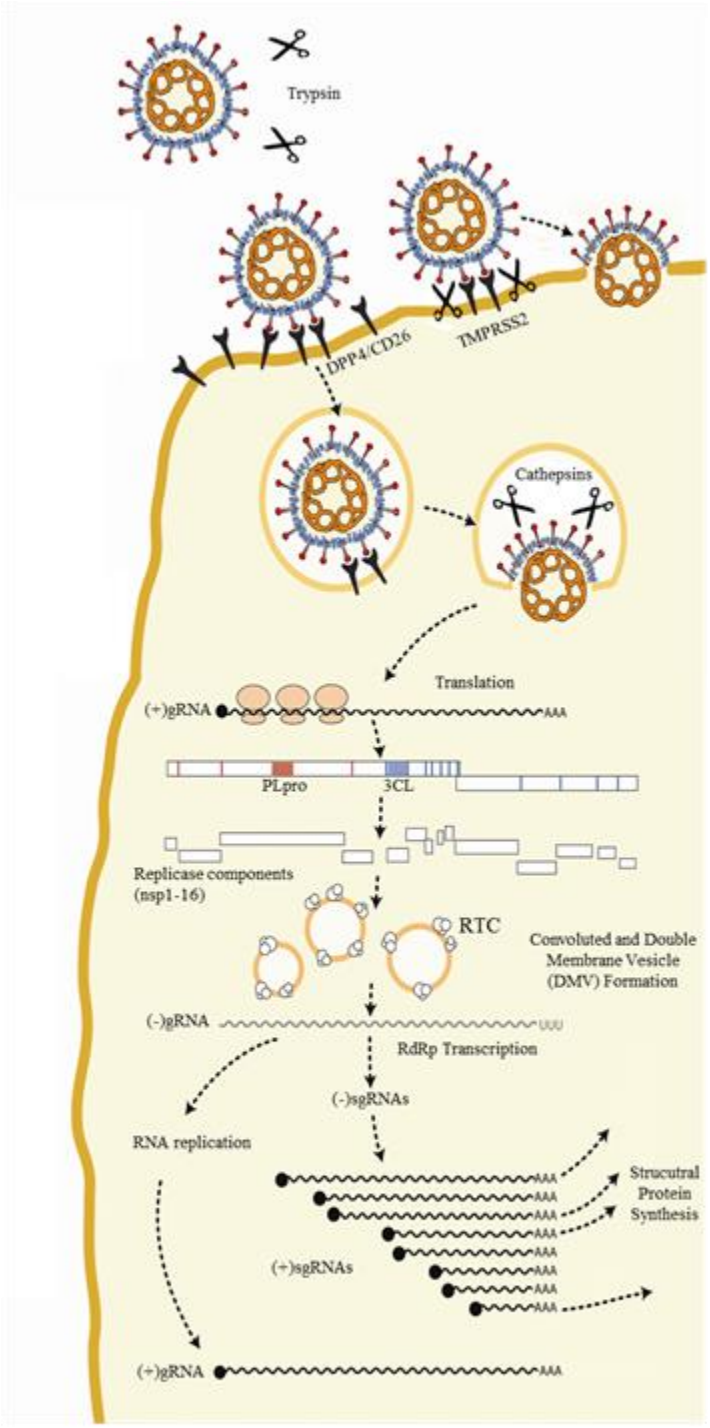

Entry Targets

- Spike glycoprotein (RBD, fusion intermediates)
- Receptor: DPP4/CD26
- Surface proteases (TMPRSS2)
- Endosomal proteases (cathepsins)

Polyprotein Processing Targets

- Papain-like protease (PLpro)
- 3C-like protease (3CLpro/Mpro)

Replicase Targets within the Replication-Transcription Complex (RTC)

- ADP-ribose-1″-phosphatase (nsp3)
- Primase (nsp8)
- RNA-dependent RNA polymerase (nsp12)
- Helicase (nsp13)
- Exonuclease (nsp14)
- N7 methyltransferase (nsp14)
- Endoribonuclease (nsp15)
- 2′ O-methyltransferase (nsp16)
- Host factors identified as being required for viral replication (kinases, cyclophilins, etc)

Fig. 1. Coronavirus entry and RNA replication targets for antiviral drug development. Targets for viral entry include the viral spike-host receptor interaction, and host proteases that cleave the viral spike to mediate fusion. Viral replicase polyprotein processing can be targeted by inhibiting the papain-like or 3C-like proteases. The enzymatic activities of the replication-transcription complexes (RTCs) on convoluted membranes and double-membrane vesicles are also attractive targets for inhibitors. From (Kilianski & Baker, 2014)

viral replication and may prevent antagonism of host innate immune responses (Barretto et al., 2005; Z. Chen et al., 2007; Devaraj et al., 2007; Frieman, Ratia, Johnston, Mesecar, & Baric, 2009; L. Sun et al., 2012). Successful inhibitors have been generated against both SARS-CoV PL^{pro} and $3CL^{pro}$ and will be discussed in more detail in the following sections.

To generate more genome copies and subgenomic mRNAs for synthesis of structural genes, the viral genome must be replicated by a series of enzymes that comprise the membrane-associated replication and transcription complex (RTC). The ADP-ribose-1″-phosphatase (nsp3), primase (nsp8), RNA-dependent RNA polymerase (RdRp, nsp12), helicase (nsp13), exonuclease and N7 methyltransferase (nsp14), endoribonuclease (nsp15), and 2′ O-methyltransferase (nsp16) are all proteins that have enzymatic activity that can be targeted by antivirals. In fact, inhibitors have been identified that can block the activity of SARS-CoV RdRp, helicase, and 2′ O-methyltransferase. After replication of the genome and generation of subgenomic mRNAs (sgmRNAs), structural and accessary proteins are translated from these sgmRNAs, assembly of the virion occurs at the endoplasmic reticulum-Golgi intermediate compartment (ERGIC), and the virion egresses through the exosomal pathway. Assembly and egress mechanisms have been targeted for inhibition in other viruses, but this strategy has not been explored for the development of coronavirus antivirals.

CELL-BASED SCREENS FOR ANTIVIRALS

SARS-CoV Entry Inhibitor Screens

Viral glycoprotein binding with its cognate receptor and the spike protein mediating viral envelope fusion with cellular membranes are necessary for infection. These steps in infection have been successfully targeted in other viruses, with two FDA approved antivirals targeting HIV-1 entry in clinical use (Henrich & Kuritzkes, 2013). The antiviral Maraviroc is a small-molecule CCR5 antagonist that inhibits the HIV-1 glycoprotein from binding to its receptor CCR5. Using a different mechanism, the antiviral Enfuvirtide inhibits viral fusion by interrupting the interaction between heptad repeat regions within the HIV-1 glycoprotein gp41. Partially based on the success of this strategy, both small-molecule and peptide inhibitors have been identified that target the entry of SARS-CoV. Here, we will review and describe the studies that used cell-based screening methods to identify these inhibitors.

The ability to evaluate of SARS-CoV entry specific inhibitors advanced with the demonstration that pseudotyped virion particles incorporating the S protein from SARS-CoV were competent for entry (Fukushi et al., 2005; Giroglou et al., 2004; Hofmann et al., 2004; Moore et al., 2004). In contrast to the previous cell-based screens based on virally induced CPE, pseudotyped lentiviral virions delivering a genome expressing GFP, luciferase, or other reporters allow for quantitative measurement and evaluation of coronaviral entry inhibitors. These assays can be used in BSL-2 laboratories and do not involve work with infectious CoVs. Using these techniques, the first demonstration of

SARS-CoV entry inhibition was achieved using pieces of the SARS-CoV S or peptides designed to interact with the S, with the goal of both approaches to block viral membrane fusion intermediates (Yuan et al., 2004; Zhu et al., 2004). These studies demonstrated that small peptides that can bind to the heptad repeat regions of the SARS-CoV S (parallel in mechanism to FDA approved HIV entry inhibitor Enfuvirtide) could inhibit viral entry/fusion.

In addition to peptide studies based on the amino acid sequence of the SARS-CoV S, compound screens were performed against SARS-CoV entry. Using a commercial screen of diverse compounds (50,240 compound screen from ChemBridge) a small-molecule inhibitor was found to inhibit SARS-CoV entry based first on virally induced CPE reduction and then prevention of pseudotyped virion entry (Kao et al., 2004). Shortly after the demonstration that small-molecule compounds could target SARS-CoV entry, Yi et al demonstrated that natural compound screens could also be used to inhibit SARS-CoV entry (Yi et al., 2004). They showed inhibition by small-molecules in a pseudotyped virion screen and identified two candidates that inhibited entry in the micromolar range. Utilizing a luciferase expressing lentiviral vector pseudotyped with S protein, molecules were screened based on luciferase expression levels of transduced cells. Two molecules, TGG and leuteolin (screened from a Chinese herbal library) were shown to have antiviral activity in the pseudotype assay and confirmed with live virus using an MTT colorimetric assay for cytotoxicity. These initial studies have evolved into three classes of inhibitor studies; small peptides that block viral fusion by interacting with SARS-CoV S, inhibition of cellular proteases that cleave the viral glycoprotein to

mediate entry, and small chemical compounds that interact with the SARS-CoV S and inhibit entry.

The peptide studies have advanced to identify necessary peptides with very high affinity interaction and potent inhibition (Liu et al., 2009; Ni et al., 2005; Struck, Axmann, Pfefferle, Drosten, & Meyer, 2012; Ujike et al., 2008; Zheng et al., 2005). Zheng et al. developed 20-mer peptides corresponding to small fragments of the SARS-CoV S protein and identified three synthetic peptides with inhibitory properties. These peptides also had additive inhibitory effects when pre-incubated in combination with cells prior to infection. To elucidate the mechanism of inhibition, the authors used molecular modeling and speculated that these 20-mer peptides interacted with faces of SARS-CoV S that are required for interaction between the monomers of S to form functional, trimeric S. Inhibition at these interfaces has not been previously observed, and suggested a novel targeting strategy for prevention of S mediated viral entry.

In addition to peptides designed to bind to the S protein, Han et al took the opposite approach and designed peptides that corresponded to residues critical for entry mediated by ACE2 (D. P. Han, Penn-Nicholson, & Cho, 2006). Using a pseudotyped MuLV and HeLa cells expressing wild-type or alanine point mutants within ACE2, they determined that many of the charged residues within alpha helices 1 and 2 (residues 22-57) have inhibitory effects on viral entry. Importantly, their studies determined that these effects could only be seen with a 20 minute adsorption, and that the commonly used 60 minute adsorption time led to a high background and couldn't properly identify inhibitors

in the pseudotype assay. Based on these studies, the authors created peptides corresponding to the amino acids from residues 22-57 and determined that these peptides had specific inhibitory activities against SARS-CoV pseudotype entry, but not entry of VSV-G psuedotypes. Overall, peptides corresponding to SARS-CoV S or ACE2 are effective at limiting entry of pseudotyped and wild-type SARS-CoV; however, none of these inhibitors have been tested further in animal models.

The inhibition of cellular factors required for SARS-CoV entry are attractive targets, as they could be less susceptible to viral escape due to mutations within the viral glycoprotein. Catalytic mutants of ACE2 had no effect on viral entry, suggesting that the enzymatic activity of coronaviral receptors is not required for entry (Moore et al., 2004). The SARS-CoV S protein requires cleavage either extracellularly by trypsin or TMPRRS2 or within the endosomal compartment by cathepsin L (Figure 1). Simmons et al. determined that cathepsin L mediates SARS-CoV S protein cleavage and that it can be pharmacologically targeted to prevent SARS-CoV S cleavage and entry (Simmons et al., 2005). In this study, a unique virus-virus membrane fusion assay was utilized. This assay involves two pseudotyped virions, one decorated with SARS-CoV S and the Avian sarcoma leukosis virus (ASLV) envelope protein, and one containing ACE2 and a luciferase expression construct. These particles can be induced to undergo fusion *in vitro*, and particles able to enter cells containing the ASLV receptor and express luciferase must have undergone viral membrane fusion upon mixing of the two pseudoparticle populations. If cathepsin L is responsible for S cleavage within endosomes, then inhibition of purified cathepsin L *in vitro* will prevent viral-viral

membrane fusion and no pseudoparticle expressed luciferase will be detected. The authors used this assay to demonstrate cathepsin L activation of SARS-CoV S and also that other endosomal cathepsins were not responsible for mediating SARS-CoV entry. Cathepsin L has been the continued target of antiviral development not only for SARS-CoV but other enveloped viruses that have a cleavage requirement within their glycoproteins, such as Ebola virus (Shah et al., 2010).

Endosomal proteases are not the only proteases that are able to activate SARS-CoV S. TMPRRS2 can activate S at the host cell plasma membrane, allowing SARS-CoV to enter without utilizing cathepsin L (Figure 1). Cell-cell fusion assays have been used to identify and characterize plasma membrane surface factors, and can be used to investigate cell surface fusion inhibitors. Cells expressing SARS-CoV S and a T7 polymerase are plated with cells expressing ACE2 and a luciferase or GFP reporter plasmid driven by a T7-dependent promoter. Upon receptor interaction and fusion, the cytoplasm from both cell types mixes, allowing for the transcription and translation of the luciferase or GFP (Shulla et al., 2011; Simmons et al., 2005). Pseudotyped virions were used by Kawase et al in their work identifying commercially available protease inhibitors targeting TMPRRS2 (Kawase, Shirato, van der Hoek, Taguchi, & Matsuyama, 2012). Inhibiting only serine proteases, which includes TMPRRS2, partially inhibited the entry of pseudotyped particles; however, also inhibiting cysteine proteases (which includes cathepsins) fully inhibited the entry of both pseudoparticles and authentic SARS-CoV. Targeting these host cell factors has been shown to be an effective way to prevent viral fusion and entry in cell culture.

Finally, small-molecule inhibitors have been screened and developed to target SARS-CoV entry. Recently, Adedeji et al used a SARS-CoV S pseudotyped HIV-Luc virus to screen a 3,000 compound library (Adedeji et al., 2013). Forty four hits were taken from this library and analyzed for specificity against SARS-CoV entry as compared to inhibition of a VSV-G enveloped HIV-Luc pseudovirus. Out of the initial 44 compounds, only 3 were found to be specific for inhibition of SARS-CoV. These counter screens highlight the importance of identifying specific compounds before undergoing further analysis of positive hits in initial screens. Further *in vitro* analysis was performed and the three compounds were identified to separately inhibit cathepsin L activity, inhibit interaction between S and ACE2, and inhibit a fusion step downstream of S-ACE2 recognition. The feasibility of chemical compound inhibition of virus entry is an established strategy to develop efficacious antivirals, especially for HIV; however, small compounds remain a relatively unexplored strategy with respect to coronaviruses. Overall, targeting viral entry of coronaviruses (especially SARS-CoV) has been demonstrated using specific cell-based assays outlined here. These strategies can be utilized for the evaluation of peptides or chemical inhibitors of S protein-receptor interaction, S-mediated fusion, or host cell factors necessary for mediating MERS-CoV and other emerging coronavirus entry.

SARS-CoV Protease and Replicase Inhibitor Screens

After entry and fusion, the SARS-CoV genome is translated into two large polyproteins from ORF1a and ORF1b. For replication to continue, these polyproteins must be cleaved by viral proteases, either 1 or 2 papain-like proteases (designated PL^{pro} or PLP1/PLP2) and the 3C-like protease ($3CL^{pro}$ or M^{pro} for main protease). This step in the replicative process has been the target of the most extensive work done to identify inhibitors for SARS-CoV replication (reviewed in(Barnard & Kumaki, 2011). SARS-CoV PL^{pro} is responsible for three cleavages while SARS-CoV $3CL^{pro}$ cleaves the polyprotein at 11 sites (Figure 1). Because the use of proteases is conserved across coronaviruses, both PL^{pro} and $3CL^{pro}$ are considered attractive targets for antiviral drug development. Much of the antiviral work performed with the coronaviral proteases has been done using *in vitro*, cell free conditions, and this work is crucial in laying the foundation for continued antiviral development. In this section, the focus continues to remain on important cell based assays and techniques to efficiently identify and validate antiviral candidates against coronavirus replication.

Some of the first SARS-CoV PL^{pro} inhibitors discovered were first screened against purified protein *in vitro* and then further characterized in infection and cell lysate assays (C Y Chou et al., 2008; Ratia et al., 2008). To determine if the inhibitors characterized were specific for SARS-CoV PL^{pro}, Ratia et al utilized a cell lysate experiment that combined purified SARS-CoV PL^{pro} with cell lysates, a tagged ubiquitin-vinyl sulfone, and the inhibitor. In this experiment, cell lysates were incubated with the

tagged ubiquitin-vinyl sulfone, and any deubiquitinating enzyme will be covalently linked via the vinyl sulfone linkage to the tagged ubiquitin. These lysates can then be analyzed by western blot to determine if deubiquitinating enzyme binding to the ubiquitin vinyl-sulfone is affected in the presence of inhibitors. In the presence of the specific SARS-CoV inhibitor, only SARS-CoV PL^{pro} binding to the tagged ubiquitin vinyl sulfone was shown to be decreased. While not strictly a cell-based method, this is a useful technique for determining the specificity of inhibitors of papain-like protease activity.

Frieman et al took an entirely cell-based approach in their screening, identification, and mechanistic evaluation of a small compound library against SARS-CoV PL^{pro} (Frieman et al., 2011). The expression and activity of SARS-CoV PL^{pro} within *S. cerevisiae* led to a slow growth phenotype, and the basis for the screen was that inhibition of PL^{pro} activity by small compounds could reverse this slow growth phenotype. Growth was measured by optical density, and from a 2000 compound library provided by the NIH, the authors generated candidate compounds that were then analyzed for their effect on PL^{pro} expression or toxicity within *S. cerevisiae.* Based on these results, the authors further screened the compounds in VeroE6 and MA104 cells for activity against SARS-CoV replication. These compounds were also tested against three different activities of SARS-CoV papain-like protease. First, the drugs were tested for their ability to inhibit cleavage of a synthetic PL^{pro} polyprotein substrate, nsp2-3, by SARS-CoV PL^{pro}. This assay uses a tagged nsp2-3 and the cleavage product, which is dependent of PL^{pro} catalytic activity, and can be visualized by western blot. The second

assay uses the deubiquitinating activity of PL^{pro} as a readout for PL^{pro} activity and inhibition. Cells are transfected with PL^{pro} and a tagged ubiquitin and then treated with inhibitors. PL^{pro} will cleave the ubiquitin molecules, resulting in a decreased smear of ubiquitinated proteins and an increased smear if the inhibitors are blocking PL^{pro} deubiquitinating activity. Finally, the authors assessed the ability of inhibitors to block the interferon antagonism properties of PL^{pro} using an IFNβ luciferase assay. Cells transfected with either poly(I:C) or a constitutively active form of RIG-I, an IFNβ luciferase reporter, and PLpro, and then were treated with inhibitors. PLpro inhibits IFNβ promoter activation in response to stimulus, so if PL^{pro} inhibitors block the ability of PL^{pro} to inhibit IFNβ activation, an increase in IFNβ promoter activity will be seen. These cell based screening techniques are good tools to assess the mechanism of inhibitors and how they inhibit papain-like proteases within cells. However, these assays are not amenable to a higher-throughput analysis of compounds, and do not offer the specific quantitation of PL^{pro} catalytic activity within cells, which is critical when attempting to optimize small compounds and build structure activity relationships.

SARS-CoV $3CL^{pro}$ has also been the target of extensive efforts to generate specific antivirals. Modeling of SARS-CoV $3CL^{pro}$ based on the structures of transmissible gastroenteritis virus (TGEV) and HCoV-229E $3CL^{pro}$ presented the likelihood of structural conservation. Rhinoviral $3C^{pro}$ inhibitors bound efficiently to HCoV-229E $3CL^{pro}$, and were later shown to form complexes with SARS-CoV $3CL^{pro}$ (K Anand, Ziebuhr, Wadhwani, Mesters, & Hilgenfeld, 2003; H. Yang et al., 2003). Based on this biochemical characterization, and the enzymatic properties of proteases, much of

the early work on $3CL^{pro}$ inhibitors was performed *in vitro* in cell-free conditions. For example, Blanchard et al used purified SARS-CoV $3CL^{pro}$ and a FRET-based *in vitro* assay to screen a large compound library of compounds for $3CL^{pro}$ inhibition (Blanchard et al., 2004). Multiple studies have used a live infection approach based on cell cytotoxicity, and then worked backwards from the hits to identify the mechanism of action of the identified inhibitors (Kao et al., 2004; Wu et al., 2004). Experiments like these are critical for the identification of lead compounds; however, cell-based assays designed to measure protease activity are needed to identify if these compounds could be efficacious in the context of viral infection.

To measure $3CL^{pro}$ inhibitors in a cell-based assay, Lin et al. created a *cis* cleavage luciferase assay (Lin et al., 2004). This involved the creation of an expression construct that encoded for SARS-CoV $3CL^{pro}$ in frame with an inserted $3CL^{pro}$ cleavage site (SAVLQSGFRK) and a downstream luciferase construct. The rationale for this design was the knowledge that when luciferase is fused to larger proteins, its activity is substantially decreased. Upon the *cis* cleavage of the $3CL^{pro}$-luciferase polyprotein, the liberated luciferase should give an increased signal. The authors demonstrated that this luciferase construct was not very active when translationally fused with a mutated $3CL^{pro}$ cleavage site. When the cleavage site was intact they witnessed a 5-25 fold increase in luciferase activity. This assay was the first demonstration of a quantitative readout for $3CL^{pro}$ activity when the protease is transiently expressed within cells.

Replicons have been developed for SARS-CoV and have been used as a platform for screening anti-coronaviral compounds (Almazan et al., 2006; Ge, Luo, Liew, & Hung, 2007; Ge, Xiong, Lin, Zhang, & Zhang, 2008). These replicons contain all of ORF1a/b from SARS-CoV in addition to the N gene (required for replication) and a reporter cassette. The N gene and reporter are both transcribed off of separate sub-genomic messenger RNAs, similar to the replication of the virus (Figure 1), meaning that the reporter can only be synthesized when the replicon is replicating correctly. These SARS-CoV replicons can be either transfected or incorporated into stable cell lines for antiviral screening. While these replicons are useful, this approach does not address the specificity of compounds screened. To determine mechanisms of action, the candidate compounds must be screened against replicase proteins in another system.

Antivirals have also been developed against the SARS-CoV helicase (Adedeji et al., 2012; Tanner et al., 2005; Yu et al., 2012), polymerase (Ahn et al., 2011; te Velthuis et al., 2010), and 2'-O-methyltransferase (Ke et al., 2012). A previous study by van Hemert et al. established a protocol to isolate and monitor the activity SARS-CoV replication complexes *in vitro* (van Hemert et al., 2008). The study performed by te Velthuis et al. used this protocol and showed that zinc-ionophores inhibited the synthesis of RNA by SARS-CoV RdRp. This method allows for the study of cell-produced replication complexes *in vitro*.

APPLICATIONS AND DEVELOPMENT OF CELL-BASED SCREENS FOR MERS-COV ANTIVIRAL SCREENING

Since the outbreak of MERS-CoV, there has been adaptation of methods used to screen for SARS-CoV inhibitors to MERS-CoV and the development of novel methods to identify potential antiviral inhibitors against MERS-CoV (Table 1). The entry of some coronaviruses, including SARS-CoV, is known to be mediated by TMPRSS2 (Figure 1). To determine if TMPRSS2 inhibition is a viable strategy to prevent MERS-CoV entry, Shirato et al targeted TMPRSS2 activity with camostat and assessed the ability of MERS-CoV to cause syncytia and to enter cells using qRT-PCR for viral RNA. They demonstrated that inhibition of TMPRSS2 activity could inhibit MERS-CoV syncytia formation and that camostat, when combined with an inhibitor of cathepsin L (Figure 1) potently inhibited MERS-CoV entry into cells (Shirato, Kawase, & Matsuyama, 2013). These data represent the first chemical inhibition of MERS-CoV entry using infectious MERS-CoV by targeting host proteases. Targeting both the MERS-CoV S and receptor (CD26/DPP4) have been shown to be effective approaches, as Gao et al designed viral fusion peptide inhibitors against the heptad repeat region HR2 of the MERS-CoV S and Ohnuma et al created monoclonal antibodies against CD26 that were able to block MERS-CoV entry (Gao et al., 2013; Ohnuma et al., 2013).

To understand how MERS-CoV infection influences and interacts with host cells, Josset et al infected a lung epithelial cell line, Calu3, with MERS-CoV and SARS-CoV and analyzed the host transcriptome (Josset et al., 2013). This approach identified host

factors to which inhibitory compounds exist, that could be exploited as antiviral therapeutics. To validate these putative inhibitors, the authors infected cells with MERS-CoV and showed that the host kinase inhibitor SB203580 had inhibitory effects on both SARS-CoV and MERS-CoV replication. This approach is useful for identifying host cell factors beneficial for replication, determining if they are druggable targets, and identifying existing inhibitors to these targets.

Based on the knowledge that cyclophilins play an important role in coronaviral infections (Pfefferle et al., 2011), de Wilde et al. used cyclosporine A to determine if cytotoxicity as a result of MERS-CoV infection is a possible readout for antiviral screening (de Wilde et al., 2013). Cyclosporin A was able to prevent MERS-CoV cytopathic effect in both Vero and Huh7 cells, verifying CPE as a read out of MERS-CoV infection, and a possible way to screen antiviral compounds against MERS-CoV. To aid in the study of MERS-CoV biology and antiviral screening, reverse genetics systems for MERS-CoV have been developed by two groups (Almazan et al., 2013; Scobey et al., 2013). The use of reverse genetics will allows for the creation of viruses expressing reporters as readouts of viral replication, and can be used to screen antiviral compounds in a more quantitative fashion. This was demonstrated by Scobey et al, who engineered a MERS-CoV encoding an RFP gene that is expressed during viral replication.

Showing inhibitory effects using the infectious virus is the critical step in developing antivirals, but screening large compound libraries or determining inhibitor mechanisms using infectious virus is not practical. Many approaches rely on using

infectious MERS-CoV as a way to determine if compounds had inhibitory effects. As MERS-CoV is highly pathogenic and is transmittable from human to human, all assays must be performed in a BSL-3 laboratory. So far, two approaches have been developed for assaying antiviral compounds at either the entry or viral protease stage of the MERS-CoV lifecycle without using infectious MERS-CoV. The first approach involves the familiar pseudotype assay that has been used to evaluate SARS-CoV entry inhibitors. Gierer et al. used VSV-luciferase pseudotyped with the MERS-CoV S to determine that MERS-CoV does not utilize any other coronaviral receptors, that TMPRSS2 and endosomal cathepsins facilitate viral entry, and that the S protein can be neutralized with MERS-CoV infected patient serum (Gierer et al., 2013). Zhao et al. also used pseudotyped virions, but for their experiments they utilized an HIV-luciferase virus pseudotyped with MERS-CoV S (G. Zhao et al., 2013). They used this system to also show that the S could be neutralized by antibodies and that a small-molecule inhibitor of HIV entry had inhibitory properties on the transduction of their pseudovirions. Gao et al used pseudotyped virions to determine that HR targeting peptides inhibit viral entry (Gao et al., 2013).

A novel, cell-based approach to assay for coronaviral protease activity was developed by Kilianski et al. and used to determine if previously identified SARS-CoV protease inhibitors had activity against MERS-CoV proteases (Kilianski, Mielech, Deng, & Baker, 2013). This work is discussed in detail later in this dissertation, but briefly, these experiments utilized a circularly permuted luciferase construct with an inserted cleavage site corresponding to either the papain-like or 3C-like protease recognition sites.

Expression vectors for both MERS-CoV PL^{pro} and $3CL^{pro}$ were able to cleave their respective biosensors when transfected together. An endpoint dual-luciferase assay with renilla luciferase as a transfection control and a live cell assay using a cell permeable luciferase substrate both showed luciferase activation when the MERS-CoV proteases were present. These assays were used to test previously identified SARS-CoV PL^{pro} and $3CL^{pro}$ inhibitors. The PL^{pro} inhibitor had no effect on the activity of MERS-CoV PL^{pro}, while the $3CL^{pro}$ inhibitor CE-5 did show inhibitory activity against MERS-CoV $3CL^{pro}$. This was the first demonstration of an efficacious antiviral compound specific to a MERS-CoV enzyme, and will lead to SARS-CoV specific compounds being further tested. The applications of this assay are not limited to MERS-CoV, as the viral papain-like protease from SARS-CoV also activated the luciferase construct. This cell-based biosensor assay is especially useful as it can be used at BSL-2 level to study the effects of compound inhibitors on coronaviral proteases in the context of a host cell. The results from this work will be discussed in more detail in the results and discussion sections in chapters III and IV.

CURRENT STATE OF CORONAVIRAL DRUG DEVELOPMENT

There are many challenges currently facing scientists who are developing coronaviral, and especially MERS-CoV, antiviral drugs. As highlighted above, there is a need for validated cell-based assays that can be used to accelerate antiviral compound discovery in the face of emerging coronavirus infections (Table 1). One issue with

Table 1. Cell-based Assays Used for Antiviral Development Against MERS-CoV
(from (Kilianski & Baker, 2014)

Cell-based Assay	For evaluation of:	References
Infectious Virus (BSL-3)		
Cytopathic Effect	TMPRSS2 MERS-CoV S Cleavage	Shirato, Kawase, & Matsuyama, 2013
	Cyclophilins required for MERS-CoV replication	de Wilde et al., 2013
Immunoflourescence	Blocking MERS-CoV S and CD26 interaction	Ohnuma et al., 2013
Viral Titer	Host Kinases Upregulated by MERS-CoV	Josset et al., 2013
qRT-PCR	TMPRSS2 MERS-CoV S Cleavage	Shirato, Kawase, & Matsuyama, 2013
Reporter Virus	Synthetic RFP expressing MERS-CoV for antiviral screening	Scobey et al., 2013
Surrogate Assays (BSL-2)		
Spike pseudotyped virus	Peptide Blockage of HR2	Gao et al., 2013
	Neutralization with patient serum	Gierer et al., 2013
	Neutralization and entry inhibition by small molecule	Zhao et al., 2013
Protease cleavage bioassay	Small molecules targeting PLpro and 3CLpro	Kilianski et al., 2013

MERS-CoV antiviral design is that only recently has a small animal model for infection been proposed. Rhesus macaques can be infected with MERS-CoV, exhibit symptoms, and respond to therapies (Emmie de Wit et al., 2013; Falzarano et al., 2013; Munster, de Wit, & Feldmann, 2013); however, the symptoms are transient and do not completely reflect the severity of the disease in humans. Unlike SARS-CoV, de Wit et al. demonstrated that MERS-CoV does not establish a productive infection in Syrian hamsters (E de Wit et al., 2013). To date, there has been only one productive infection in a small animal model. Mice transduced with a replication-deficient adenovirus expressing the human CD26 were able to support infection and replication within the lung (J. Zhao et al., 2014). In addition to the generation of better animal models for MERS-CoV, more work needs to be done to develop broad-spectrum inhibitors that would work against the common human coronaviral pathogens like HCoV-NL63, HCoV-229E, HCoV-OC43, or HCoV-HKU1. Development of inhibitors that also target these common viruses would allow for clinical trials on the effectiveness of antiviral drugs against endemic and possible emergent coronaviruses such as MERS-CoV. While antiviral therapies are being developed against coronaviral proteases, there are still many unknowns about their role, apart from polyprotein cleavage, during viral infection. In the following section, I will explore the papain-like protease from coronaviruses and what role its multiple functions might have on viral replication and pathogenesis.

THE PAPAIN-LIKE PROTEASE AS A MULTIFUNCTIONAL ENZYME

While antiviral therapies are being developed against coronaviral proteases, there are still many unknowns about their role, apart from polyprotein cleavage, during viral infection. Multi-functionality of viral enzymes is a common theme due to the genetic economy necessary to encode all of the functions necessary for viral replication in limited coding space. Despite being the largest of the RNA viruses, this theme continues for coronavirus enzymes. The papain-like protease (PLP or PLpro) is a coronavirus enzyme with multiple functions apart from its primary role during viral replication. After the coronavirus genome enters the cytoplasm, it is translated by host ribosomes into two large polyproteins, pp1a and pp1b. These polyproteins comprise the non-structural proteins that must be liberated by protease cleavage for replication complex formation and the continuation of the viral replication cycle. Papain-like proteases are responsible for cleavage through the recognition of a consensus LXGG↓ motif located between non-structural proteins at the n-terminal end of the polyproteins. Some coronaviruses, such as SARS-CoV and MERS-CoV, only encode one papain-like protease responsible for cleavage between nsp1-2, 2-3, and 3-4 (Harcourt et al., 2004; Kilianski et al., 2013). Other coronaviruses, like the prototypic animal model MHV and human coronaviruses HCoV-NL63 and HCoV-229E encode two papain-like proteases. PLP1 is responsible for cleavage between nsp1-2 and 2-3 while PLP2 is responsible for cleavage between nsp3-4 (reviewed in (Mielech, Chen, Mesecar, & Baker, 2014).

In addition to this conserved role in viral replication, evidence has emerged for auxiliary functions of coronavirus papain-like proteases. Predicted structural characteristics, and the RLRGG↓ (similar to the CoV PLP LXGG↓ recognition site) motif recognized by host deubiquitinating enzymes, led to the hypothesis that PLpro is able to cleave ubiquitin and/or ubiquitin-like protein modifiers from host cell proteins (Sulea, Lindner, Purisima, Menard, & Ménard, 2005). This hypothesis was supported by *in vitro* evidence of ubiquitin cleavage and further supported by the cleavage of ubiquitin from host cell proteins in transfected cells (Barretto et al., 2005; Lindner et al., 2005). With the resolution of the first crystal structure of a coronavirus papain-like protease, SARS-CoV PLpro, came the realization that the structure of PLpro has homology to human deubiquitinating enzymes, specifically the ubiquitin-specific protease (USP) class of enzymes (Ratia et al., 2006). Deubiquitinating activity was not unique to SARS-CoV PLpro, as MERS-CoV PLpro, transmissible gastroenteritis virus (TGEV) PLP1, HCoV-NL63 PLP2, and MHV PLP2 all have the ability to cleave ubiquitin either *in vitro* or within transfected cells (Z. Chen et al., 2007; Mielech, Kilianski, Baez-Santos, Mesecar, & Baker, 2014; G. Wang, Chen, Zheng, Cheng, & Tang, 2011; Wojdyla et al., 2010). Coronaviruses are not the only viruses to encode deubiquitinating enzymes; however the role for this activity during infection and how it relates to virus pathogenesis is still very much unknown.

VIRAL DEUBIQUITINATING ENZYMES

Ubiquitin and its conjugation and de-conjugation play a major role in the signaling pathways required for the innate immune system to recognize and defend against viral infections. In the constant evolutionary battle between viruses and their hosts, viruses have evolved proteins capable of disrupting the ubiquitin conjugation needed for the activation of many innate immune pathways (Figure 3). Viral deubiquitinating enzymes have evolved across very distinct viral families (Table 1). Discovery of deubiquitinating enzymes within tegument proteins in the herpesviruses has been linked to innate immune antagonism and viral latency (Inn et al., 2011). Adenovirus proteinase has also been shown to possess deubiquitinating activity (Balakirev, Jaquinod, Haas, & Chroboczek, 2002). Nidoviruses encode proteases necessary for the cleavage of viral polyproteins during replication, and some of these proteases have been identified as deubiquitinating enzymes (reviewed in Mielech, Chen, Mesecar, & Baker, 2014). Of note, equine arteritis virus (EAV) PLP2 has been co-crystalized with ubiquitin, and this structure has allowed for the creation of mutant viruses that lack deubiquitinating activity and induce some proinflammatory cytokines (van Kasteren et al., 2013). However, a full profile of the effect of loss of DUB activity in cell culture and *in vivo* relevance to pathogenesis has not been addressed.

The evolution of viral DUBs indicates their importance during infection, so determining the specificities of virally encoded DUBs is an important area of study. Some useful information can be taken from what is known about host cell DUBs when

Table 2. Identified viral deubiquitinating enzymes

Virus Family	*DUB/putative DUB*	*Domain Structure*	*Reference*
Adenoviridae	Avp	~UCH	(Balakirev et al., 2002)
Arteriviridae	PLP2 (PRRS)	OTU	(Z. Sun, Li, Ransburgh, Snijder, & Fang, 2012; van Kasteren et al., 2012)
	PLP (EAV)	OTU	(van Kasteren et al., 2012)
Bunyaviridae	vOTU (CCHFV)	OTU	(Akutsu et al., 2011; Capodagli et al., 2011; James et al., 2011)
Coronaviridae	PLpro (SARS-CoV)	USP	(Barretto et al., 2005; Lindner et al., 2005; Ratia et al., 2006)
	PLP2 (MHV)	Unk	(Clementz et al., 2010; G. Wang et al., 2011)
	PLP2 (NL63)	Unk	(Z. Chen et al., 2007)
	PLpro (MERS-CoV)	Unk	(Mielech, Kilianski, et al., 2014; X. Yang et al., 2013)
	PLP2 (PEDV)	Unk	(Xing et al., 2013)
	PLP 1 (TGEV)	USP	(Wojdyla et al., 2010)
Nairoviridae	nsp2	OTU	(van Kasteren et al., 2012)
Herpesviridae	BPLF1 (EBV)	htUSP	(Whitehurst et al., 2009)
	Orf64 (KSHV)	htUSP	(Gonzalez, Wang, & Damania, 2009)
	UL48 (CMV)	htUSP	(Gredmark, Schlieker, Quesada, Spooner, & Ploegh, 2007)
	pUL36 (Pseudorabies)	htUSP	(Bottcher et al., 2008; Lee et al., 2009)

thinking about how SARS-CoV PLpro might function during infection. PLpro has ubiquitin-specific protease (USP) class homology, and the USP class of DUBs is the largest class and most well studied. The ubiquitin-specific proteases all share a similar catalytic domain structure and many have thumb, palm, and zinc finger domains. Despite these shared characteristics, the USP class of DUBs can have great variation, and thus interaction between these proteases and ubiquitin or ubiquitin-like modifiers can vary. The structure of USP21 has been solved in complex with a linear di-ubiquitin molecule linked to aldehyde (Y Ye et al., 2011). In this crystal structure, the di-ubiquitin molecule interacts primarily with the fingers domain, and there is an interaction between the second ubiquitin protein and the zinc ion bound by the fingers. It is also shown that USP21 is able to cleave all forms of ubiquitin and the ubiquitin-like modifier ISG15, which is an important antiviral gene upregulated by interferon signaling (Y Ye et al., 2011).

This promiscuity in ubiquitin and ubiquitin-like modifier cleavage could be advantageous for a viral DUB like PLpro. Additionally, the USP-ubiquitin interactions at sites distant from the catalytic site could provide potential sites for mutagenesis which may modify ubiquitin interaction. Mutating certain residues might provide for affinity changes between the DUB and different ubiquitin chains, creating the possibility of a PLpro with affinity for only a specific type of ubiquitin chain or ubiquitin-like modifier. Mutagenesis of residues distant from the catalytic site might also allow for loss of ubiquitin interaction while maintaining the critical interactions between PLpro and viral substrates. Using the crystal structure of SARS-CoV PLpro with Ub-aldehyde as

outlined in the following sections could allow for the separation of protease activity against the viral polyprotein from deubiquitinating activity by targeting residues distant from the active site of PLpro.

INNATE IMMUNE SIGNALING PATHWAYS, PLPRO, AND UBIQUITIN

In addition to its role in viral replication and its deubiquitinating activity, PLpro has been shown to act as an innate immune antagonist in transfected cells (Clementz et al., 2010; Devaraj et al., 2007; Frieman et al., 2009; S. W. Li et al., 2011; L. Sun et al., 2012). PLpro was cloned out of SARS cDNA with the soluble domain of PLpro comprising amino acids 1541-1855 of ORF1a. This construct prevents activation of IRF3 and NFκB when these pathways are stimulated. Interestingly, IRF3 antagonism is seen in a catalytic mutant PLpro, where NFκB antagonism is completely dependent on catalytic activity (Clementz et al., 2010; Devaraj et al., 2007). As SARS-CoV doesn't induce a robust interferon response at early stages in infection, it is thought that either SARS-CoV RNA is able to hide from cytoplasmic RNA sensors like RIG-I or MDA5, and/or that SARS-CoV encodes antagonists to actively block the innate immune system from activation, or a combination of the two (reviewed in (Totura & Baric, 2012). PLpro can act as a deubiquitinase, and because ubiquitin has been implicated as a major modification in the regulation of innate immune signaling pathways, the deubiquitinating activity of PLpro might play a major role in the innate immune antagonism properties of SARS-CoV PLpro.

The innate immune system acts as the first line of defense against viral infections within host cells (reviewed in (Wilkins & Gale Jr, 2010). It is comprised of sensors of viral infections called pattern recognition receptors (PRRs) and many downstream effectors, which act as signal transducers, viral restriction factors, and transcription factors. Upon sensing of viral proteins, viral nucleic acids, or changes in the cell which are characteristic of viral infection, PRRs become activated and initiate signaling cascades which lead to the production of antiviral genes. These antiviral genes include critical antiviral proteins like ISG15, the IFIT family of proteins, type-I interferons, and various cytokines and chemokines. Type-I interferons are important signaling molecules, and signal in an autocrine and paracrine manner to alert other cells that a nearby cell is virally infected. This response is known to be suppressed during SARS-CoV infection, and in vitro data suggests that the deubiquitinating and deISGylating activity of PLpro might contribute to the lack of an innate immune response seen during the early stages of SARS-CoV infection.

Ubiquitination plays a crucial role in the activation of the innate immune system in response to viral infection. Viruses have evolved mechanisms to deconjugate ubiquitin within infected host cells, and it has been hypothesized that viral DUB activity might disrupt innate immune signaling in infected cells (reviewed in (Viswanathan, Fruh, & DeFilippis, 2010). In response to the detection of viral RNA through the PRRs RIG-I and MDA5, RIG-I and MDA5 are activated by phosphorylation and either directly ubiquitinated or interact with unanchored poly-ubiquitin chains (Jiang et al., 2012; Zeng et al., 2010). This allows for the activation of downstream effector MAVS, which acts to

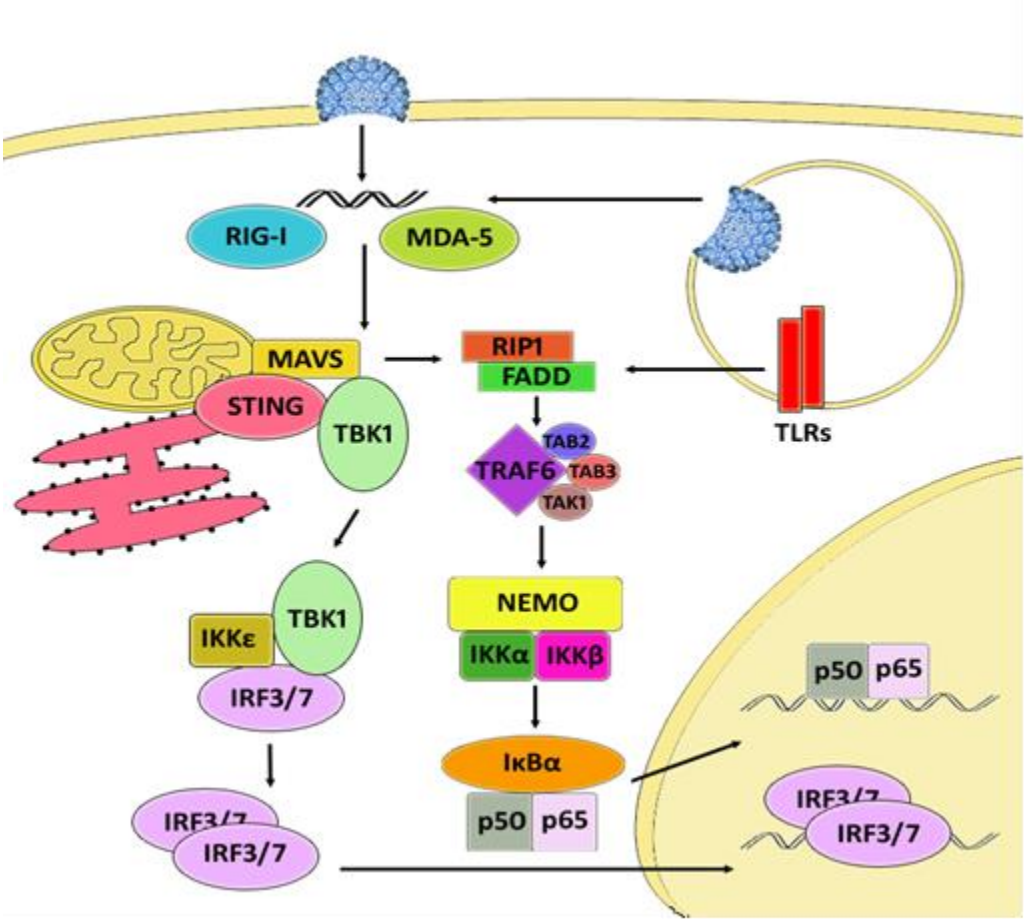

Figure 2. Major innate immune pathways regulated during viral infection. Upon viral entry at either the plasma membrane or from endosomes, viral nucleic acids are exposed to pattern recognition receptors like RIG-I, MDA5. These proteins are dependent upon ubiquitin for their signaling function, and activate the recruitment of MAVS, STING, and TBK1. This complex is important for downstream signaling leading to the activation of transcription factors IRF3/7 and for the phosphorylation and polyK-48 ubiquitination of IκBα. This leads to its degradation and liberates NFκB to access the nucleus and, along with IRF3/7, activate transcription of key interferon and innate immune genes.

recruit STING and TBK1 to a signaling complex that is important for the activation of transcription factors NFκB, IRF3, and IRF7 (Hou et al., 2011). MAVS and STING are k63-linked ubiquitinated while the degradation of IκBα, required for NFκB activation, is mediated by K48-linked ubiquitination (Figure 3). Upon degradation of IκBα, NFκB is then free to become phosphorylated and enter the nucleus, where it is a critical transcription factor (along with IRF3/7) necessary for the upregulation of interferons, cytokines/chemokines, and ISGs. The role for K48-liked ubiquitination in the activation of NFκB is well characterized and so this pathway will serve as a model for the effect of SARS-CoV PLpro deubiquitinating activity on innate immune antagonism.

ISG15, a ubiquitin-like modifier, has recently been identified as an important interferon stimulated gene in the defense of cells from viral infection (Lenschow et al., 2005, 2007). Expressed in response to type-I interferon signaling, ISG15 is conjugated to newly synthesized proteins or released extracellularly, and both forms of ISG15 have antiviral properties (Lenschow, 2010). How ISG15 mediates broad-spectrum antiviral activity is unknown, but similar to ubiquitination, many viruses have evolved mechanisms to prevent ISG15 antiviral activity. Virally encoded proteases such as CCHFV L protease with OTU domain structure are able to cleave ISG15 from host proteins, and cleavage prevents the antiviral effects of ISG15 in mouse models (Akutsu, Ye, Virdee, Chin, & Komander, 2011; James et al., 2011; Lenschow et al., 2007). In addition to DUB activity, SARS-CoV PLpro can cleave ISG15 efficiently (Lindner et al., 2005, 2007; Ratia, Kilianski, Baez-Santos, Baker, & Mesecar, 2014). The cleavage of ubiquitin and ISG15 might be a critical mechanism for prevention of innate immune

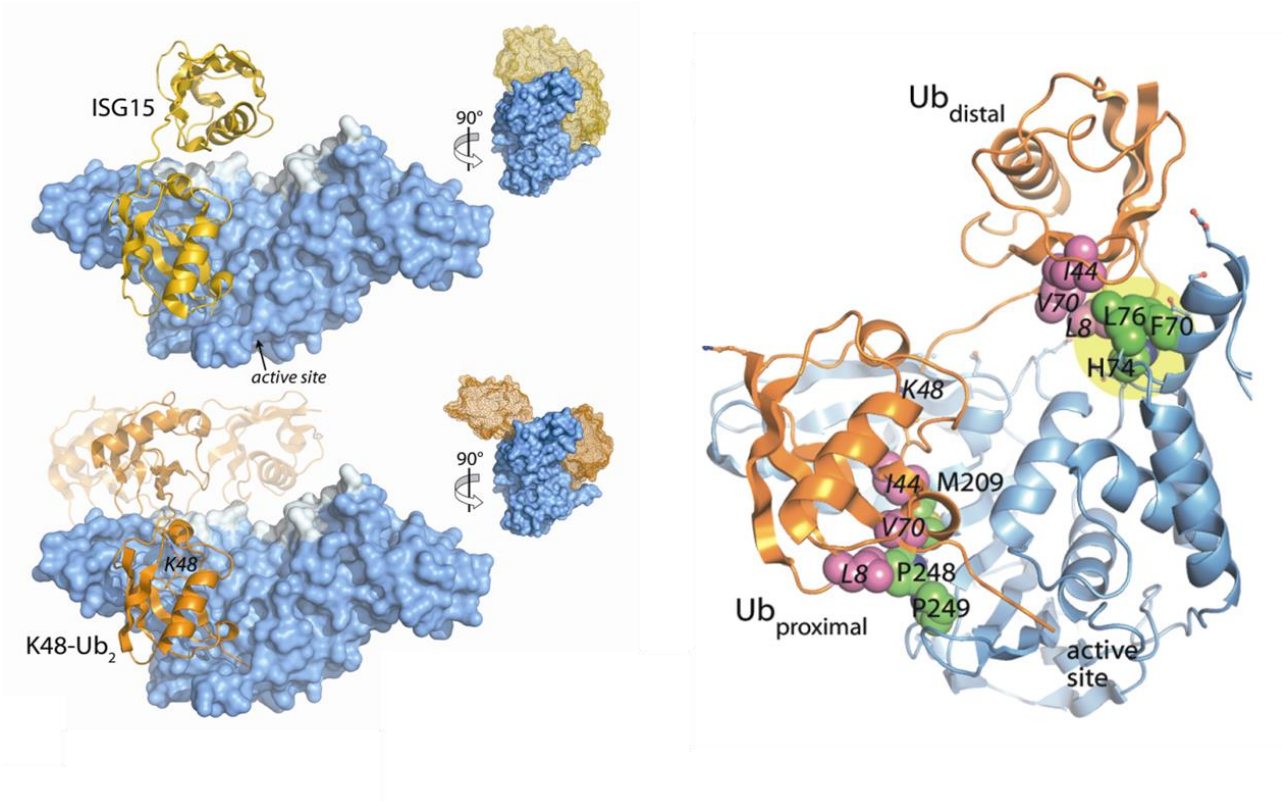

Figure 3. Modeling of ISG15 and K48-Ub from crystal structure of SARS-CoV PLpro bound to Ub-aldehyde. A) The dark orange structure on the right is the single ubiquitin molecule bound to aldehyde co-crystalized with PLpro in blue. The white region of PLpro represents the ridge. The lighter orange and yellow ribbon structures of K48-Ub and ISG15 represent modeling on how these chains interact with PLpro based on the Ub-aldehyde/PLpro co-crystal structure. B) The residues in green (PLpro) are interact with the I44 patch on ubiquitin at the hydrophobic patch (M209, P248, P249) and are predicted to interact with the I44 patch on the second ubiquitin molecule in a K48-linked chain at the ridge region (F70, H74, L76). From (Ratia et al., 2014)

responses during SARS-CoV infection, so understanding how PLpro affects these pathways is important for understanding the pathogenesis of SARS-CoV infection.

DETERMINING A ROLE FOR SARS-COV PLPRO DEUBIQUITINATING ACTIVITY

To investigate if PLpro deubiquitinating or deISGylating activity plays a role in innate immune antagonism, we sought to separate the polyprotein cleavage and deubiquitinating activities. This separation would allow for the independent examination of the role of DUB activity in innate immune antagonism and may also allow for DUB inactive PLpro mutants to be engineered into infectious SARS-CoV. In order to examine how PLpro and ubiquitin interact, PLpro and a ubiquitin aldehyde molecule were co-crystalized together and analyzed by x-ray crystallography. There are two interacting faces that were determined by the crystal structure and by modeling various ubiquitin chain linkages onto that single ubiquitin structure (Figure 3a). The PLpro-ubiquitin interaction surface determined by crystal structure (Figure 3b) contains a polar patch, with important residues R167, M207, and Y208; and a hydrophobic patch with interactions mediated by M209, and P248 and P249 are important. It is clear that structurally, these residues are important, but it is possible that other residues in close proximity to these patches could also influence the affinity of PLpro for ubiquitin. To gain further insight into PLpro-poly ubiquitin interactions, K48-linked di-ubiquitin and ISG15 were modeled onto the single ubuqituin molecule co-crystalized with PLpro. In

these models, PLpro is predicted to interact with both K48-liked ubiquitin and ISG15 in a similar manner (Figure 3a).

The second molecule of ubiquitin in K48-linked chains (and the second half of ISG15) extend upward from the catalytic site and are modeled to interact with a region of PLpro on the thumb domain. We termed this region the ridge, and it is highlighted in more detail in the ribbon diagram (Figure 3b). There are residues that extend outward from the core of PLpro and are predicted to interact with a stretch of amino acids on K48-Ub. Because these residues are far away from the core domain and catalytic triad of PLpro, we predict that mutagenizing these residues will not affect polyprotein cleavage ability. However, we predict that these residues will be crucial for PLpro and poly-ubiquitin chain interaction, and thus could be important for PLpro DUB activity. The modeling of these chains suggest that the ridge residues F70, H74, and L76 are responsible for interaction between PLpro and both K48-Ub and ISG15 (Figure 3b). Residues in both the hydrophobic patch and the ridge region of SARS-CoV PLpro will be targeted for mutagenesis in order to separate PLpro viral polyprotein cleavage from PLpro DUB and/or deISGylating activity. If these mutants retain polyprotein cleavage ability but lose deubiquitinating or deISGylating activity, then the relevance of this activity and how it relates to innate immune antagonism can be determined experimentally.

The goal of my dissertation work is to develop a novel biosensor for the detection of coronavirus papain-like and 3C-like protease activity from multiple coronaviruses of

the alpha and beta coronavirus genus. This work will aid the rapid identification of potential antiviral compounds that are needed for emerging coronaviruses like MERS-CoV. Additionally, the roles for the multiple functions exhibited by SARS-CoV PLpro during viral infection are unknown. I will utilize PLpro-ubiquitin co-crystal structure to create targeted mutations that are predicted to disrupt the affinity between PLpro and ubiquitin and abrogate the deubiquitinating activity of SARS-CoV PLpro. This separation of protease and deubiquitinating activity will allow for the examination of PLpro DUB activity and its contribution to innate immune antagonism.

CHAPTER II

MATERIALS AND EXPERIMENTAL METHODS

CELLS AND TRANSFECTIONS

HEK293T cells were cultured in Dulbecco's modified Eagle's medium (DMEM) containing 10% fetal calf serum (FCS), and 2% glutamine. For transfection experiments, cells were plated in cell-bind plates (Corning) and when cells were approximately 70% confluent, they were subjected to transfection using TransIT-LT1 transfecting reagent (Mirus) according to the manufacturer's suggested protocol.

PROTEASE EXPRESSION PLASMIDS

The sequence of the MERS-CoV PLpro (accession number: AFS88944; ORF1a amino acids 1483-1802) was codon-optimized and synthesized (GenScript), and cloned into pcDNA3.1-V5/His-B (Invitrogen) (Supplementary Fig 1) to generate pMERS-CoV PLpro. A catalytically inactive mutant (cysteine 1592 changed to alanine, designated CA) was generated using site-directed mutagenesis by two-step overlapping PCR approach using primers (Supplementary Table 1). The MERS-CoV nsp4-5-6N region (ORF1a amino acids 2741 to 3561) was synthesized (GenScript) and cloned into pcDNA3.1-V5/His-B (Invitrogen) (Supplementary Fig. 2) to generate pMERS-

pp3CLpro. Specific mutations in the catalytic residues (C3395 in nsp5) and putative cleavage site of nsp5/6 (Q3553/S3554) were generated by using QuikChange II XL site-directed mutagenesis kit (Stratagene) with primers listed in Supplementary Table 1. SARS-CoV PLpro was generated previously (Ratia et al., 2006).

BIOSENSOR EXPRESSION PLASMIDS

The pGlo-30F vector backbone (Promega) is a circularly permuted *Photuris pennsylvanica* luciferase optimized for expression in cell culture (32). Oligonucleotides corresponding the amino sequence RLKGG (for PLpro) or VRLQS (for 3CLpro) were ligated into the BamHI and HindIII restriction enzyme cleavage sites (Supplementary Table 1) and screening for the inserts was performed by restriction enzyme digestion to confirmation of the presence of engineered AflII (RLKGG) or PstI (VRLQS) sites. The resulting plasmids were designated pGlo-30F-RLKGG and pGlo-30F-VRLQS.

TRANS-CLEAVAGE ASSAY

293HEK cells were transfected with constructs expressing nsp2-3-GFP and SARS-CoV PLpro-V5 wild type, catalytic mutant (C112A) or ridge mutants. Cells were incubated for 24 hours and then lysed with IkBα lysis buffer (20mM Tris (pH 7.5), 150mM NaCl, 1mM EGTA, 1mM EDTA, 1% Triton X-100, 2.5mM Na pyro-phosphate, 1mM Beta-glycerophosphate, 1mM Na ortho-vanadate, 1ug/ml Leupeptin). Lysates were

subjected to centrifugation at 4C and the cytoplasmic contents were added to 2X sample buffer and separated by SDS-PAGE on a 10% PAGE gel (BioRad). Samples were transferred to PVDF immunoblotted with anti-GFP (Life Technologies) and anti-V5 (Invitrogen).

PAPAIN-LIKE PROTEASE EXPRESSION PLASMIDS

The sequence of the MERS-CoV PLpro (accession number: AFS88944; ORF1a amino acids 1483-1802) was codon-optimized and synthesized (GenScript), and cloned into pcDNA3.1-V5/His-B (Invitrogen) (Supplementary Fig 1) to generate pMERS-CoV PLpro. A catalytically inactive mutant (cysteine 1592 changed to alanine, designated CA) was generated using site-directed mutagenesis by two-step overlapping PCR approach using primers (Supplementary Table 1). The MERS-CoV nsp4-5-6N region (ORF1a amino acids 2741 to 3561) was synthesized (GenScript) and cloned into pcDNA3.1-V5/His-B (Invitrogen) (Supplementary Fig. 2) to generate pMERS-pp3CLpro. Specific mutations in the catalytic residues (C3395 in nsp5) and putative cleavage site of nsp5/6 (Q3553/S3554) were generated by using QuikChange II XL site-directed mutagenesis kit (Stratagene) with primers listed in Supplementary Table 1.

TRANS-CLEAVAGE ASSAY FOR PLPRO

HEK293T cells in 12-well plates were transfected using TransIT-LT1 transfection reagent (Mirus) with 25 ng nsp2/3-GFP plasmid and increasing amounts of pcDNA-MERS-CoV PLpro expression plasmids. At 24 hours post transfection, cells were lysed with 300µl of Lysis Buffer A containing 4% SDS, 3% dithiothreitol (DTT), and 0.065M Tris, pH 6.8. Proteins were separated by SDS-PAGE and transferred to PVDF membrane in transfer buffer (0.025M Tris, 0.192M glycine, 20% methanol) for 1 hour at 65V at 4°C. The membrane was blocked using 5% dried skim milk in TBST buffer (0.9% NaCl, 10mM Tris-HCl, pH7.5, 0.1% Tween 20) over night at 4°C. The membrane was incubated with polyclonal rabbit anti-GFP antibody (Life Technologies) followed by incubation with HRP-conjugated donkey-anti-rabbit secondary antibody (SouthernBiotech). To verify expression of PLpro, the membrane was probed with mouse anti-V5 antibody (Invitrogen); mouse anti-calnexin (CellSignal) antibody was used to detect a host cell protein as a loading standard; HRP-conjugated goat-anti-mouse (SouthernBiotech) was used as the secondary antibody. Secondary antibody was detected using Western Lighting Chemiluminescence Reagent Plus (PerkinElmer) and visualized using FluoroChemE Imager.

BIOSENSOR ENDPOINT ASSAY

HEK293T cells were transfected with 150 ng pGlo-30F-RLKGG or pGlo-30F-VRLQS, 25ng pRL-TK (Promega), and increasing amounts of protease expression

plasmid. Transfections were equalized to 500 ng per well with empty pcDNA3.1-V5/His-B vector. At 20 hours post transfection, cells were lysed with 1X passive lysis buffer (Promega) and 25µl of lysate was assayed for luciferase activity using 96-well white bottom assay plates (Corning) and dual luciferase activating reagents (Promega).

BIOSENSOR LIVE-CELL ASSAY

HEK293T cells (96-well format, 0.4µl TranIT-LT1 per well) were transfected with 37.5 ng pGlo-30F vector, pGlo-30F-RLKGG or pGlo-VRLQS, 2 ng pRL-TK (Promega), and either 37.5 ng for SARS-CoV PLpro or 25 ng MERS-CoV 3CLpro DNA. Transfections were equalized to 125 ng with empty vector pcDNA3.1-V5/His-B. At 13 hrs post transfection, GloSensor (Promega) reagent (diluted 1:50 in culture medium) was added to each well. Plates were imaged using a luminometer (Veritas) every hour for 2 hours. Cells were then treated with indicated concentration of drug or volume equivalent of DMSO and imaged every hour for 4 hours.

WESTERN BLOT DETECTIONS OF MERS-PP3CLPRO CLEAVAGE PRODUCTS

To determine catalytic activity of MERS-pp3CLpro, HEK293T cells in 24-well CellBind plates were transfected with increasing amounts of pcDNA-pp3CLpro expression plasmid DNA. At 20 hours post transfection cells were lysed in 100µl of

Lysis buffer A followed by western blotting as described above. The protein level of pp3CLpro and its cleaved products were detected using mouse anti-V5 antibody (Invitrogen). After probing with anti-V5, the membrane was treated with stripping buffer (62.5mM Tris-Cl, pH 6.8, 2% SDS, 100mM 2-beta-mercaptoethanol) and re-blotted using a mouse monoclonal antibody to beta-actin (Ambion). HRP-conjugated goat-anti-mouse (Southern Biotech) was used as the secondary antibody.

DEUBIQUITINATING ASSAY

293T cells in 12-well Cell-Bind plate (Corning) are transfected (LT1, Mirus) with 300ng FLAG-Ub and either 125ng, 250ng, or 500ng of pcDNA3.1-SARS-PLpro per well. Cells were incubated for 18hrs then lysed with IkBα lysis buffer (20mM Tris (pH 7.5), 150mM NaCl, 1mM EGTA, 1mM EDTA, 1% Triton X-100, 2.5mM Na pyro-phosphate, 1mM Beta-glycerophosphate, 1mM Na ortho-vanadate, 1ug/ml Leupeptin) and incubated for 20min on ice. Lysates were subjected to centrifugation at 4C and the cytoplasmic contents were added to 2X sample buffer and separated by SDS-PAGE on a 4-20% gradient gel (BioRad). Gel was transferred to PVDF using semi-dry apparatus (BioRad) and immunoblotted with anti-FLAG (Sigma), anti-V5 (Invitrogen), and anti-calnexin (BD).

DEISGYLATING ASSAY

To determine deISGylating activity MERS-CoV PLpro HEK293T cells in 12-well plates were transfected with 10, 25, 50, and 100ng of pCDNA-MERS-PLpro wild type or catalytic mutant and 250ng ISG15-myc, 125ng UbcH8, 125ng Ube1L, and 125ng Herc5. 20 hours post transfection cells were lysed with lysis buffer (20mM Tris (pH 7.5), 150mM NaCl, 1mM EGTA, 1mM EDTA, 1% Triton X-100, 2.5mM Na pyrophosphate, 1mM beta-glycerophosphate, 1mM Na ortho-vanadate, 1ug/ml leupeptin). Proteins were separated by SDS-PAGE and transferred to PVDF membrane using a semi-dry transfer apparatus (BioRad).

Iκbα PHOSPHORYLATION ASSAY

293T cells in 12-well Cell-Bind plate (Corning) are transfected (LT1, Mirus) with 500ng of pcDNA3.1-SARS-PLpro per well. Cells are incubated for 16hrs then treated with TNFα (Roche) at 20ng/ml for 0, 5, 10, 15, 30, or 60 minutes. Cells are then harvested in Iκbα lysis buffer (20mM Tris (pH 7.5), 150mM NaCl, 1mM EGTA, 1mM EDTA, 1% Triton X-100, 2.5mM Na pyro-phosphate, 1mM Beta-glycerophosphate, 1mM Na ortho-vanadate, 1ug/ml Leupeptin) directly on ice. Lysates were subjected to centrifugation at 4C and the cytoplasmic contents were added to 2X sample buffer and separated by SDS-PAGE on a 10% PAGE gel (BioRad). Gel was transferred to PVDF using semi-dry apparatus (BioRad) and immunoblotted with anti-pIkBα (CellSignaling), anti- Iκbα (CellSignaling), anti-V5 (Invitrogen) and anti-calnexin (BD).

CORONAVIRUS PLASMID MUTAGENESIS

Wild-type pcDNA3.1-PLpro-V5 was mutated using either QuikChange XL (Agilent) or ChangeIT (Affymetrix) mutagenesis kits following the manufacturer's instructions. Briefly, primers were synthesized according to the kit manufacturer's specifications (Table 2). After PCR mutagenesis, DNA was digested with Dpn1 to remove template plasmid and then transformed into XL-10 gold ultracompetent cells (Agilent). Cells were plated on Amp+ LB plates and colonies selected for mini-prep growth and plasmid prep. Selected clones were sent for sequencing using CMV-F primer encoded within pcDNA3.1.

Iκbα-HA DEGRADATION ASSAY

HEK293 cells were plated in 60mm dishes and transfected with 3ug pcDNA3.1 – PLpro and 250ng pIkBα-HA per dish (Mirus LT-1) (S. Sun, Elwood, & Greene, 1996). Cells were incubated for 24hrs, media, removed, and fresh media containing TNFα (Roche) at a final concentration of 20ng/ml was added and incubated with cells. Cells were incubated with TNFα for the indicated time points. Cells were then lysed with an IkBα lysis buffer: 20mM Tris (pH 7.5), 150mM NaCl, 1mM EGTA, 1mM EDTA, 1% Triton X-100, 2.5mM Na pyro-phosphate, 1mM Beta-glycerophosphate, 1mM Na ortho-vanadate, 1ug/ml Leupeptin. Lysates were kept on ice and centrifuged at 14000xg for 10min at 4C. After centrifugation, supernatant was added to equal volume 2x sample buffer, boiled for 5min, and then immediately run on 10% SDS-PAGE gel. Gel was

transferred to PVDF using a semi-dry blot apparatus (TransBlot Turbo, Bio-Rad) and blocked in 5% milk overnight. Antibodies were used at a concentration of 1:5000 (mαHA, Covance; mαV5, Invitrogen). Western blots were quantified using a Typhoon Image Scanner and ImageQuant5. $p < .05$ indicates a significant difference from WT PLpro transfected cells and was determined using a student t test with Systat.

NFκB LUCIFERASE REPORTER ASSAY

HEK293 cells were plated in Cell-Bind™ 24-well plates (Corning) and transfected with 50, 100, or 150ng of pcDNA3.1 – PLpro plasmid, 50ng pNFκB-luc, and 25ng pRL-TK (Renilla control) per well in triplicate (Mirus LT-1). Cells were incubated for 12hrs, media removed, and fresh media containing TNFα (Roche) at a final concentration of 10ng/ml was added and incubated with cells for 4hrs. Cells were then lysed with passive lysis buffer and wells assayed for dual luciferase expression (Promega) by luminometer. $p < .05$ indicates a significant difference from mock transfected cells and was determined using a student t test with Systat.

SARS-COV REPLICON GROWTH AND PURIFICATION

DH10B cells (Invitrogen) were thawed on ice, and it is extremely important to keep all materials on ice to prevent arc during the electroportation. Add small volume (~1ul) DNA to 20ul cells in prechilled eppendorf tube, incubate for 15min. DNA is

electroporated in .1cm cuvette using recommended protocol for DH10B cells (2kV, 200 ohms, 25uF; 1 pulse). Make sure that the cells cover the entire length of the bottom of the electroporation chamber. After electroporation, add 1ml SOC media to the cells and transfer to a 15ml culture tube and shake at 255 rpm for 1hr. Plate 200ul of cells on Chl plate, incubate ON at 37C then pick colony and grow ON at 37C in similar conditions for MAXI-PREP. Cells are lysed according to Qiagen Large Construct kit (Qiagen).

SARS-COV REPLICON MUTAGENESIS

To incorporate the mutations created within the B clone of the infectious clone SARS-CoV plasmid set into the BAC replicon, bacterial artificial chromosome recombineering was used. A detailed protocol is available from the NCI (Warming, Costantino, Court, Jenkins, & Copeland, 2005) and is on file in the Wiethoff and Baker laboratories.

SARS-COV REPLICON N GENE QRT-PCR

HEK293T cells were transfected with Lipofectamine2000 (Invitrogen) at1ug pBAC-Rep per 12-well plate well and incubated for 24 or 48 hours. Cells were then lysed using RNA lysis buffer (Qiagen RNeasy kit). RNA was purified from cell lysates using the RNeasy kit and cDNA synthesized using a cDNA synthesis kit (SA Biosciences). cDNA was used for qPCR using primers for SARS-CoV N gene

subgenomic RNA (primers..) and RPL13 (host control) transcripts (BioRad). Data is normalized to RPL13. Performed in triplicate; n=2

CHAPTER III

RESULTS

ASSESSING ACTIVITY AND INHIBITION OF MERS-COV PAPAIN-LIKE AND 3C-LIKE PROTEASES USING LUCIFERASE-BASED BIOSENSORS

Cloning and expression of MERS-CoV papain-like protease (PLpro)

To determine if the predicted papain-like protease domain of MERS-CoV can be expressed in trans as a functional protease, the MERS-CoV PLpro domain was codon optimized, cryptic splice sites removed, synthesized and cloned into pcDNA3.1 for transient transfection studies (Figure 4). The synthetic MERS-CoV PLpro extends from amino acids 1485 to 1802 of ORF1a, with the addition of 2 amino acids at the N-terminus to allow efficient translation (methionine and alanine) and a V5 epitope tag on the c-terminus. A catalytic mutant MERS-CoV PLpro was generated by mutating the catalytic cysteine residue (amino acid 1594) to an alanine. To evaluate protease activity in cell culture, plasmid DNA expressing the wild-type or catalytic mutant forms of MERS-CoV PLpro were transfected into HEK293T cells along with a plasmid DNA expressing the SARS-CoV nsp2-3-GFP substrate. The nsp 2-3-GFP substrate is commonly used to assess the cleavage ability of transiently expressed CoV papain-like proteases (Frieman et al., 2009). We detected evidence of processing of the nsp2-3-GFP substrate in the

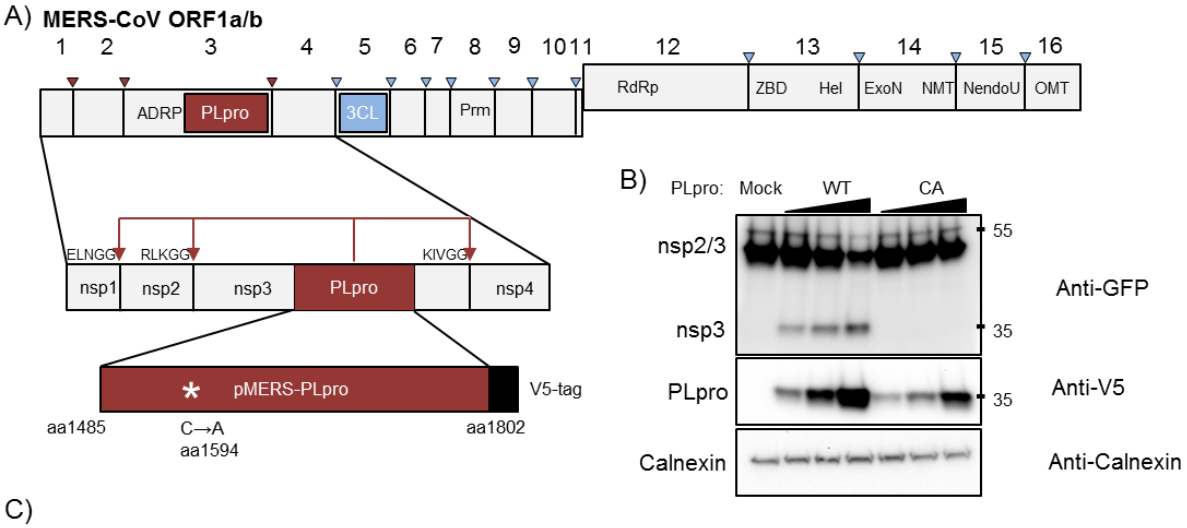

C)

```
MERS-1484 TIEVLVTVDGVNFRTVVLNNKNTYRSQLGCVFFNGADISDTIPDEKQNGHSLYLADNLTADETKALKELYGPVDPTFLHRF
HKU4-1526 NIEVLVTIDGVNFRTVILNDTTTFRKQLGATFYKGVDISDAFPTVKMGGESLFVADNLSESEKVVLKEYYGTSDVTFLQRY
HKU5-1560 NVDVLVTIDGVNFRTVVLNNTTTYRVQLGSVFYKGSDISDTIPTEKMSGEAVYLADNLSEAEKAVLSEVYGTADTAFLHRY
SARS-1541 -VKVFTTVDNTNLHTQLVDMSMTYGQQFGPTYLDGADVTKIKPHVNHEGKTFFVLPS-DDTLRSEAFEYYHTLDESFLGRY
 MHV-1609 KVDVLCTVDGVNFRSCCVAEGEVFGKTLGSVFCDGINVTKVRCSAIYKGKVFFQYSDLSEADLVAVKDAFGFDEPQLL-KY

                                  *
MERS YSLKAAVHGWKMVVCDKVRSLKLSDNNCYLNAVIMTLDLLKDIKFVIPALQHAFMKHKGGDSTDFIALIMAYGNCTFGAPDDASRL
HKU4 YSLQPLVQQWKFVVHDGVKSLKLSNYNCYINATIMMIDMLHDIKFVVPALQNAYLRYKGGDPYDFLALIMAYGDCTFDNPDDEAKL
HKU5 YSLLALVKKWKYTVHDGVKSLKLNSNNCYVNVTMLMLDMLKEIKFIVPALQAAYLKHKGGDSTEFIALIMAYGDCTYGEPDDASRL
SARS MSALNHTKKWKFPQVGGLTSIKWADNNCYLSSVLLALQQL-EVKFNAPALQEAYYRARAGDAANFCALILAYSNKTVGELGDVRET
 MHV YTMLGMCK-WSVVVCGNYFAFKQSNNNCYINVACLMLQHL-SLKFPKWQWQEAWNEFRSGKPLRFVSLVLAKGSFKFNEPSDSIDF

                                  # #                                 # #
MERS LHTVLAKAELCCSARMVWREWCNVCGIKDVVLQGLKACCYVGVQTVEDLRARMTYVCQCGGERHRQLVEHTTPWLLLSGTPNEKLV
HKU4 LHTLLAKAELTVSAKMVWREWCTVCGIRDIEYTGMRACVYAGVNSMEELQSVFNETCVCGSVKHRQLVEHSAPWLLVSGLNEVKV-
HKU5 LHTILSKAELTTQAKMVWRQWCNVCGVQDTTTTGLKACIYVGMNSLDELHATHEECCQCGDVRKRQLVEHNAPWLLLSGLNEAKVM
SARS MTHLLQHANLE-SAKRVLNVVCKHCGQKTTTLTGVEAVMYMGTLSYDNLKTGVSIPCVCGRDATQYLVQQESSFVMMSAPPAE---
 MHV MRVVLREADLS-GATCNLEFVCK-CGVKQEQRKGVDAVMHFGTLDKGDLVRGYNIACTCGS-KLVHCTQFNVPFLICSNTPE----

                  *                 *                                                  %Identity
MERS ---TTSTAPDFVAFNVFQGIETAVGHYVHARLKGGLILKFDSGTVSKTSDWKCKVTDVLFPGQKYSSDC-
HKU4 ---STSTDPIYRAFNVFQGVETSVGHYVHIRVKDGLFYKYDSGSLTKTSDMKCKMTSVWYPTVRYTADCN      59.87%
HKU5 TPTSQSAGPDYTAFNVFQGVETSVGHYLHVRVKDNLLYKYDSGSLSKTSDMKCKMTDVYYPKQRYS----      62.07%
SARS ---YKLQQGTFLCANEYTG-NYQCGHYTHITAKETL-YRIDGAHLTKMSEYKGPVTDVFYKETSYTTTI-      30.82%
 MHV ---GRKLPDDVVAANIFTG--GSVGHYTHVKCKPKYQL-YDACNVNKVSEAKGNFTDCLYLKNLK-----      28.57%
```

Figure 4. Activity of MERS-CoV PLpro. A) Schematic diagram of MERS-CoV ORF1ab with predicted PLpro cleavage sites indicated; pMERS-PLpro corresponds to amino acid residues 1485-1802. ADRP - ADP-ribose-1"-monophosphatase, PLpro – papain-like protease, 3CL – 3-chymotrypsin-like protease, Prm – Primase, RdRp – RNA dependent RNA polymerase, ZBD – zinc binding domain, Hel – Helicase, ExoN – exoribonuclease, NMT – N7 methyltransferase, NendoU – endoribonuclease, OMT – 2′ O-methyltransferase B) Trans-cleavage activity of MERS-PLpro. pMERS-PLpro and plasmid DNA expressing the SARS-CoV nsp2-3-GFP substrate were transfected into HEK293T cells, lysates harvested at 24 hrs post-transfection, and protein expression analyzed by western blotting with the indicated antibodies. C) Alignment of the PLpro domains from selected betacoronaviruses using ViPR software MUSCLE alignment algorithm; identical residues highlighted in orange, * = catalytic residues; # = zinc-binding cysteines; underlined residues in SARS-PLpro indicate flexible loop that binds specific inhibitors. Accession numbers: MERS-CoV aa1484-1802 (JX869059); BCoV-HKU4 aa1526-1844 (NC_009019); BCoV-HKU5 aa1560-1878 (NC_009020); SARS-CoV aa1541-1855 (AY278741); MHV aa1609-1911 (NC_001846). From (Kilianski et al., 2013)

presence of the catalytically active form of MERS-CoV PLpro, but not in the presence of the catalytic mutant MERS-CoV PLpro (Figure 4B). These data confirm that the putative papain-like protease domain located within nsp3 of the MERS-CoV genome indeed functions as a papain-like protease capable of cleaving LXGG-containing polyprotein substrates.

Comparison of MERS-CoV PLpro to other coronavirus PLPs by sequence homology

Alignment of the PLpro domain of MERS-CoV with the PLpro domains of other beta coronaviruses including SARS-CoV, bat coronaviruses HKU-4 and HKU-5 and the murine coronavirus, mouse hepatitis virus (MHV) revealed the conservation of the catalytic triad (Cys-1594, His-1759 and Asp-1774), and the four cysteine residues that comprise the zinc-binding fingers domain (Cys-1672, 1675, 1707 and 1709). However, the overall sequence identity between MERS-CoV PLpro and SARS-CoV PLpro is low, at only 30% amino acid identify (Fig. 4C). MERS-CoV PLpro also contains a canonical RLKGG site located between the catalytic histidine at position 1759 and the catalytic aspartic acid at position 1774. This cleavage site is unique to MERS-CoV, but due to the proximity to the catalytic residues, it is unlikely this cleavage site would be accessible for PLpro cleavage. However, further experiments must be done to address the functionality of this putative cleavage site.

Exploiting a biosensor assay to evaluate MERS-CoV PLpro activity

Developing assays to rapidly detect the activity of coronavirus proteases is a key step toward the goal of evaluating specific and pan-coronavirus protease inhibitors. Therefore, we developed a luciferase-based biosensor assay to measure protease activity within transfected cells. The system takes advantage of an inverted, circularly-permuted luciferase construct (pGlo-30F) separated by an engineered site corresponding to the canonical coronavirus PLpro cleavage recognition sequence, RLKGG (Figure 5A). The protease recognition site is limited in size, and because coronaviral proteases recognize short consensus sequences within the viral polyprotein, only five amino acids were engineered into the construct.

The five amino acid cleavage site contains the consensus LXGG motif necessary for recognition by coronaviral papain-like proteases, so this substrate should be recognized by MERS-CoV PLpro and other coronavirus PLPs (Barretto et al., 2005; Kanjanahaluethai, Jukneliene, & Baker, 2003; Ratia et al., 2006). The inactive form of luciferase is expressed within transfected cells and upon cleavage by a viral protease recognizing the engineered cleavage site, there is a conformational change into an active form of luciferase. Protease activity is measured quantitatively upon endpoint lysis of the cells and incubation with luciferase substrate reagents, or using a live-cell approach to examine kinetics of protease activity. This system is based on the pGloSensor caspase 3/7 system that has been used previously to evaluate protease activity in live cells and animal models, and similar systems that were used to evaluate viral protease activity in

an *in vitro* translation system (B. F. Binkowski et al., 2011; B. Binkowski, Fan, & Wood, 2009; Galban et al., 2013; Oka et al., 2011).

To determine if this system can be used to examine MERS-CoV PLpro activity, the MERS-CoV PLpro expression plasmid in addition to pGlo-RLKGG and renilla luciferase plasmids were transfected into HEK293T cells. The cells were lysed 20 hours post transfection and a dual-luciferase assay was performed on the lysates, assessing the firefly luciferase activity generated by cleavage of the pGlo-RLKGG substrate, and the renilla luciferase activity to control for transfection efficiency and toxicity. Wild-type MERS-CoV PLpro recognized and cleaved the pGlo-RLKGG substrate, resulting in luciferase induction of 10-fold above mock (Fig. 5B). A dose response with increasing amounts of protease expression leads to higher levels of luciferase activity. The catalytic mutant PLpro did not cleave the substrate and there is no detectable increase in luciferase activity above background. To evaluate MERS-CoV PLpro activity in real time, we exploited an assay based on detecting luciferase activity using a live cell readout. The firefly luciferase encoded in the pGlo reporter can be detected in live cells using a cell-permeable luciferase activator substrate, GloSensor, added to tissue culture media during incubation (B. Binkowski et al., 2009). HEK293T cells in a 96-well format were transfected with MERS-CoV PLpro (wild-type or catalytic mutant) and the pGlo-RLKGG expressing substrate. At 15 hours post-transfection, the cells were incubated in GloSensor reagent and monitored for luciferase activity using a luminometer. Cells expressing MERS-CoV PLpro showed a 10-fold increase over mock as early as 1 hour after GloSensor incubation, and luciferase activity continued to increase over the duration

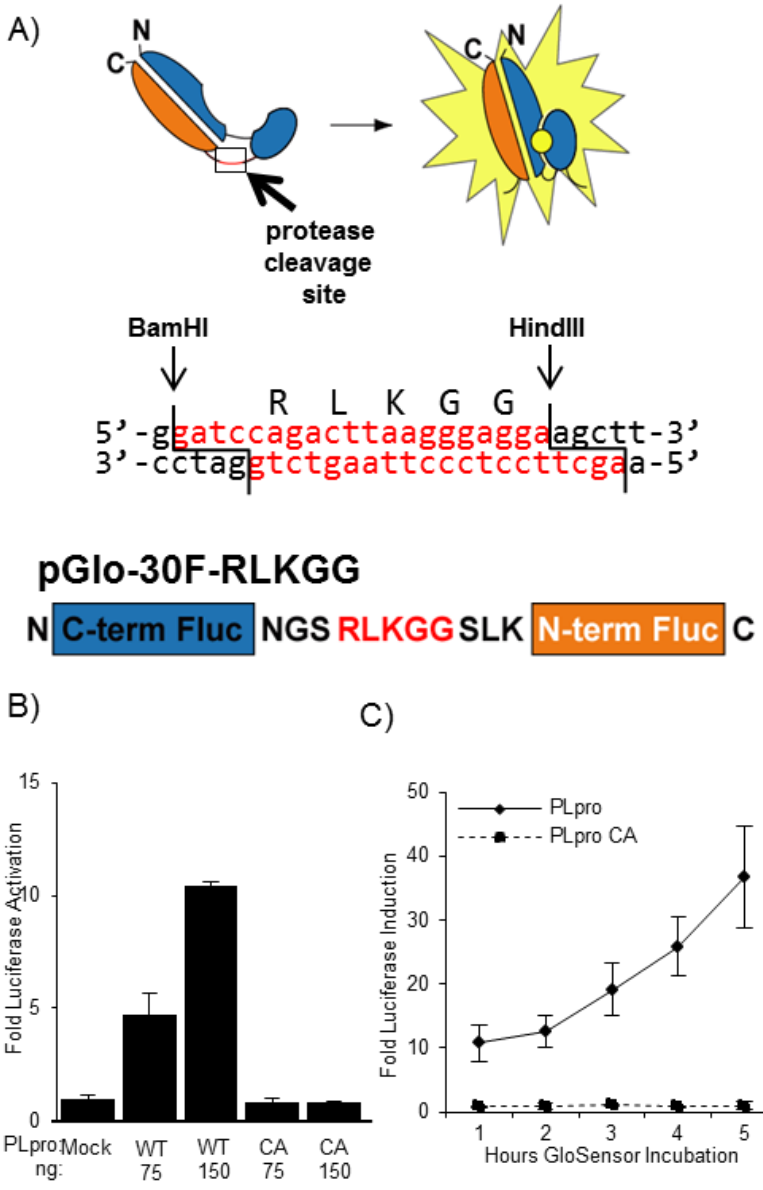

Figure 5. Biosensor assay detecting MERS-PLpro activity in cell culture. A) Diagram depicting the circularly permuted luciferase construct linked by the protease cleavage site, RLKGG, for assessing CoV PLpro activity. B) Expression of MERS-PLpro activates the biosensor. HEK293T cells are co-transfected with pGlo-30F-RLKGG and either pMERS-PLpro or pMERS-PLpro-CA. At 20 hours post transfection, cells were lysed and assayed using the dual luciferase assay. Experiment was performed in triplicate with error bars representing the standard deviation of the mean. C) Live-cell assay of MERS-PLpro activity. Cells are co-transfected with pGlo-30F-RLKGG and either pMERS-PLpro or pMERS-PLpro-CA. At 14 hrs post transfection, cells were incubated with Glosensor reagent and luminescence was read hourly. Experiment was performed in triplicate with error bars representing the standard deviation of the mean. From (Kilianski et al., 2013)

of the

of the experiment (Figure 5C). The catalytic mutant MERS-CoV PLpro expressing cells show no increase over the mock transfected cell background. The mock transfected cells gave an extremely low background in the live cell assay (only ~15 luciferase units) allowing for excellent sensitivity of protease activity.

Using the biosensor assay to evaluate a previously validated SARS-CoV PLpro inhibitor

Initial screening of the existing SARS-CoV PLpro inhibitor, benzodioxolane derivative 15g (BD-15g) against MERS-CoV PLpro revealed no significant inhibition (Figure 6) (Ghosh et al., 2010). One possible explanation for the specificity of BD-15g for SARS-CoV PLpro over MERS-CoV PLpro is that the inhibitor associates with a flexible loop that differs between SARS-CoV PLpro and MERS-CoV PLpro (underlined in Fig. 4B and shown in (Ratia et al., 2008)). This loop has been shown to close upon BD-15g binding to SARS-CoV PLpro, and the loop closure prevents the substrate from accessing the active site. Because there are differences in the amino acid sequence in the flexible loop, it is possible that BD-15g cannot bind the loop of MERS-CoV PLpro, leaving the active site accessible to substrate. Overall, these results validate the use of the biosensor assay, with a known positive control, for evaluating the specificity of small molecule inhibitors directed against CoV PLpros. Further work is needed to identify inhibitors that block MERS-CoV PLpro or are broadly inhibitory to CoV PLpros.

Cloning and expression of MERS-CoV 3C-like protease (3CLpro)

To evaluate MERS-CoV 3CLpro activity, a nsp4-5-6N-V5 codon optimized, splice-site removed DNA was synthesized encoding amino acids 2741 (N-terminus of nsp4) to 3561 (within nsp6) and cloned into the pcDNA3.1 expression vector and designated pMERS-pp3CLpro (for polyprotein-containing the nsp5/3CLpro domain). The 3CLpro cleavage site between nsp5/6 was either retained, resulting in expression of MERS-3CL protease that cleaves between nsp4/5 and nsp5/6 and is untagged; or with a mutated nsp5/6 cleavage site (pMERS-pp3CLpro-AA), resulting in a protease that cleaves the nsp4/5 site but should retain the V5-epitope tag on the nsp5-6N-V5 C-terminus (Fig. 7A). Currently there are no antibodies available to detect MERS-CoV 3CLpro, therefore we relied on detection of cleavage intermediates and epitope-tagged products to assess expression and activity.

To determine if the MERS-pp3CLpro expresses an active protease, we transfected plasmid DNA into HEK293T cells and harvested cell lysates at 20 hours post-transfection for western blot evaluation. As expected, the wild-type pp3CLpro protease cleaves the polyprotein, generating a nsp5-6N-V5 product that can be detected by western blotting (Figure 7B). As expected, this product is more abundant when the nsp5/6 cleavage site is mutated (compare WT-QS to WT-AA). The nsp6-V5 product is predicted to be only 5.6kD, and was undetectable by western blot in the WT-QS sample. The catalytic mutant pMERS-pp3CLpro-CA does not generate the cleavage product, instead generating

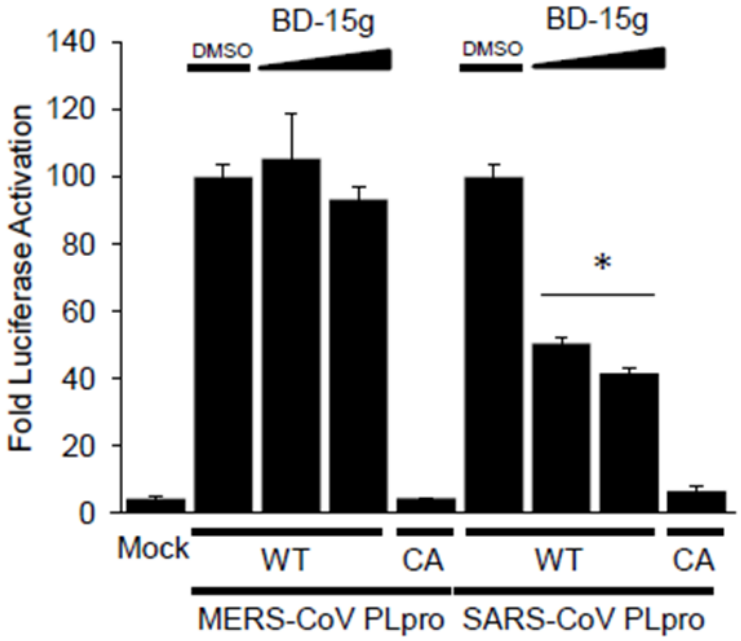

Figure 6. A previously identified SARS-CoV inhibitor does not inhibit MERS-CoV PLpro. HEK293T cells were transfected with the wild-type (WT) or catalytic mutant (CA) SARS-CoV PLpro or MERS-CoV PLpro and pGlo-RLKGG constructs for 13hrs then treated with 12.5 or 6.25uM BD-15g for 3hrs or with the equivalent volume of DMSO diluted in media. Cells were then lysed in PLB and assayed for dual luciferase activity. Experiment was performed in triplicate with error bars representing the standard deviation of the average. * = p<.005 as determined with student's T-test between DMSO and drug treated cells. From (Kilianski et al., 2013)

a polyprotein of the expected size and an aggregate that does not efficiently enter the SDS-PAGE gel, presumably because of the trans-membrane domain that remains in the polyprotein (Figure 7C, asterisk). These results demonstrate that activity of the MERS-CoV 3CLpro and the requirement for the catalytic cysteine residue Cys-3395.

Evaluation of MERS-CoV 3CLpro activity using the luciferase biosensor

To generate a biosensor 3CLpro substrate, we evaluated the predicted 3CLpro cleavage sites in MERS-CoV pp1ab and noted that the predicted cleavage sites for MERS-CoV 3CLpro conform to the consensus cleavage sites for previously characterized CoV 3CLpros (Chuck, Chow, Wan, & Wong, 2011). Oligonucleotides encoding the consensus cleavage site (VRLQ/S) were synthesized and ligated into pGlo-30F to generate the pGlo-30F-VRLQS biosensor for CoV 3CLpro activity (Figure 8A). Transfecting cells with plasmid DNA encoding pMERS-pp3CLpro, pGlo-VRLQS and renilla luciferase reporters and lysing the cells after 20 hours allowed for the evaluation of MERS 3CLpro activity. Recognition of the pGlo-VRQLS cleavage site engineered into the luciferase biosensor resulting in a 250-fold increase in luciferase activity above the level detected in mock transfected cells. We also noted a dose response of the reporter relative to increasing expression of 3CLpro (Figure 8B). The catalytic mutant 3CLpro did not generate significant luciferase activity above background. To determine if we could detect MERS 3CLpro activity in the live-cell kinetic assay, we transfected HEK293T cells with the protease and substrate plasmid DNAs and evaluated activity

using the Glosensor assay as described above. The wild-type 3CLpro construct led to a rapid activation of luciferase, with a 50-fold increase detectable only 1 hour after incubation with the substrate reagent (Figure 8C). This activation increased to levels of >300-fold above mock after 5 hours of incubation. The catalytic mutant 3CLpro was not capable of cleaving the luciferase biosensor, and there was no increase over mock in the live cell assay.

Identification of a SARS-CoV 3CLpro inhibitor that blocks MERS-CoV 3CLpro activity

The structure for the MERS-CoV 3CLpro in complex with a peptidomemetic inhibitor termed N3 was recently solved, and significant structural similarities between SARS-CoV and MERS-CoV 3CLpro were noted (Ren et al., 2013). These results suggest that broadly reactive 3CLpro inhibitors may block MERS 3CLpro activity. To test this hypothesis, the efficacy of antiviral drugs optimized for inhibition of SARS-CoV 3CLpro that were also shown to block murine coronavirus replication (Ghosh et al., 2008) were tested for the ability to block MERS-CoV 3CLpro activity. The antiviral inhibitor tested is a 5'-chloropyridine ester designated CE-5. Structural studies by Verschueren and colleagues showed that this class of benzotriazole esters acts as suicide inhibitors by covalently modifying the catalytic cysteine residue necessary for protease activity (Verschueren et al., 2008). This drug inhibits SARS-CoV 3CLpro activity *in vitro* in addition to inhibiting viral replication in SARS-CoV infected VeroE6 cells and

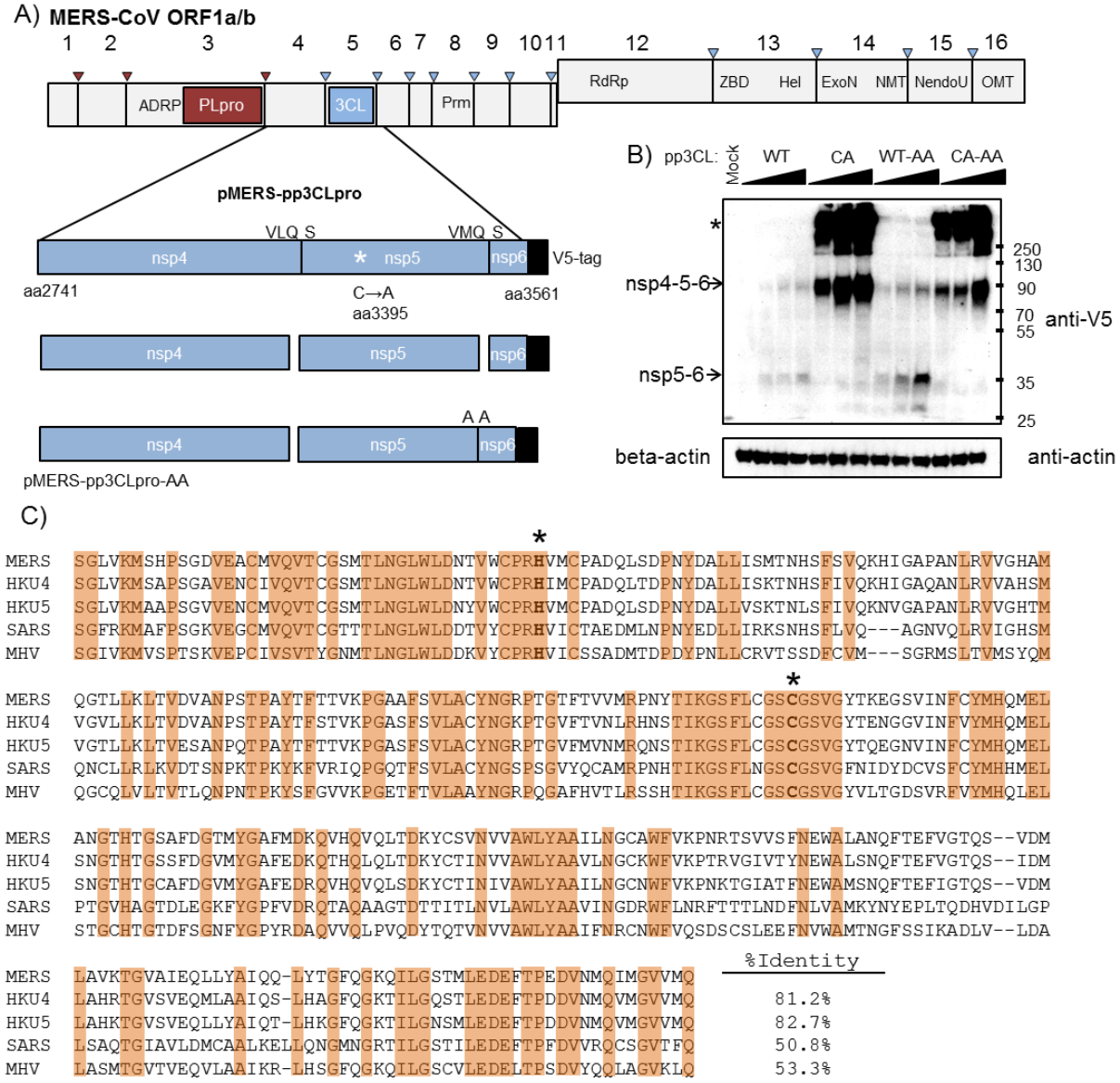

Figure 7. MERS-CoV 3CLpro activity. A) Schematic diagram of the 3CLpro domain and predicted cleavage sites in ORF1a/b. The region corresponding to the amino acid residues 2741-3561 spanning nsp4-5-6 was synthesized, cloned and designated pMERS-pp3CLpro; the catalytic cysteine was changed to alanine; and the nsp5/6 cleavage site Q/S was changed to AA. B) Expression and activity of 3CLpro. pMERS-pp3CLpro was transfected into HEK293T cells, lysates prepared at 20 hrs post-transfection and protein products analyzed by western blotting; anti-V5 detects polyprotein and processed products, anti-beta-actin was used to monitor protein loading. * = protein aggregates C) Alignment of 3CLpro regions from selected betacoronaviruses. Alignments were performed using ViPR software MUSCLE alignment algorithms. Sequence identity is indicated in orange; catalytic residues are boxed in red. * = catalytic residues. Accession numbers are listed in Fig. 1. From (Kilianski et al., 2013)

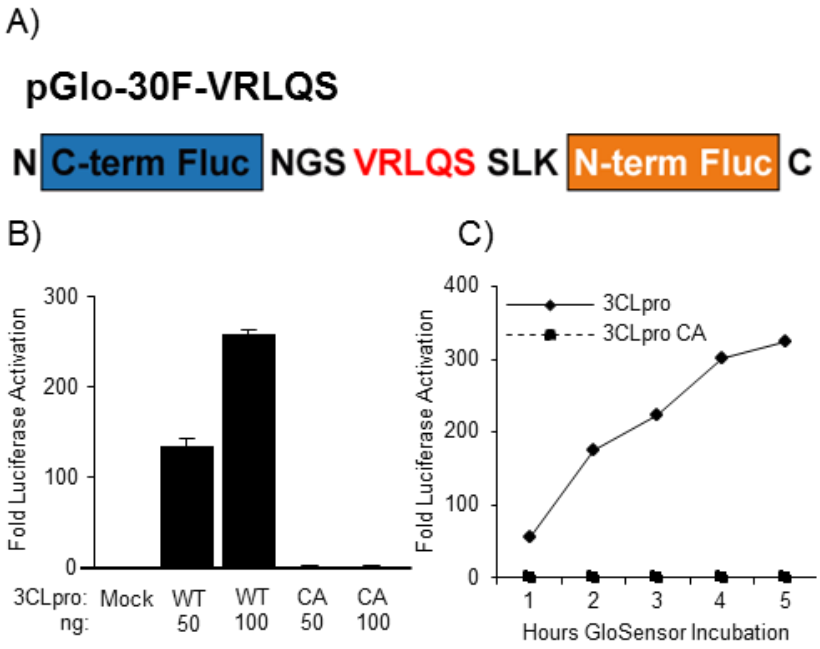

Figure 8. Biosensor assay detecting MERS-3CLpro activity in cell culture. A) Diagram depicting the circularly permuted luciferase construct linked by the protease cleavage site, VRLQS, for assessing CoV 3CLpro activity. B) Expression of MERS-pp3CLpro activates the biosensor. HEK-293T cells were co-transfected with pGlo-VRLQS and pMERS-pp3CLpro expressing either wild type or catalytic mutant (CA) of 3CLpro. At 20 hours after transfection, cells are lysed and assayed for luciferase activity. Experiment was performed in triplicate with error bars representing the standard deviation of the mean. C) MERS-CoV 3CLpro activity is detected in a live-cell assay. Cells were transfected as above and at 14 hours, incubated with GloSensor reagent. Luciferase activity is assayed in live cells every hour using a luminometer. Experiment was performed in triplicate with error bars representing the standard deviation of the mean. From (Kilianski et al., 2013)

m

murine coronavirus replication in DBT cells. Because of the structural similarity between SARS-CoV and MERS-CoV 3CLpro, it is possible that 3CLpro inhibitors like CE-5 will be cross-reactive and have inhibitory properties against MERS-CoV 3CLpro.

The efficacy of the SARS-CoV 3CLpro inhibitor CE-5 was tested against MERS-CoV 3CLpro using the pGlo-VRLQS biosensor assay. To determine if CE-5 inhibited MERS-CoV 3CLpro, cells were transfected with the pGlo-VRLQS construct, renilla luciferase plasmid, and MERS-CoV 3CLpro wild-type and catalytic mutant expression constructs. After 14 hours of transfection, CE-5 was added to the media at a final concentration of 50uM, 25uM, 12.5uM, and 6.25 uM and incubation continued for 6 hours. The cells were lysed and assayed for luciferase activity to measure the amount of reporter activity (Figure 9A). The luciferase levels measured for the MERS-CoV 3CLpro wild-type were set to 100%. The drug treatment inhibited the activity of MERS-CoV 3CLpro to 30% of DMSO-treated cells at a maximum dose of 50uM. The endpoint evaluation of CE-5 indicated an EC50 in cell culture of ~12.5uM.

To evaluate the real-time effects of CE-5 inhibition of MERS-CoV 3CLpro, the live cell protease cleavage assay described earlier was used. HEK293T cells transfected with pGlo-VRLQS, renilla luciferase plasmids and MERS-CoV 3CLpro were incubated in GloSensor reagent then measured for luminescence beginning at 14hrs post transfection. We noted the expected increase in luciferase activity in the DMSO-treated group, while the luciferase activity in the CE-5 treated cells declined sharply (Figure 9B). The efficacy of this previously reported SARS-CoV 3CLpro inhibitor to act on MERS-CoV

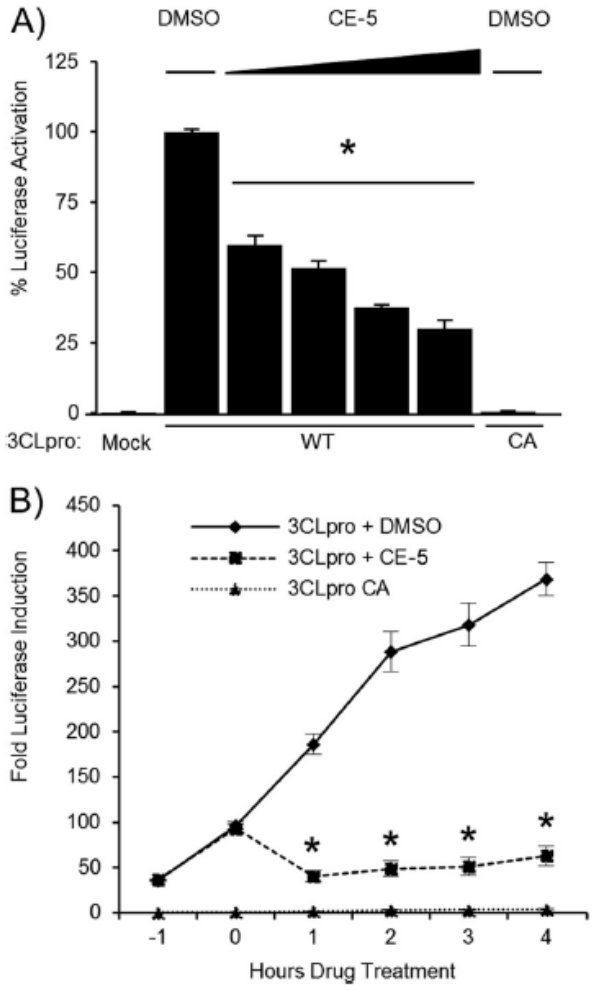

Figure 9. CoV 3CLpro inhibitor CE-5 blocks MERS-3CLpro activity. A) MERS-CoV 3CLpro activity is inhibited by CE-5. HEK293T cells were transfected with the wild-type (WT) or catalytic mutant (CA) pMERS-pp3CLpro and pGlo-VRLQS DNA, incubated for 14 hrs then treated with 6.25, 12.5, 25, or 50 uM CE-5 or DMSO for 6 hrs. Cells were lysed and assayed for dual luciferase activity. Experiment was performed in triplicate with error bars representing the standard deviation of the mean. * = p<.005 as determined with student's T-test between DMSO and drug treated cells. B) MERS-CoV 3CLpro activity is inhibited by CE-5 in the live cell assay. HEK293T cells were transfected with the wild-type (WT) or catalytic mutant (CA) pMERS-pp3CLpro and pGlo-VRLQS for 13 hours, incubated with GloSensor reagent for 1 hr, then treated with 50 uM CE-5 or DMSO. Luciferase activity was assayed in live cells every hour using a luminometer. Experiment was performed in triplicate with error bars representing the standard deviation of the mean. * = p<.005 as determined with student's T-test between DMSO and drug treated cells. From (Kilianski et al., 2013)

3CLpro is consistent with broad-spectrum inhibition. Further studies are needed to identify if other compounds with inhibitory activity against SARS-CoV proteases may have inhibitory affects against MERS-CoV.

EVALUATING PROTEASE ACTIVITY AND MULTIFUNCTIONALITY OF PUTATIVE PAPAIN-LIKE PROTEAES FROM ALPHA AND BETA CORONAVIRUSES

Identification, cloning, and expression of putative coronaviral PLPs

The adaption of the pGlo assay to papain-like proteases from SARS-CoV and MERS-CoV and to the 3CLpro from MERS-CoV demonstrated the ability of the assay to quantitatively evaluate the cleavage from a diverse range of coronaviral proteases. There has been some demonstration, including with MERS-CoV, of 3CLpro inhibitors having broad-spectrum activity. However, broad spectrum activity of inhibitors against the papain-like proteases has not been demonstrated. To aid in the development of broad-spectrum papain-like protease inhibitors, we sought to express, characterize, and use the pGlo assay to evaluate the activity and inhibition of a broad range of putative coronaviral papain-like proteases.

The PLpro or PLP2 from human coronaviruses OC43, HKU1, 229E and PLP2 from feline infectious peritonitis virus (FIPV) have never been expressed or characterized, much less been evaluated for inhibition by specific antiviral compounds. To accomplish this, the putative PLP2 domains from the above viruses were synthesized based on the starting point of a predicted UBL domain (a domain upstream that is present

in SARS-CoV PLpro and MHV PLP2 crystal structures unpublished data from (Ratia et al., 2006), and extended until about 40 amino acids after the catalytic aspartic acid residue. These putative domains were cloned into pcDNA3.1 and catalytic mutants were created by mutating the cysteine residue of the catalytic triad to alanine. The mutants were assessed for their ability to cleave the synthetic SARS-CoV nsp2-3-GFP construct, cleave ubiquitin, cleave ISG15, and activate the pGlo substrate in transfected cells.

The mutants were first characterized with the nsp2-3-GFP trans-cleavage assay used to determine if the MERS-CoV PLpro domain we synthesized was active (Figure 10). Each PLP was transfected at 500ng with 25ng of nsp2-3-GFP per well and incubated for 20 hours. Cell lysates were then immunoblotted for GFP, calnexin (loading control), and V5. The SARS-CoV PLpro, MERS-CoV PLpro, and HCoV-NL63 PLP2 all cleaved the polyprotein as reporter previously, while the catalytic mutants could not (Figure 10). The putative PLP domains for HCoV-OC43, HCoV-HKU1, HCoV-299E, and FIPV had varying levels of nsp2-3-GFP cleavage, and the hypothesized catalytic residues targeted for mutagenesis all disrupted protease activity. While the difference in nsp2-3-GFP cleavage was expected, because the substrate is of SARS-CoV origin, the expression differences were unexpected. All of the molecular weights were predicted to about the same, yet there were size and expression level differences seen especially with HCoV-229E PLP2 and FIPV PLP2. HCoV-299E PLP2 does not display a sharp band when examined by western blot, and FIPV is a much stronger band and of a considerably

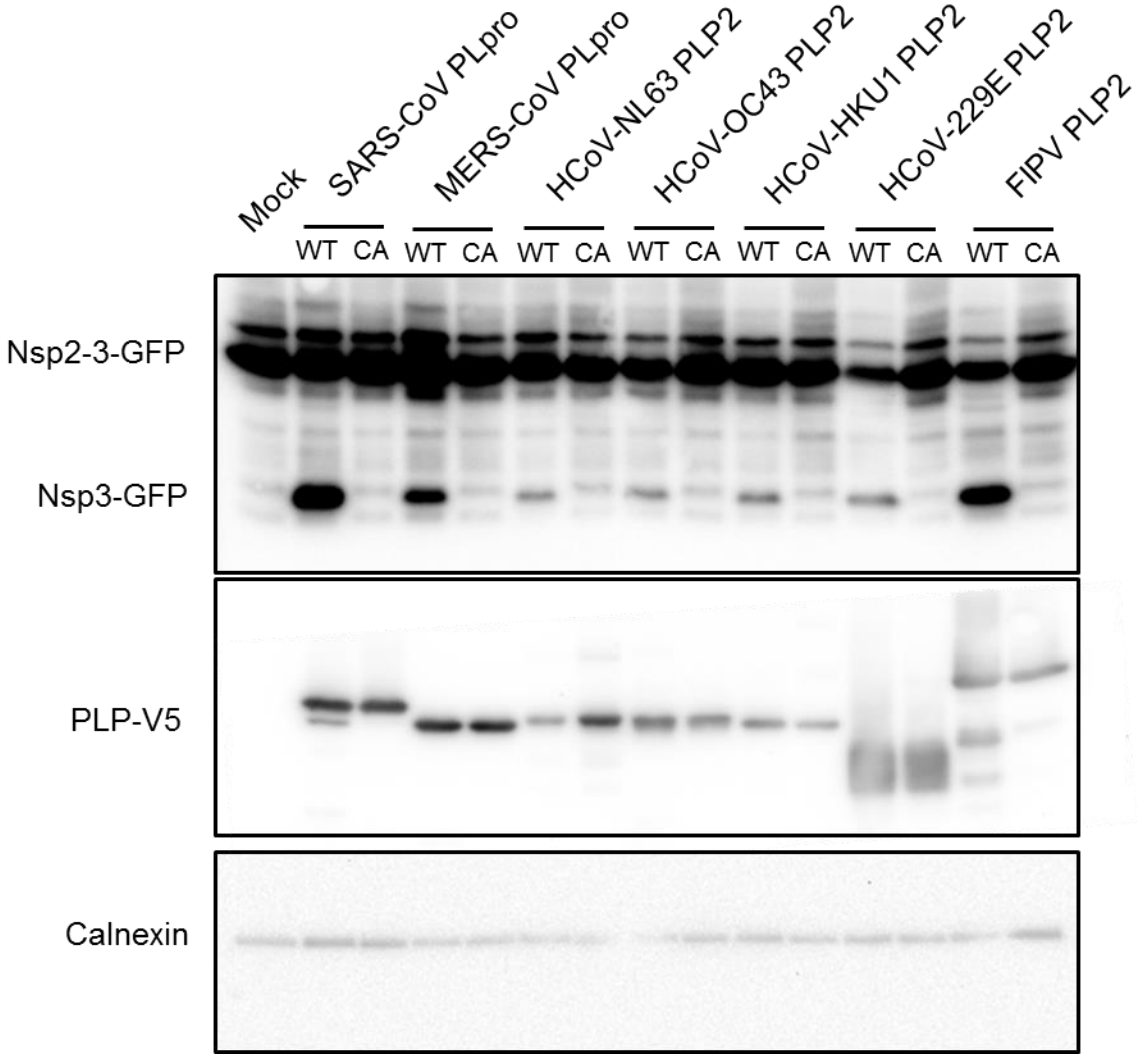

Figure 10. Trans-cleavage ability of putative papain-like proteases from alpha and beta coronaviruses. HEK293T cells were transfected with constructs expressing nsp2-3-GFP and SARS-CoV PLpro-V5. Lysates were immunoblotted with anti-GFP, anti-calnexin, and anti-V5.

higher molecular weight.

Putative CoV PLPs possess deubiquitinating activity and deISGylating activity

The trans-cleavage assay showed that each of the putative PLP domains encode functional proteases that recognize the LXGG motif characteristic of coronavirus papain-like proteases. To determine if these PLPs also possess the multifunctionality seen in other coronaviruses, transfection experiments were performed to assess the deubiquitinating and deISGylating activity of these PLPs within the context of the cell. The deubiquitinating activity of coronavirus papain-like proteases can be analyzed by transfecting the protease with a tagged ubiquitin construct into 293T cells. If the PLP acts as a deubiquitinating enzyme, then the levels of host cell proteins conjugated to ubiquitin will be less than mock transfected cells or cells transfected with the catalytic mutant PLPs when cell lysates are analyzed by western blot. Fellow graduate student Anna Mielech performed this experiment, and demonstrated that all of the putative PLP domains possess deubiquitinating activity (Figure 11A). Similar to the trans-cleavage activity, the relative levels of DUB activity varied, with some PLPs acting as more efficient DUBs (SARS, NL63, FIPV) and some only displaying DUB activity when transfected at higher doses (OC43, HKU1, 229E). Each of the catalytic mutants was unable to deconjugate ubiquitin from the host cell proteins and the amount transfected

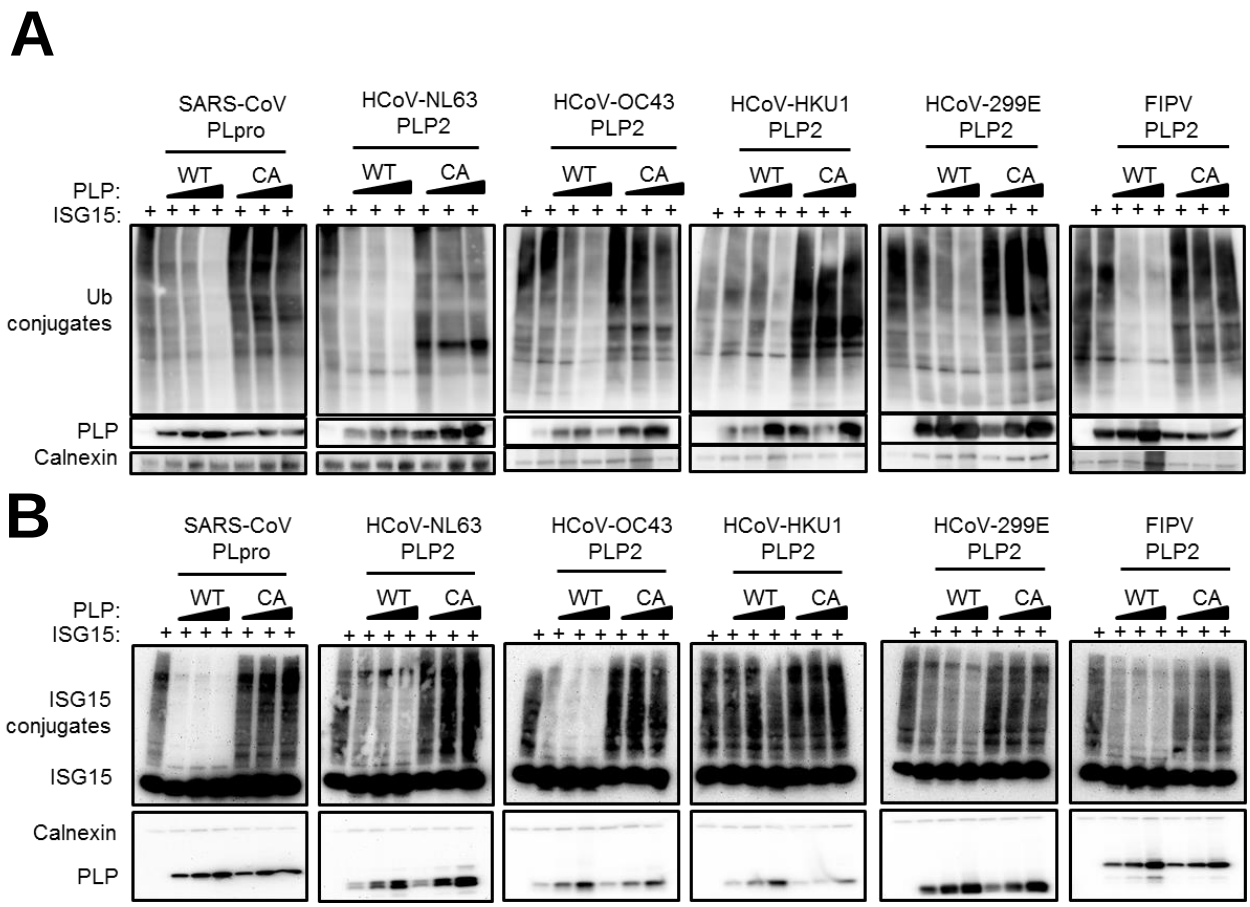

Figure 11. Deubiquitinating and deISGylating activity of putative papain-like proteases from alpha and beta coronaviruses. 293T cells in 12-well Cell-Bind plate (Corning) are transfected (LT1, Mirus) with 300ng FLAG-Ub and either 125ng, 250ng, or 500ng of pcDNA3.1-SARS-PLpro per well. Cells were incubated for 18hrs then lysed with IkBα lysis buffer Lysates were separated by SDS-PAGE on a 4-20% gradient gel (BioRad). Gel was transferred to PVDF using semi-dry apparatus (BioRad) and immunoblotted with anti-FLAG (Sigma), anti-V5 (Invitrogen), and anti-calnexin (BD). B) HEK293T cells in 12-well plates were transfected with 10, 25, 50, and 100ng of pCDNA-MERS-PLpro wild type or catalytic mutant and 250ng ISG15-myc, 125ng UbcH8, 125ng Ube1L, and 125ng Herc5. 20 hours post transfection cells were lysed with lysis buffer. Proteins were separated by SDS-PAGE and transferred to PVDF membrane using a semi-dry transfer apparatus (BioRad).

had no effect on the overall ubiquitin profile of the transfected cells.

To determine if these proteases have deISGylating activity in addition to deubiquitinating activity, a transfection-based deISGylating assay was performed. Cells were transfected with a myc tagged ISG15, the ISG15 conjugation machinery (Ube1L, UbcH8, Herc5), and the PLPs characterized earlier in increasing doses. Varying levels of deISGylating activity were seen among the PLPs, with only HCoV-HKU1 PLP2 showing very limited, if any, deISGylating activity (Figure 11B). Interestingly, there didn't seem to be a clear correlation between the proteases ability to cleave ubiquitin substrates from host cell proteins and their ability to cleave ISG15. For example, HCoV-OC43 PLP2 has some deubiquitinating activity, but it's only discernable at higher doses. However, OC43 PLP2 has very efficient deISGylating activity, with deconjugation seen even at the lower transfected (125ng) doses. Despite these differences, all of the putative domains tested exhibit both deubiquitinating and deISGylating activity (with the possible exception of HCoV-HKU1 PLP2).

The usefulness of the pGlo system with regards to antiviral screening was demonstrated with the identification of the first small molecule inhibitor that had inhibitory effects on the 3C-like protease of MERS-CoV (Figure 12). A necessary goal in coronavirus research is develop inhibitors that are both broad-spectrum and FDA approved for use in human infections, and currently none of these goals have been met. To aid in the search for broad spectrum inhibitors, it's possible the pGlo system could be used to determine if small molecules have inhibitory effects against multiple coronavirus

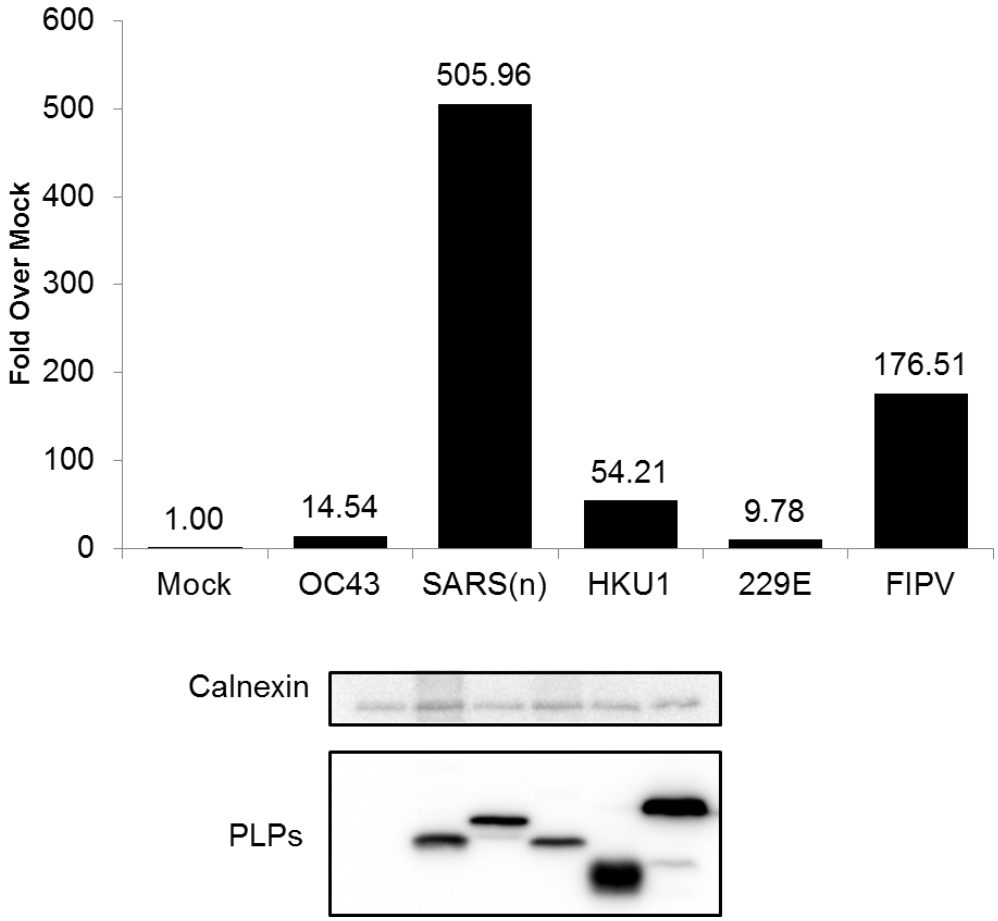

Figure 12. pGlo-RLKGG activation by the putative papain-like proteases from alpha and beta coronaviruses. Cells are co-transfected with pGlo-30F-RLKGG and the noted papain-like protease. At 14 hrs post transfection, cells were incubated with Glosensor reagent and luminescence was read hourly. Results above are of the 5hr timepoint after GloSensor addition.

proteases in a cell-based system. The previously putative proteases characterized above were transfected into cells with the pGlo-RLKGG construct and assayed using the live-cell protocol. After five hours of live transfected cells being incubated with the GloSensor substrate, all of the proteases activated the pGlo substrate to some degree (Figure 12). These levels of activation, ranging from 10-500 fold above mock, correlate very well to the trans-cleavage assay, with SARS-CoV PLpro and FIPV PLP2 showing the greatest activation while the PLPs from HCoV-OC43, HCoV-229E, and HCoV-HKU1 all had lower levels of pGlo cleavage. The ability of each protease to recognize and cleave the pGlo-RLKGG substrate is an excellent start towards implementing these cell-based approaches to more rapidly and accurately identify potential broad-spectrum coronavirus protease inhibitors.

SEPARATING THE MULTIFUNCTIONALITY OF SARS-COV PLPRO

Residues within the ridge region of SARS-CoV PLpro are important for NFκB antagonism

Previous *in vitro* experiments determined that specific residues within the ridge region of SARS-CoV PLpro are required for WT levels of ubiquitin and ISG15 cleavage but not critical for viral substrate recognition (Ratia et al., 2014). As mentioned previously, many cellular pathways require ubiquitination for signal transduction. Particularly important to these experiments is the NFκB pathway, which requires K48-linked ubiquitination of the inhibitor IkBα for its degradation and the release of NFκB

inhibition. SARS-CoV PLpro is a known inhibitor of the NFκB pathway (Clementz et al., 2010; Frieman et al., 2009), however the mechanism is unknown. We hypothesized that SARS-CoV PLpro inhibits NFκB activation at the step of IkBα degradation by cleaving the K48-linked ubiquitin that targets IkBα for degradation. This degradation frees NFκB from inhibition, allowing it to access the nucleus and activate transcription.

To first determine if PLpro inhibits the NFκB pathway at the level of IkBα, levels of phosphorylated IkBα were measured by western blot in cells expressing WT PLpro. If PLpro inhibits the NFκB pathway upstream of IkBα, then the phosphorylation (which is required for the ubiquitination and subsequent degradation of IkBα) of IkBα will also be blocked. When cells are stimulated with TNFα and lysed, the levels of phosphorylated IkBα rapidly rise (Figure 13). This phosphorylation precedes IkBα degradation, which happens after 15min of stimulation. When cells are transfected with WT PLpro, the phosphorylation of IkBα is unchanged, indicating that the presence of PLpro does not affect the upstream elements of the NFκB pathway. However, IkBα does not get normally degraded in response to TNFα in the presence of PLpro, suggesting that PLpro is having a direct effect on the degradation of IkBα.

With the knowledge that SARS-CoV PLpro NFκB antagonism occurs at IkBα, a role for PLpro deubiquitinating activity on the NFκB pathway could be answered using PLpro mutants that were deficient in DUB activity (Ratia et al., 2014). If SARS-CoV PLpro uses its deubiquitinating activity to inhibit the NFκB pathway, there will be a loss of IkBα stabilization in response to stimuli in cells transfected with PLpro

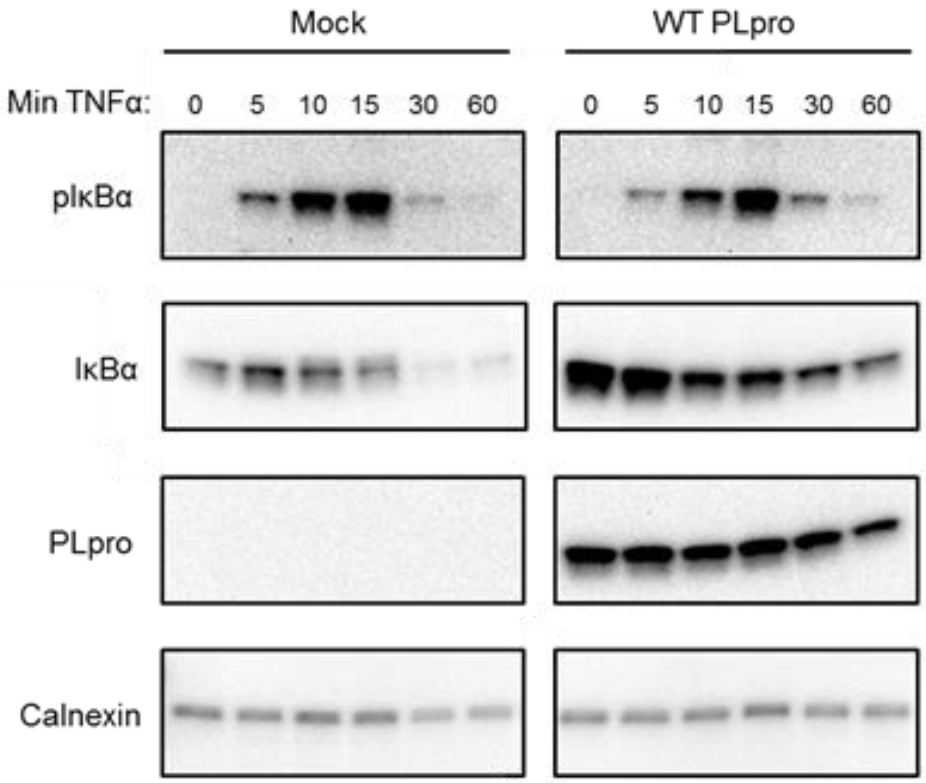

Figure 13. PLpro does not block phosphorylation of IκBα. HEK293 cells were transfected with wild-type PLpro. After 16hrs incubation, cells were stimulated with TNFα (20ng/ml) for indicated times. Cells were then lysed using an IkBα lysis buffer and lysates were analyzed by 10% SDS-PAGE and western blotted.

DUB mutants. To test this hypothesis, we will utilize a tagged version of IkBα to determine the turnover in cells transfected with WT or mutant PLpro. If NFκB antagonism is due to cleaving K48-Ub from IkBα, then PLpro mutants will lose the ability to prevent the turnover of IkBα in response to stimuli. 293T cells were transfected with plasmid DNA encoding IkBα-HA and either PLpro WT or the indicated PLpro mutant. At 16 hours post transfection, cells were treated with TNFα to induce ubiquitination and degradation in IkBα. The protein levels of IkBα and PLpro were monitored by western blotting (Figure 14A). We found that IkBα was 2-fold more abundant in cells expressing PLpro. In addition, there was no detectable degradation of IkBα in the presence of PLpro after treatment with TNFα. In contrast, IkBα response to TNFα treatment was the same as mock in the presence of either the catalytic mutant of PLpro (C112A) or F70S (Figure 14A and B) and the combination mutants (Figure 14C).

These data suggested that PLpro K48-Ub cleavage activity was responsible for NFκB antagonism. However, these mutants could also be protease impaired, which would cloud the NFκB data interpretation as well as prevent the reverse engineering of these mutations into infectious virus (PLpro catalytic activity is required for viral polyprotein cleavage). To determine if the PLpro mutants retained protease activity, we evaluated them in a trans-cleavage assay and found F70S and the other mutants retained the ability to process the nsp2-3 substrate (Figure 15). These results are consistent with the in vitro findings and indicate that the PLpro mutants are proteolytically active but impaired for NFκB antagonism.

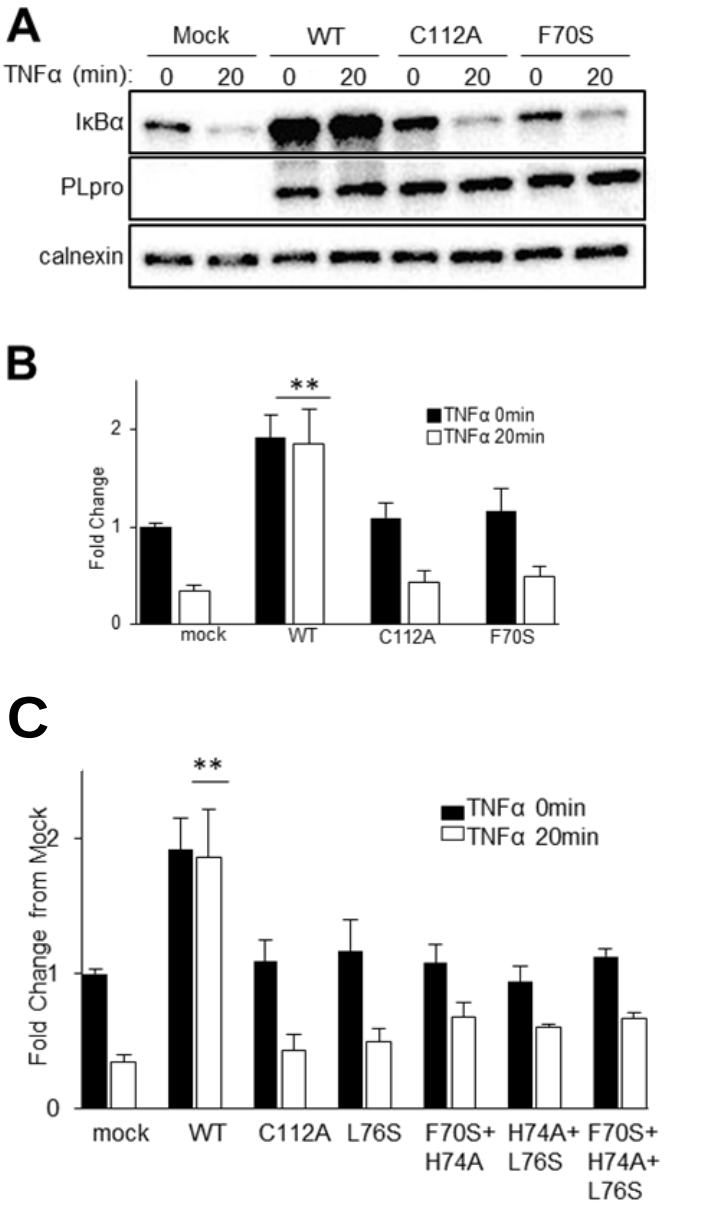

Figure 14. NF-κB activation is affected by wild-type but not DUB mutants of PLpro. (A) HEK293 cells were transfected with IkBα-HA and the indicated PLpro. After 16hrs incubation, cells were stimulated with TNFα (20ng/ml) for 20 minutes. Cells were then lysed using an IkBα lysis buffer and lysates were analyzed by 10% SDS-PAGE and western blotted. (B)(C) Quantification of IκBα using Fluorchem E System and AlphaView software (Protein Simple). ** = The levels of IkB-HA were significantly increased in the presence of WT PLpro compared to mock, C112A, and F70S ($p<.05$) by mixed ANOVA and there was no decrease after TNFα treatment ($p=.675$) by Dunnet t-test. From (Ratia et al., 2014)

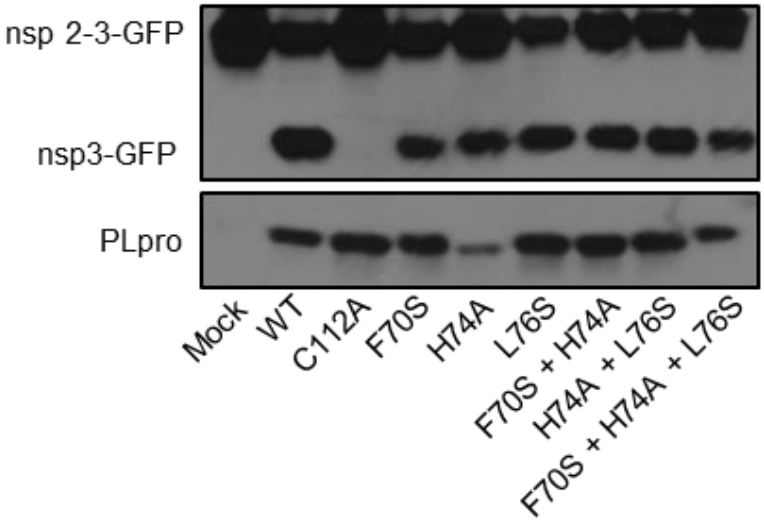

Figure 15. PLpro ridge mutants retain nsp2-3 cleavage ability. 293HEK cells were transfected with constructs expressing nsp2-3-GFP and SARS-CoV PLpro-V5 wild type, catalytic mutant (C112A) or ridge mutants. Cells were incubated for 24 hours at 37°C and then lysed with lysis buffer A. Lysates were run on 10% SDS-PAGE and Western blot was performed using anti-GFP and anti-V5. From (Ratia et al., 2014)

To determine if the proteolytic activity or the DUB activity was important for antagonism of the NF-kB mediated activation of transcription, we evaluated PLpro WT, catalytic mutant, and F70S PLpro in a dual-luciferase reporter assay containing an NFκB reporter fused to firefly luciferase. In mock transfected cells, the NFκB-dependent reporter is potently activated by the addition of media containing TNFα. This activation is antagonized when cells are transfected with wild-type PLpro in a dose-dependent manner. In contrast, the PLpro catalytic mutant and F70S mutant are unable to antagonize this pathway (Figure 16A). There were some cases of intermediate phenotypes with the single and combination mutants (L76S), but in general all of the ridge mutations had some effect on PLpro NFκB antagonism (Figure 16B). These reporter results, combined with the IkBα degradation assay, indicate that PLpro deubiquitinating activity is required for the antagonism of the NFκB pathway, an important mediator of the innate immune system in response to a viral infection.

The ridge mutations cause SARS-CoV PLpro to lose its innate immune antagonism properties, however the effect of these mutations on general deubiquitinating activity within transfected cells is unknown. SARS-CoV PLpro has been shown to have broad deubiquitinating activity in transfected cells, so mutants designed to be deficient in K48-Ub binding should have decreased DUB profiles when analyzed by immunoblot. To determine if PLpro ridge mutants were deficient in general DUB activity, 293T cells were transfected with PLpro and FLAG-Ub and the transfected cells were lysed and the ubiquitination pattern of host cell proteins were analyzed (Figure 17). Wild-type PLpro cleaved ubiquitin from a broad range of host cell substrates in a dose-dependent manner.

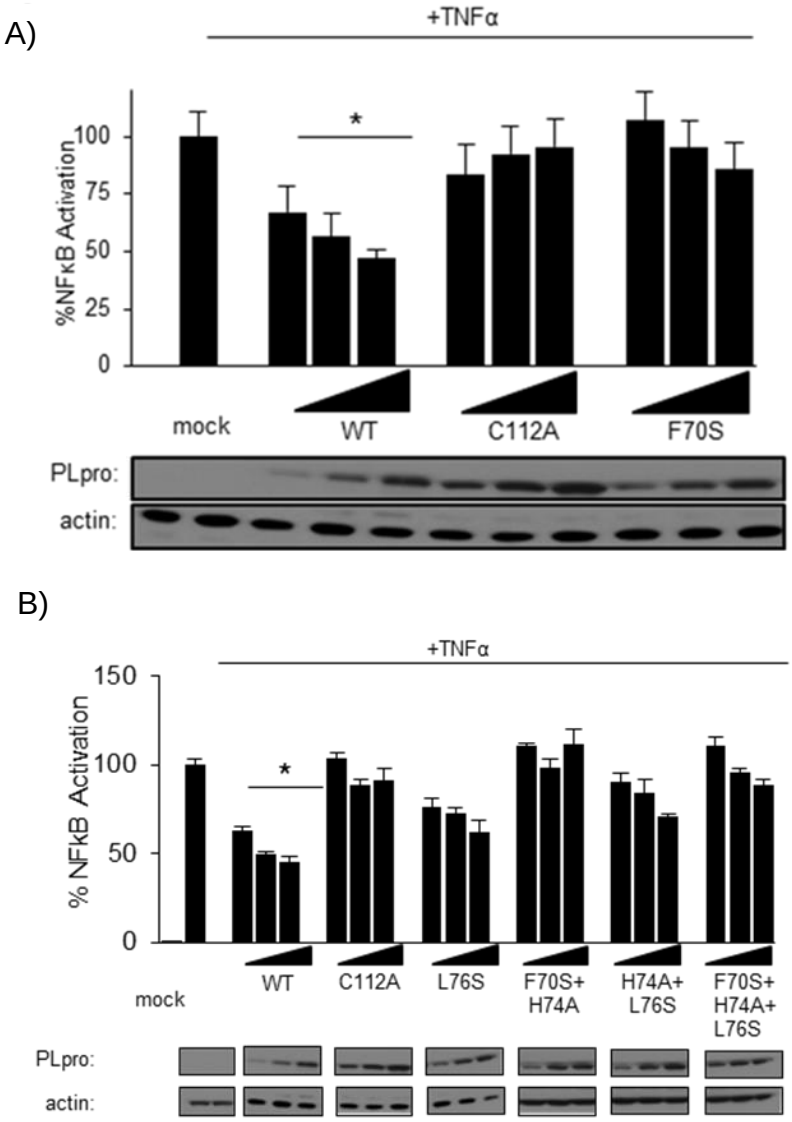

Figure 16. PLpro ridge mutants lose NFκB reporter antagonism. A) B) 293HEK cells were transfected with a construct containing a firefly luciferase reporter driven by an NFκB dependent promoter and a Renilla luciferase under control of a constitutive promoter. After 12hrs, TNFα was added to a final concentration of 10ng/mL and the cells were incubated for an additional 4hrs. Cells were lysed in passive lysis buffer and 25ul of lysate was used in Promega's Dual Luciferase Reporter Assay. Results are normalized to induction of NFκB reporter activity by TNFα. Panels below are western blots of the lysates using anti-V5 for detection of PLpro and anti-actin as a protein loading control. Experiments were performed in triplicate and repeated twice. * = $p < .05$ statistical difference from mock transfected cells by student t-test. From (Ratia et al., 2014)

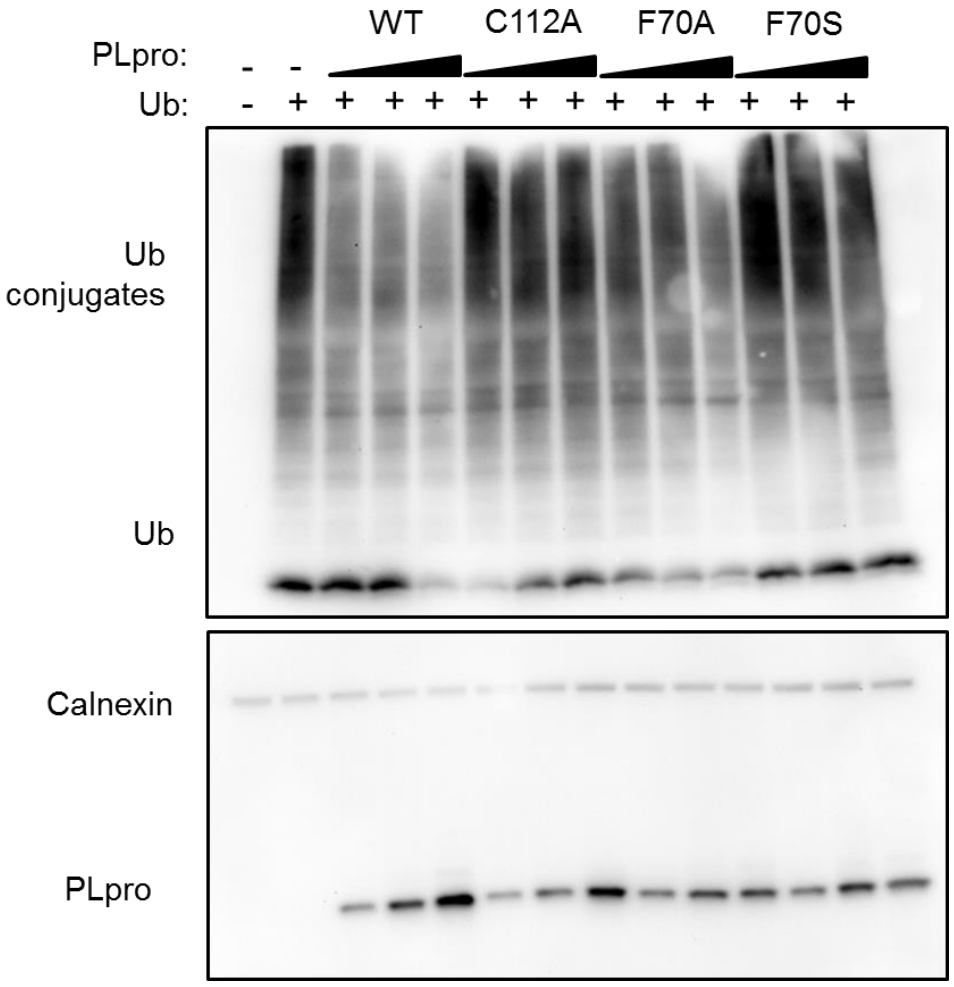

Figure 17. PLpro ridge mutants at residue F70 are deficient in ubiquitin cleavage . HEK293T cells were transfected with expression plasmids encoding FLAG-Ub and the indicated PLpro. 18hrs post transfection, cells were lysed and immunoblotted for FLAG-Ub, calnexin, and PLpro-V5. From (Ratia et al., 2014)

The catalytic mutant C112A was unable to cleave ubiquitin while the ridge mutants F70A and F70S were deficient in ubiquitin cleavage. These data agree with the previous results from the NFκB pathway analysis and further demonstrate that the PLpro ridge mutants are deficient in ubiquitin binding and cleavage.

The importance of the phenylalanine at position 70 was evident in the above experiment, where mutations that changed both the polarity (nonpolar to polar F70S) and the size of the amino acid side chain (large to small F70A) had noticeable effects on the deubiquitinating activity of SARS-CoV PLpro. van Karsteren et al achieved the separation of DUB and protease activity by only making size alterations to the amino acid side chains important for ubiquitin interaction in the viral OTU domain of EAV PLP2 (van Kasteren et al., 2013). These viruses were also replication competent, and there was no need (or viruses were not viable) for making polarity changes to the side chains of interaction amino acids. Because of the effects of F70S in innate immune antagonism experiments, and because of the need to reverse engineer these mutations into infectious virus, it was important to determine if a mutation which could have less potential side effects (F70A) would have a similar loss in NFκB antagonism. To determine this, the IkBα degradation and NFκB reporter assays were run side-by-side with F70A and F70S. Additionally, F70A and F70S were also tested together for their ability to cleave the nsp2-3 substrate. F70A has a similar phenotype to F70S, as it lost the ability to stabilize IkBα (Figure 18A), exhibited a loss of NFκB antagonism (Figure 18B), but still retained 18the ability to cleave the nsp2-3 synthetic viral substrate (Figure 18C). Mutations at the F70 position affect the ability of SARS-CoV PLpro to efficiently cleave ubiquitin while

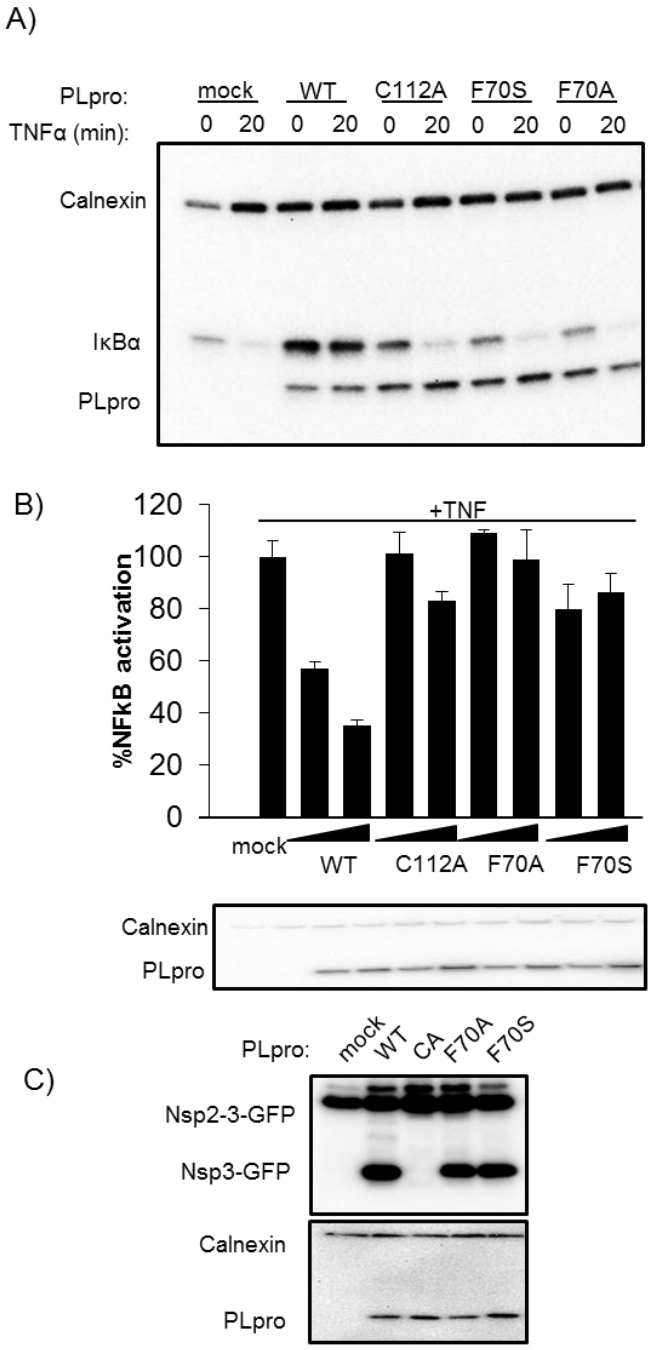

Figure 18. NF-κB antagonism, but not protease activity, is affected by PLpro F70 mutants. (A) HEK293 cells were transfected with IkBα-HA and the indicated PLpro. After 16hrs incubation, cells were stimulated with TNFα (20ng/ml). Lysates were analyzed by 10% SDS-PAGE and immunoblotted for anti-HA, anti-calnexin, and anti-V5. (B) 293HEK cells were transfected with NFκB-reporter and Renilla luciferase control constructs and the indicated PLpro. After 12hrs, TNFα was added to a final concentration of 10ng/mL and the cells were incubated for an additional 4hrs. Results are normalized to induction of NFκB reporter activity by TNFα. Panels below are western blots of the lysates using anti-V5 for detection of PLpro and anti-actin as a protein loading control. Experiments were performed in triplicate and repeated twice. * = $p < .05$ statistical difference from mock transfected cells by student t-test (C) HEK293T cells were transfected with constructs expressing nsp2-3-GFP and SARS-CoV PLpro-V5 . Lysates were immunoblotted with anti-GFP, anti-calnexin, and anti-V5. From (Ratia et al., 2014)

also being deficient in innate immune antagonism. Importantly, both mutations that affect the size or charge of the amino acid side chain responsible for ubiquitin interaction have effects on PLpro function, which allows for more flexibility when constructing infectious virus using reverse genetics.

Replication differences in SARS-CoV replicons containing F70S and F70A mutations

After showing that mutations within the ridge of SARS-CoV PLpro had effects on innate immune antagonism, the next step was to determine if these mutations had any effect on the replication of SARS-CoV. To do this in the BSL2 laboratories at Loyola, the replicon system for SARS-CoV was obtained from the laboratories of Luis Enjuanes (Almazan et al., 2006). The SARS-CoV replicon is based on the fact that the replication cycle of coronaviruses can occur by transcribing the viral RNA encoding ORF1ab and by providing the N gene needed to encapsulate the viral RNA, and replication of the viral genome does not require any of the structural genes that are necessary for the formation of viral particles. ORF1ab contains the replicase genes needed for the creation of viral replication sites on double membrane vesicles (Figure 1) and the RdRp which is necessary to replicate the genome and produce subgenomic messenger RNAs. By transfecting a bacterial artificial chromosome (BAC) encoding ORF1ab and the N gene produced by a subgenomic mRNA after replication begins, it was determined that replication of the vRNA and production of N gene RNA occurred in transfected cells

(Almazan et al., 2006). By engineering the F70S and F70A mutations into the replicon BAC using recombineering, the replication competency of SARS-CoV containing these ridge mutations can be assessed in a BSL2 laboratory without creating infectious virus.

After creating both F70S and F70A replicons using recombineering (methods), they were transfected into 293T cells in addition to the WT replicon. Their replication levels were compared after 24 and 48hrs by lysing the cells, isolating RNA, making cDNA, then using qPCR to quantitate the levels of replicon produced N gene present in the transfected cells (Figure 19). The wild-type SARS-CoV replicon efficiently produced N gene over a period of two days. The F70S replicon failed to initiate efficient replication, and after 48 hours the levels of replication were low and did not increase from 24 hours. Surprisingly, the replicon containing the F70A mutation replicated far more successfully, only slightly lagging behind WT replication after 24 hours and catching up to the level of replication seen at 48 hours in the WT. The exact reproducibility of this experiment was not great; however, the trends represented in this experiment were reflective of the reproduced experiments.

The hydrophobic pocket of SARS-CoV PLpro is important for interaction with ubiquitin

In addition to the ridge region of SARS-CoV PLpro, the crystal structure of PLpro and ubiquitin aldehyde revealed a hydrophobic pocket closer to the active site that interacts with the hydrophobic Ile44 patch on ubiquitin (Figure 3). The mutations within

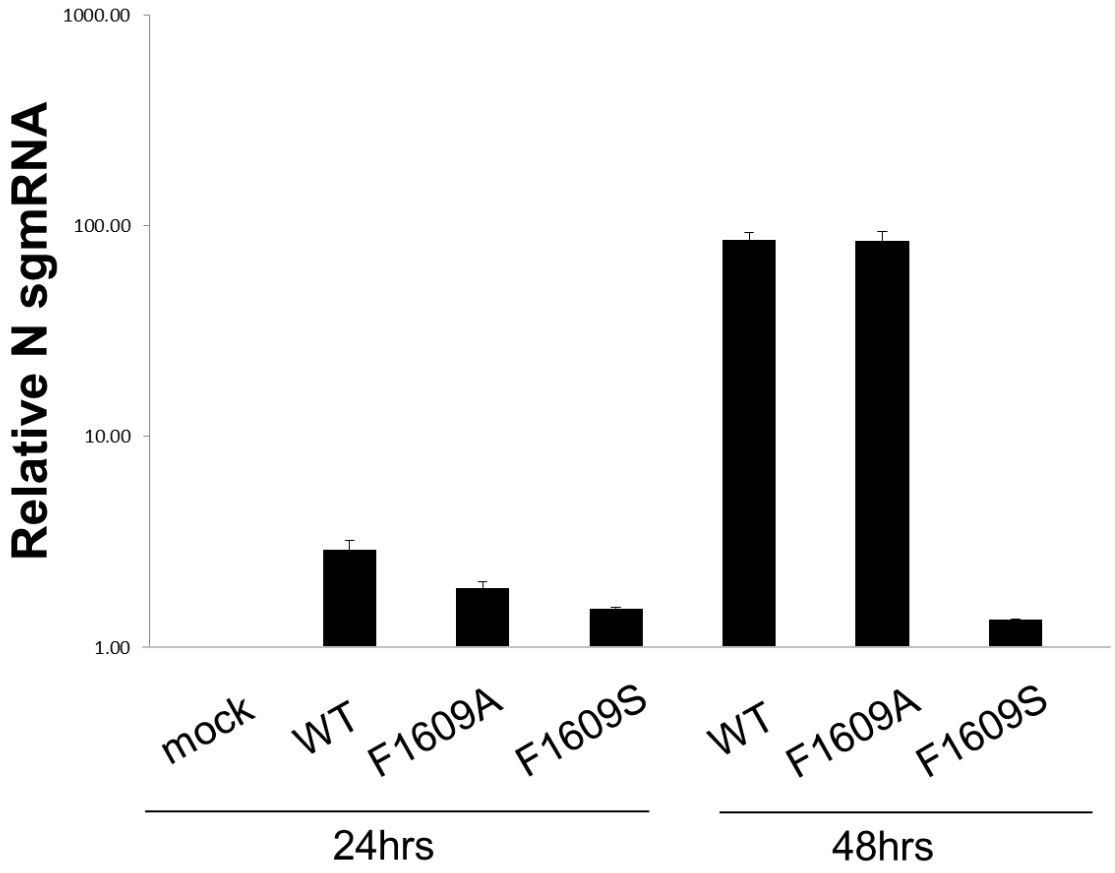

Figure 19. Efficient replication in SARS-CoV replicons containing F1609A mutation. B) HEK293T cells were transfected with 1ug pBAC-Rep for 24/48hrs. RNA was purified from cell lysates, cDNA was made from the RNA, and qPCR performed for N gene (SARS-CoV) and RPL13 (host control) transcripts. Data is normalized to RPL13. Performed in triplicate; n=2

the ridge region are predicted to only affect the affinity of PLpro for ubiquitin linked through the lysine residue at position 48. Other linkages, such as K63, adopt a conformation that would lead to chains extending from the first ubiquitin that do no contact the residues in PLpro that are important for interaction with K48 linkages. The loss of K48-linked ubiquitin chain interaction by PLpro ridge mutants allows for us to ask specific questions about K48-linked deubiquitination (in host pathways such as NFκB), however, it's possible that PLpro interacts with other ubiquitin chains and that cleavage of non K48-linked chains is important for PLpro antagonism of host responses. To determine if these residues are critical for ubiquitin interaction and potentially for innate immune antagonism, the hydrophobic pocket residue mutants M209A and Q233E were created, as well as a double mutant M209A+Q233E and a triple mutant F70A+M209A+Q233E which includes mutations within both the ridge and hydrophobic pocket of PLpro.

To determine if the hydrophobic pocket or combination mutations had any effect on innate immune antagonism, I again utilized the NFκB reporter assay and trans-cleavage assays to select the best mutants to analyze further. The NFκB assay was performed exactly like the assays for the ridge mutants, and the single hydrophobic pocket mutant PLpros, M209A and Q233E, the double mutant M209A+Q233E, and a triple mutant F70A+M209A+Q233E were analyzed for their ability to antagonize the NFκB pathway. After induction with TNFα, wild-type PLpro blocked activation of the NFκB reporter as shown previously. The catalytic mutant C112A is unable to antagonize the NFκB pathway and the mutants had varying results (Figure 20). The single mutants

within the hydrophobic pocket had intermediate phenotypes, suggesting that these mutations only partially affected the ability of PLpro to interact with and cleave K48-linked ubiquitin chains. When these mutations were combined, the effect was synergistic and the M209A and Q233E mutant lost the ability to antagonize the NFκB pathway. The same effect was seen when the ridge mutation F70A was combined with the hydrophobic pocket mutations in the triple mutant.

With the proximity of the hydrophobic pocket to the active site, the evaluation of the trans-cleavage activity for the PLpro mutants is especially important. To determine if the NFκB results were a result of authentic protease-deubiquitinating activity separation or merely the result of interrupting active site conformation, the mutant proteases were expressed with the nsp2-3 construct used previously to characterize the PLpro ridge mutants (Figure 21). Again, as demonstrated previously, wild-type PLpro cleaves the nsp2-3-GFP efficiently while the catalytic mutant (C112A) cannot. Despite the hydrophobic pocket being close to the active site, all of the mutants retained the ability to cleave the nsp2-3-GFP construct . When combined with the NFκB antagonism data, it suggests that these mutations might separate protease from deubiquitinating activity.

To attempt to quantitate the protease activity of the SARS-CoV PLpro hydrophobic pocket mutants, the pGlo assay used for antiviral drug screening of MERS-CoV proteases was used to measure cleavage. Cells were transfected with the pGlo-RLKGG substrate and the PLpro mutants, and the cleavage potential of these mutants was examined using the live-cell pGlo assay. The results were a surprising contrast to the

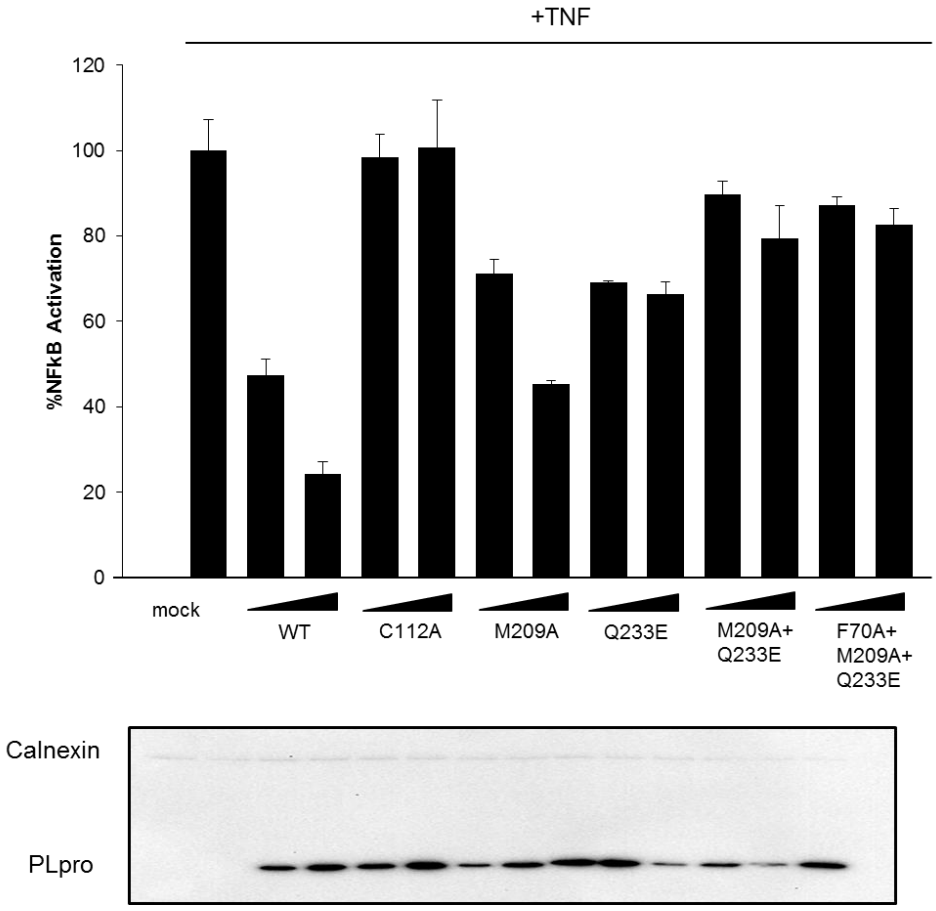

Figure 20. Hydrophobic pocket mutations affect SARS-CoV PLpro NFκB antagonism. 293HEK cells were transfected with NFκB-reporter and Renilla luciferase control constructs and the indicated PLpro. After 12hrs, TNFα was added to a final concentration of 10ng/mL and the cells were incubated for an additional 4hrs. Results are normalized to induction of NFκB reporter activity by TNFα. Panels below are western blots of the lysates using anti-V5 for detection of PLpro and anti-actin as a protein loading control. Experiments were performed in triplicate and repeated twice.

trans-cleavage assay detailed above (Figure 22). The wild-type SARS-CoV PLpro was the most efficient PLpro in its cleavage and recognition of the pGlo substrate and the catalytic mutant showed no substrate activation over time. The single mutant PLpros, M209A and Q233E, were less efficient, but not much less than WT. However, combining mutations further decreased the cleavage rate in this assay, and when the F70A mutation was added to M209A+Q233E, PLpro had the lowest rate of cleavage over time. This assay has not been used before to determine the rate of PLpro protease activity, and these results have not been correlated to activity of the PLpro domain within nsp3 in the context of viral infection. Until these mutations are reverse engineered into the virus, it's hard to conclude anything about their relative activity. However, we can say that all of these mutants are active when compared to the catalytic mutant (C112A). This assay complements both the trans-cleavage assay and we can say that all the PLpro mutants have some level of protease activity and are not completely impaired.

The NFκB assay suggests that protease and deubiquitinating activities have been separated by introducing mutations into the hydrophobic pocket. To determine if these mutations led to a decrease in the global DUB activity of PLpro, cells were transfected with a FLAG-tagged ubiquitin construct and the mutant PLpro. Similar to the experiment with the ridge mutants, if the mutants are deficient in ubiquitin cleavage, then you would expect more conjugated host proteins to remain detectable by immunoblot of the lysates. While the F70A mutant within the ridge of PLpro had reduced ubiquitin cleavage, the double hydrophobic pocket mutant (M209A+Q233E) and the combination

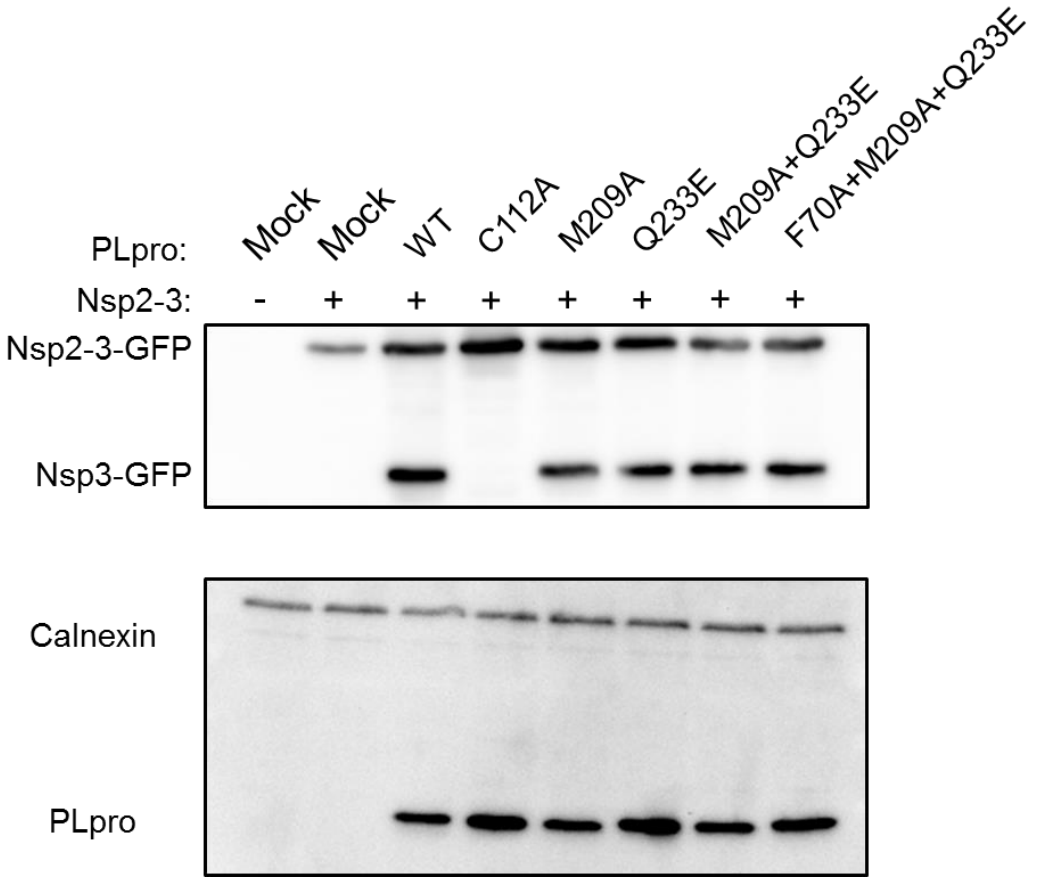

Figure 21. Hydrophobic pocket mutations do not affect SARS-CoV PLpro nsp2-3 recognition and cleavage. 293HEK cells were transfected with constructs expressing nsp2-3-GFP and SARS-CoV PLpro-V5 wild type, catalytic mutant (C112A) or ridge mutants. Cells were incubated for 24 hours and then lysed with IkBα lysis buffer. Samples were transferred to PVDF immunoblotted with anti-GFP (Life Technologies), anti-calnexin (BD) and anti-V5 (Invitrogen).

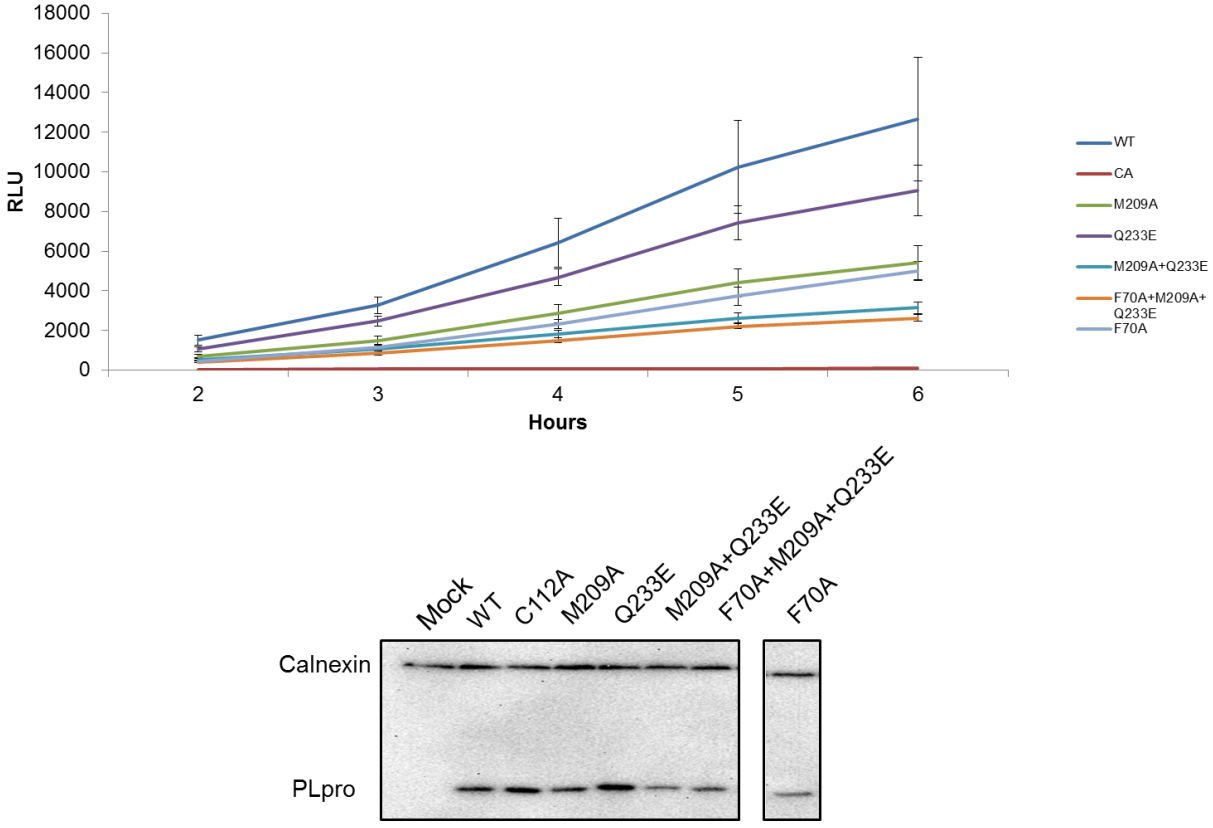

Figure 22. Hydrophobic pocket mutations have varying effects on SARS-CoV PLpro pGlo recognition and cleavage. Cells are co-transfected with pGlo-30F-RLKGG and either SARS-CoV WT or mutant PLpro. At 14 hrs post transfection, cells were incubated with Glosensor reagent and luminescence was read hourly. Experiment was performed in triplicate with error bars representing the standard deviation of the mean. Samples were transferred to PVDF and immunoblotted with anti-calnexin (BD) and anti-V5 (Invitrogen) to confirm protease expression.

ridge and hydrophobic pocket mutant (F70A+M209A+Q233E) all had a severe decrease in the deubiquitinating activity within transfected cells to almost mock transfected and catalytic mutant levels (Figure 23). This data links the trans-cleavage and NFκB results to a lack in deubiquitinating activity and supports the role of DUB activity in SARS-CoV PLpro mediated NFκB antagonism.

Since the mutations within the hydrophobic pocket interrupt direct binding with a single ubiquitin molecule, these mutations should also affect how ubiquitin-like molecules interact with PLpro. ISG15 is a di-ubiquitin-like molecule and has been demonstrated to have antiviral effects when expressed. SARS-CoV and MERS-CoV PLpro have been shown to cleave ISG15 (deISGylating activity) *in vitro* and in transfected cells (Barretto et al., 2005; Lindner et al., 2005; Sulea et al., 2005). It has been hypothesized that this activity could allow SARS-CoV and MERS-CoV to evade inhibition by ISG15; however this hypothesis has never been tested. When ISG15 is modeled onto PLpro using the ubiquitin-aldehyde co-crystal structure, it mimics the interaction between PLpro and ubiquitin-aldehyde (primarily because ISG15 looks like two ubiquitin molecules in a K48-linkage) (Figure 3A). Because the above data demonstrates the importance of residues F70 within the ridge, and M209 and Q233 within the hydrophobic pocket on PLpro-ubiquitin interaction, these mutants were analyzed in an assay to measure deISGylation.

To determine if the ridge and hydrophobic pocket mutations affect deISGylating activity of SARS-CoV PLpro, WT and mutant PLpro was transfected into cells along

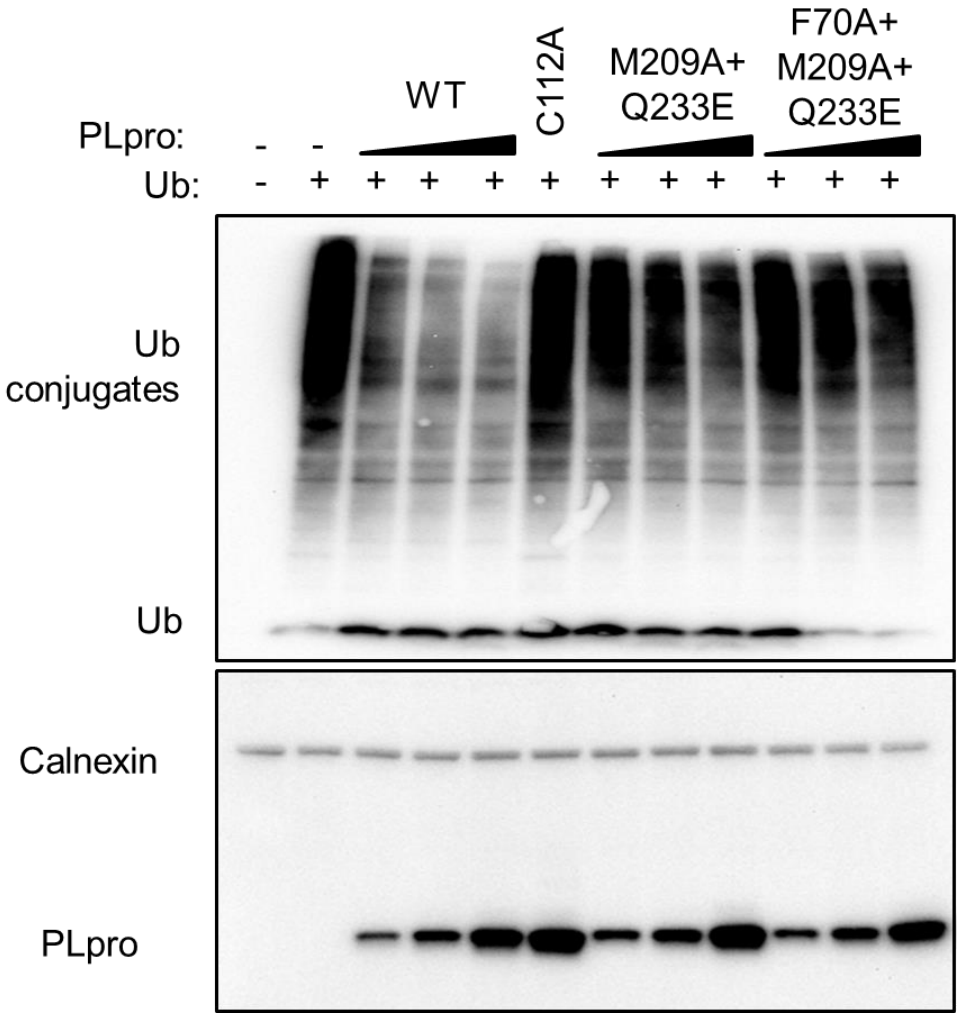

Figure 23. Hydrophobic pocket mutations are impaired in their ability to cleave ubiquitin from cellular substrates. HEK293T cells were transfected with expression plasmids encoding FLAG-Ub and the indicated PLpro. 18hrs post transfection, cells were lysed and immunoblotted for FLAG-Ub, calnexin, and PLpro-V5.

with a tagged ISG15 and the machinery needed to conjugate ISG15 to host cell proteins. If the mutants are defective in ISG15 cleavage, then more conjugated host cell proteins will be seen in cells transfected with mutant PLpro by immunoblot of cell lysates. In a dose dependent manner, WT PLpro is able to cleave ISG15 from host cell proteins (Figure 24) very efficiently, as the doses used in this experiment are 10, 25, and 50ng of PLpro plasmid DNA where for the DUB assay it was 125, 250, and 500ng. These results were surprising giving the effect of these mutations on DUB activity, however, a lot was learned from this experiment. First, the amounts of PLpro transfected had to be much less to see the dose-dependent increase of deISGylation. This indicates that the affinity and rate of cleavage for ISG15 is much great than ubiquitin, and this finding supports *in vitro* data reaching the same conclusion. Second, while these residues are critical for ubiquitin binding, they seem to be less important for interaction with ISG15. This could be due to other surfaces on PLpro that are important for interaction with ISG15; surfaces that couldn't be deduced by modeling based on the interaction between PLpro and ubiquitin.

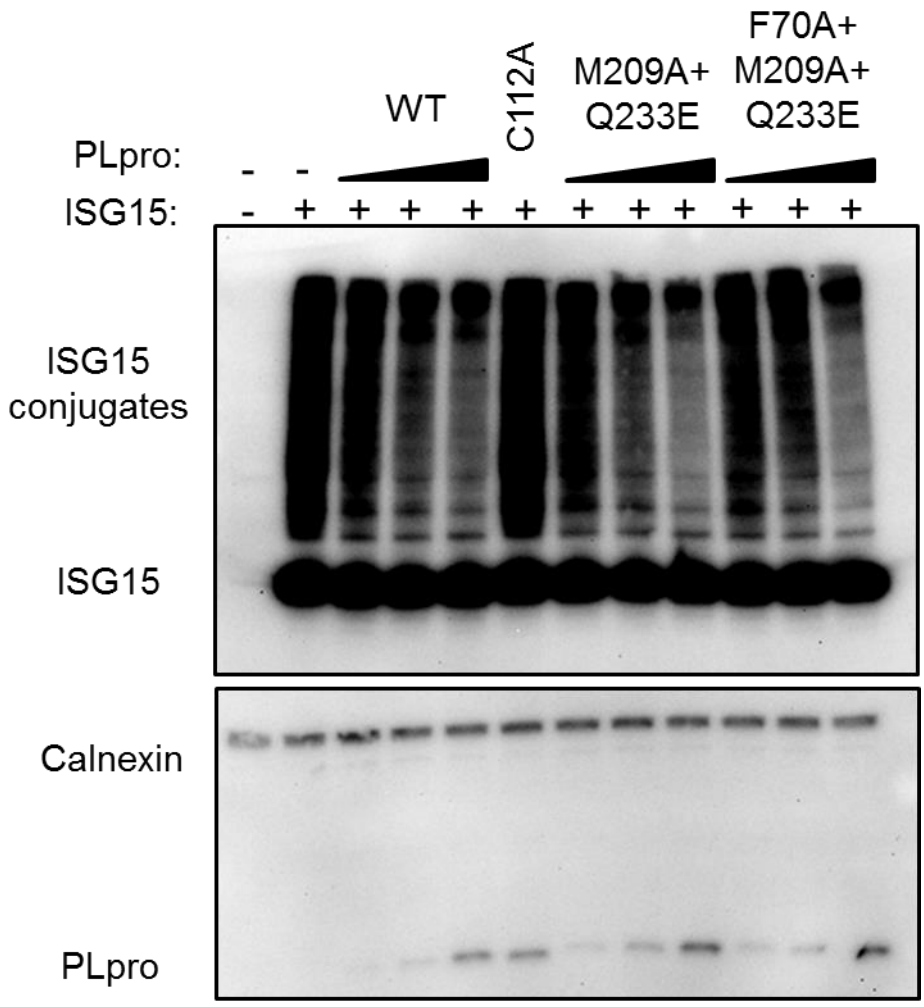

Figure 24. Hydrophobic pocket mutations have little impact on SARS-CoV PLpro deubiquitinating activity. HEK293T cells were transfected with expression plasmids encoding myc-ISG15, its conjugation machinery, and the indicated PLpro. 18hrs post transfection, cells were lysed and immunoblotted for myc-ISG15, calnexin, and PLpro-V5.

CHAPTER IV

DISCUSSION

Understanding the biology of coronaviruses is important, especially as zoonotic coronaviruses of high pathogenicity like SARS-CoV and MERS-CoV have no approved therapeutics for human use. My work has contributed to understanding coronavirus biology in multiple ways. By utilizing conserved protease cleavage sites, I developed luciferase-based biosensors that are activated by coronavirus proteases. This is a novel platform for rapid identification of inhibitors that work to block protease activity within transfected cells (Kilianski et al., 2013). We have also characterized previously putative papain-like proteases from alpha and beta coronavirus groups, and demonstrated that the multifunctionality of PLPs is conserved despite very little sequence identity. These proteases are also able to cleave the protease biosensor, establishing a platform for screening compounds thought to have broad-spectrum coronavirus activity. Finally, I have separated the protease and deubiquitinating activity of SARS-CoV PLpro by targeting residues critical for the interaction with ubiquitin for site directed mutagenesis (Ratia et al., 2014). These mutants are impaired in ubiquitin cleavage from host cell proteins and lose the ability to antagonize the NFκB pathway, and important innate immune pathway downstream of cytosolic RNA sensors. This is the first demonstration of using coronavirus DUB mutant proteases to define mechanisms of host innate immune antagonism, and this work links the DUB activity of SARS-CoV PLpro with the NFκB

pathway, a critical host pathway whose antagonism could influence the innate immune response to viral infection.

MERS-COV PROTEASE INHIBITORS AND THE PGLO SYSTEM

Middle East respiratory syndrome coronavirus (MERS-CoV) continues to be a threat to public health, remaining in the human population and causing over 150 laboratory-confirmed infections since late 2012. MERS-CoV has spread from the Middle East to Europe via infected individuals, and increasing amounts of data is suggesting some sustained human-to-human transmission in addition to multiple introductions from natural reservoirs is occurring (Cotten et al., 2014). As mentioned previously, no FDA approved anti-coronaviral treatments exist, so any laboratory confirmed MERS-CoV infected individuals have no consistent treatment options (Al-Tawfiq & Memish, 2014). Ribavirin and interferon (a very broad spectrum antiviral cocktail) have been shown to potentially have human applications, but treatment of patients with this cocktail has not been effective (Al-Tawfiq, Momattin, Dib, & Memish, 2014; Falzarano et al., 2013). To combat the threat of emerging coronaviruses such as SARS-CoV, MERS-CoV, or a coronavirus that emerges in the future; specific antivirals approved for human use are necessary.

Contributing to the lack of coronavirus drug development are the lack of cell-based assays to rapidly evaluate inhibitors on MERS-CoV or future emergent coronavirus enzymes (Kilianski & Baker, 2014). To aid in the screening of antivirals already shown

to have inhibitory effects against SARS-CoV proteases, I developed a luciferase-based biosensor to detect MERS-CoV papain-like and 3C-like protease activity and quantitatively assess the effects of inhibitors on protease activity. The biosensor is a circularly-permuted luciferase construct with a protease recognition and cleavage site inserted at a location that, only after cleavage, confers an active confirmation of luciferase that can recognize its substrate and create light. This technology was previously used for primarily *in vitro* work, and my adaptation was the first time coronavirus proteases have been quantitatively measured within cells.

Based on the catalytic residues that are conserved in coronavirus papain-like proteases, we outlined the MERS-CoV PLpro domain starting with the ubiquitin-like domain found in SARS-CoV PLpro (Ratia et al., 2006) and culminating with a stretch of amino acids 40 residues after the catalytic aspartic acid (again, based on a similar boundary to SARS-CoV PLpro) (Figure 4). This strategy has worked previously for NL63 PLP2, however MHV PLP2 required some domain extension to create a protease that was optimally functional and crystalizable (Chen et al, in preparation). The work of defining a putative protease can be difficult, especially as sequence identity between PLPs is low, but the knowledge that coronavirus papain-like protease structure is relatively conserved makes this easier. The MERS-CoV PLpro definition turned out to be correct, as we expressed a protease that was active in both trans-cleavage and pGlo assays (Figures 4 and 5). Not only was MERS-CoV PLpro an active protease, it also has the same multifunctionality seen in SARS-CoV PLpro (Mielech, Kilianski, et al., 2014). MERS-CoV PLpro functions as a deubiquitinating and deISGylating enzyme with the

ability to block host innate immune pathways. Despite the lack of crystal structure, the fact that MERS-CoV PLpro is an active protease with functions conserved with SARS-CoV PLpro indicates that despite the lack of sequence homology, structural similarities probably exist.

Based on the potential structural similarity, it's possible that inhibitors designed to work against SARS-CoV PLpro might have inhibitory properties against MERS-CoV PLpro. The possibility of inhibition of PLpro as an antiviral strategy was first demonstrated by Han et al who used zinc ions to block the activity of SARS-CoV PLpro (Y.-S. S. Han et al., 2005). The same group then identified thiopurine analogues as a method of selective and reversible inhibition of PLpro *in vitro* (C Y Chou et al., 2008). Later that year, Ratia et al discovered another type of selective, non-covalent, and reversible inhibitor that not only blocked SARS-CoV PLpro activity *in vitro,* but also blocked SARS-CoV replication in cell culture (Ratia et al., 2008). This inhibitor led to a series of inhibitors designed to more efficiently bind to SARS-CoV though a flexible loop adjacent to the active site (Baez-Santos et al., 2014; Ghosh et al., 2009, 2010). When this loop is bound by the inhibitors, the active site becomes inaccessible to the viral polyprotein and other substrates. These inhibitors are specific against SARS-CoV, although *in vitro* there might be some broad-spectrum activity that has not yet been observed with transfected enzyme or with live virus (Baez-Santos et al., 2014).

To determine if this series of inhibitors has the ability to block MERS-CoV PLpro activity, we utilized the pGlo assay to quantitatively assess inhibition by the compound

BD-15g (Ghosh et al., 2010) (Figure 6). The compound had no inhibitory effect against MERS-CoV PLpro while it inhibited SARS-CoV PLpro activity as expected. After years of using structure activity relationships and perfecting the inhibitors to bind tightly to the SARS-CoV PLpro loop structure, it is possible that this refinement excluded BD-15g from binding to the loop present in MERS-CoV PLpro. This is especially apparent when you examine the region in MERS-CoV PLpro that corresponds to the flexible loop in SARS-CoV PLpro (Figure 4). Based on x-ray crystallography of these series of inhibitors interacting with SARS-CoV PLpro, it's known that the polar tyrosine residue within the flexible loop is critical for interaction with the inhibitor. The residues within the MERS-CoV PLpro loop, if the loop exists (it might also be smaller than the loop in SARS-CoV PLpro), is unlikely to bind the inhibitor in a similar fashion to the SARS-CoV PLpro loop. It would be interesting to return to the original inhibitor study (Ratia et al., 2008) to determine if any of the compounds that were less potent against SARS-CoV might have some broad spectrum activity. With the pGlo assay for MERS-CoV PLpro established, screening multiple inhibitors against both PLPs is straightforward

In addition to papain-like proteases, 3C-like proteases are also responsible for coronavirus polyprotein cleavage. The 3C-like protease from SARS-CoV comprises all of non-structural protein 5, and the "3C-like" nomenclature comes from the sequence similarity to other 3C proteases (notably from picornaviruses) and from the presence of a chymotrypsin like fold within 3CLpro (Kanchan Anand et al., 2002; Gorbalenya, Koonin, Donchenko, & Blinov, 1989). 3CLpro recognizes viral polyprotein cleavage sites between nsps 4/5 through 15/16 via a consensus glutamine residue at P1 with some

preference around the cleavage site (based on *in vitro* work) (Chuck et al., 2011) and probably major contributions from viral polyprotein secondary and tertiary structure. In contrast to PLpro, SARS-CoV 3CLpro has been a popular target for the development of antiviral drugs, with a variety of compounds identified to have inhibitory activity (reviewed in (Barnard & Kumaki, 2011; Kilianski & Baker, 2014). Since the outbreak of MERS-CoV, there has been no reporter small compound inhibitor of any MERS-CoV enzyme, including 3CLpro. To determine if previously validated SARS-CoV inhibitors block MERS-CoV 3CLpro activity, we created an expression construct for MERS-CoV 3CLpro and first tested to see if it was active in cleavage and pGlo assays.

To maintain the optimum conformation and thus the most active protease possible, we expressed 3CLpro in the context of a polyprotein (Figure 7). nsp4 (which is a transmembrane protein), nsp5 (3CLpro), and the n-terminus of nsp6 fused with a V5 tag were synthesized into two expression constructs. One expression construct retained the 3CLpro cleavage sites between nsp4/5 and nsp5/6 while the other construct had a mutation that abrogated the nsp5/6 cleavage site. This second construct was made because the WT construct would result in complete liberation of nsp5 with no tag, and since no antibodies exist against MERS-CoV nsp5, retaining the tag would allow for us to visualize its expression better by western blot. Both of these constructs were active in the cleavage assay and the pGlo assay, with the pGlo assay yielding very high values for luciferase activation, from 250-300 fold above mock in the endpoint assay (Figure 8). I have shown that pGlo also works very well for MHV 3CLpro, demonstrating that despite

the difference between papain-like and 3C-like proteases, both can activate the pGlo assay efficiently.

As reviewed earlier, many potential 3CLpro inhibitors have been characterized for SARS-CoV, so I took one of the inhibitors that had has been demonstrated to have efficient anti-SARS activity and low toxicity, CE-5, and tested its activity against MERS-CoV 3CLpro (Figure 9). CE-5 is a covalent modifier of the catalytic cysteine utilized by 3CLpro and inhibits SARS-CoV and MHV replication in cell culture (Ghosh et al., 2008). When added to cells transfected with MERS-CoV 3CLpro and pGlo-VRLQS, CE-5 effectively inhibited 3CLpro activity. This inhibition was seen in both the endpoint and live cell assays. With the knowledge that this inhibitor is a suicide inhibitor, it was interesting to observe a slight climb after the addition of the drugs towards WT levels in the live cell assay (Figure 9B). This climb is indicative of a suicide inhibitor, because as the inhibitor binds, new 3CLpro is translated in the cell and the concentration of the drug is less than it was upon initial inhibition. When applying the pGlo assay to a higher throughput approach to identify lead compounds, looking at the dynamics of inhibition could indicate the mechanism of inhibition by a certain compound. In many applications, suicide and covalent inhibitors are not desired, so these compounds could be screened out with this process and other lead compounds with more desired mechanisms can be chosen.

My work with the MERS-CoV proteases contributed to the coronavirus field in a number of ways. The expression and activity of both MERS-CoV PLpro and 3CLpro

demonstrates the location of these proteases within the MERS-CoV genome and gives a platform for assessing the multifunctionality of PLpro and screening antiviral inhibitors against PLpro and 3CLpro. Determining that the series of PLpro inhibitors we tested had no effect on MERS-CoV PLpro saves significant time by ruling out further screening with this class of compound. Again, it would be interesting to return to some of the first compound hits against SARS-CoV PLpro and test them using the pGlo assay. The identification of CE-5 as a potential MERS-CoV inhibitor is the first demonstration of a small molecule inhibitor for a MERS-CoV enzyme, and not only identifies a potential antiviral for MERS-CoV, but also validates the usefulness of pGlo to screen antiviral compounds without the need for *in vitro* purification.

The experiments involving pGlo raise some important questions regarding the future applications of the system. In a set of experiments not described here, both PLP and 3CLP pGlo constructs were unable to be activated by MHV. However, when the soluble PLP2 and 3CLpro constructs were transiently expressed, they were able to activate the biosensor. Infection with MHV either prevents the biosensor from being synthesized properly or shields the cytoplasmic and soluble pGlo construct from the membrane-associated and potentially privileged environment where PLPs and 3CLps reside during replication. Both of these are possibilities, and both scenarios have been extensively studied in coronavirus biology. During coronavirus infection, non-structural protein 1 (nsp1) acts as a translation inhibitor, and this activity is conserved in both SARS-CoV and MERS-CoV, although the mechanisms might vary (citations). In the MHV infection experiments, cells were transfected for up to 18hrs prior to infection with

MHV. This length of transfection should ensure that there is an ample amount of pGlo present in the cytoplasm at the time of infection. Since little is known about the half-life and turnover of pGlo in transfected cells, it is possible that the amount transfected or the time of transfection did not allow a sufficient amount of pGlo to accumulate. Its also possible that upon nsp1 translation after infection with MHV, the pGlo construct was quickly degraded without the synthesis of new pGlo due to the translation inhibition by nsp1.

While nsp1 could contribute to the lack of pGlo activation during MHV infection, another possibility is that both the papain-like and 3C-like proteases are sequestered on membrane structures that are inaccessible to the cytoplasm during MHV infection. Membrane rearrangement during coronavirus replication provides scaffolding for the replicative enzymes to congregate and initiate replication of the viral genome and production of sub-genomic mRNAs for the production of the coronaviral structural proteins (Gosert, Kanjanahaluethai, Egger, Bienz, & Baker, 2002; Harcourt et al., 2004; Snijder et al., 2006). These membrane structures are ER-derived and are formed into double membrane vesicles and convoluted membrane networks by the coronavirus non-structural proteins 3,4, and 6 (Angelini, Akhlaghpour, Neuman, & Buchmeier, 2013; Reggiori et al., 2010). What is currently unclear is if the replication complexes remain on the internal or external surfaces of these membranes and if they remain accessible to the cytoplasm within infected cells. Dissection of these vesicles in other viruses, such as HCV, has revealed that small pores exist in many of the vesicles, allowing energy and molecular building blocks like nucleotides and amino acids to access the replication

machinery on the interior of the vesicles (Paul & Bartenschlager, 2013; Romero-Brey et al., 2012). Ultra-structural imaging of arterivirus and coronavirus replication structures have not been as conclusive, as connections between the inside of the membrane vesicles and the cytosol have not been seen (Knoops et al., 2008, 2012) This visual evidence, as well as experiments on isolated DMV associated replication complexes, strongly support membrane protection of replication structures (van Hemert et al., 2008). One potential strategy to bypass the membrane sequestration of replication complexes is to also localize the pGlo construct to the sites of viral replication. This can be accomplished by tethering the pGlo construct to a transmembrane protein, nsp4, that is encoded naturally by the coronaviral genome. Expressing this tethered form of pGlo could potentially localize the pGlo construct to the membranes that are being hijacked for coronavirus replication and allow for it to be activated during coronavirus infection. In addition to creating a biosensor for coronavirus infection, this assay could contribute to the understanding of coronavirus replication complex formation. If pGlo could be activated when located on membranes, then the hypothesis of membrane protection of replication complexes within DMVs to hide replication intermediates from sensors in the cytosol would be further supported.

With the proof of principle work for the pGlo biosensor demonstrated here, there are a multitude of applications for the biosensor in the future. A potential use that we are exploring (and that I will discuss in the following section) is to use the biosensor to screen for broad spectrum inhibitors against a larger group of coronavirus PLPs and/or 3CLpros in the context of the cell. This method removes the *in vitro* purification, *in vitro*

activity, cellular permeability, and cellular toxicity steps. The *in vitro* work can be very difficult and time consuming, especially with coronavirus sequences which can be toxic to bacteria used to produce purified proteins. Combining many of the *in vitro* experiments into a single experiment, which is possible with the pGlo assays, will definitely accelerate the discovery and evaluation of broad spectrum coronavirus antivirals. This is important for two main reasons: the emergence of zoonotic coronaviruses with the potential for pathogenesis in humans; and the lack of human models to test anti-coronavirus inhibitors.

While pGlo has advantages over some of the traditional methods for inhibitor identification, it also has roadblocks to overcome before it might be a wide-spread technique for other uses than identifying protease inhibition by previously validated compounds. Specifically, the reagents needed to perform luciferase-based assays in high throughput are cost prohibitive. Cell-based approaches currently utilize more qualitative measures or measures that rely on cell lysis and fluorescence (Kilianski & Baker, 2014). For example, inhibitors of the hepatitis C protease have been identified using a pseudo cell-based system where the viral protease's activity against a FRET peptide in the absence of presence of inhibitor is analyzed after cell lysis (Bühler & Bartenschlager, 2012; Konstantinidis et al., 2007). As technology advances in the field of cell-based luminescence, prices will be reduced and then it might make economic sense to move towards more quantitative cell based approaches for the identification of novel small compound inhibitors, such as pGlo.

The rapid emergence of viruses like SARS-CoV and MERS-CoV means that effective therapies need to be tested rapidly and be available to public health authorities as soon as possible. Currently, there is no human model for coronaviruses that can be used to test antiviral compounds, mainly because no broad spectrum antivirals exist that will inhibit not only highly pathogenic coronaviruses like MERS-CoV, but also common-cold causing coronaviruses such as HCoV-229E or HCoV-HKU1. If inhibitors were identified that could block protease activity from both types of coronaviruses, then these inhibitors could be tested in human models of disease for their efficacy. This increases the likelihood of FDA approval while allowing for the demonstration of inhibitory compounds that would work against coronaviruses in humans. To develop assays to explore the possibility of broad-spectrum PLP inhibitors, we characterized the PLPs from previously uncharacterized alpha and beta coronaviruses and determined if they had conserved multifunctionality and if they activated the pGlo construct.

CONSERVED MULTIFUNCTIONALITY OF THE PAPAIN-LIKE PROTEASES FROM ALPHA AND BETA CORONAVIRUSES

The papain-like proteases from coronaviruses are conserved, as one or two PLPs are necessary to cleave the viral polyprotein at the n terminus. While these proteases likely exist in all coronaviruses, many of these PLPs have not been characterized for their ability to cleave viral polyproteins or for the identification of multifunctionality that is seen in SARS-CoV, MERS-CoV, NL-63, porcine epidemic diarrhea virus (PEDV),

transmissible gastroenteritis virus (TGEV), and MHV. To determine if this multifunctionality is a conserved function of coronavirus papain-like proteases, we attempted to cast a wide net by expressing putative papain-like protease domains from human coronaviruses HCoV-OC43, HCoV-HKU1, HCoV-229E and the feline coronavirus FIPV (Figure 25A). These proteases were defined in a similar way to MERS-CoV, extending the protease on both ends from the conserved catalytic triad resulting in constructs of 324aa in length. When aligned, it's obvious that there is little sequence identity (Figure 25B). When compared to the similarity between MERS-CoV and SARS-CoV PLpro (30%), it's not surprising that these proteases from both alpha and beta coronavirus groups do not have much amino acid sequence homology. To determine if these putative proteases are in fact proteases and are multifunctional, we evaluated their activity in trans-cleavage, deubiquitinating, and deISGylating assays.

All of the putative protease domains expressed had activity against nsp2-3-GFP in transfected cells (Figure 10) and possessed deubiquitinating and deISGylating (except possibly HCoV-HKU1 PLP2) activity (Figure 11). This data supports the hypothesis that while the sequence homology between coronavirus PLPs is low, there is structural conservation that allows for similar recognition of the viral polyprotein as well as cellular substrates like ubiquitin and ISG15. The varying levels of protease, DUB, and deISGylating activity are especially interesting, as the results between the experiments do not necessarily line up. For example, HCoV-OC43 PLP2 has intermediate DUB activity when compared with the other CoV PLPs expressed; however, it has excellent relative deISGylating activity. HCoV-HKU1 has DUB activity, but no detectable deISGylating

A)

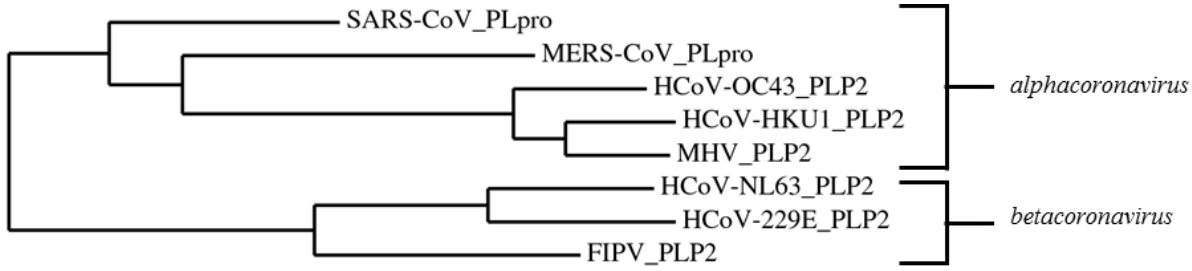

B)

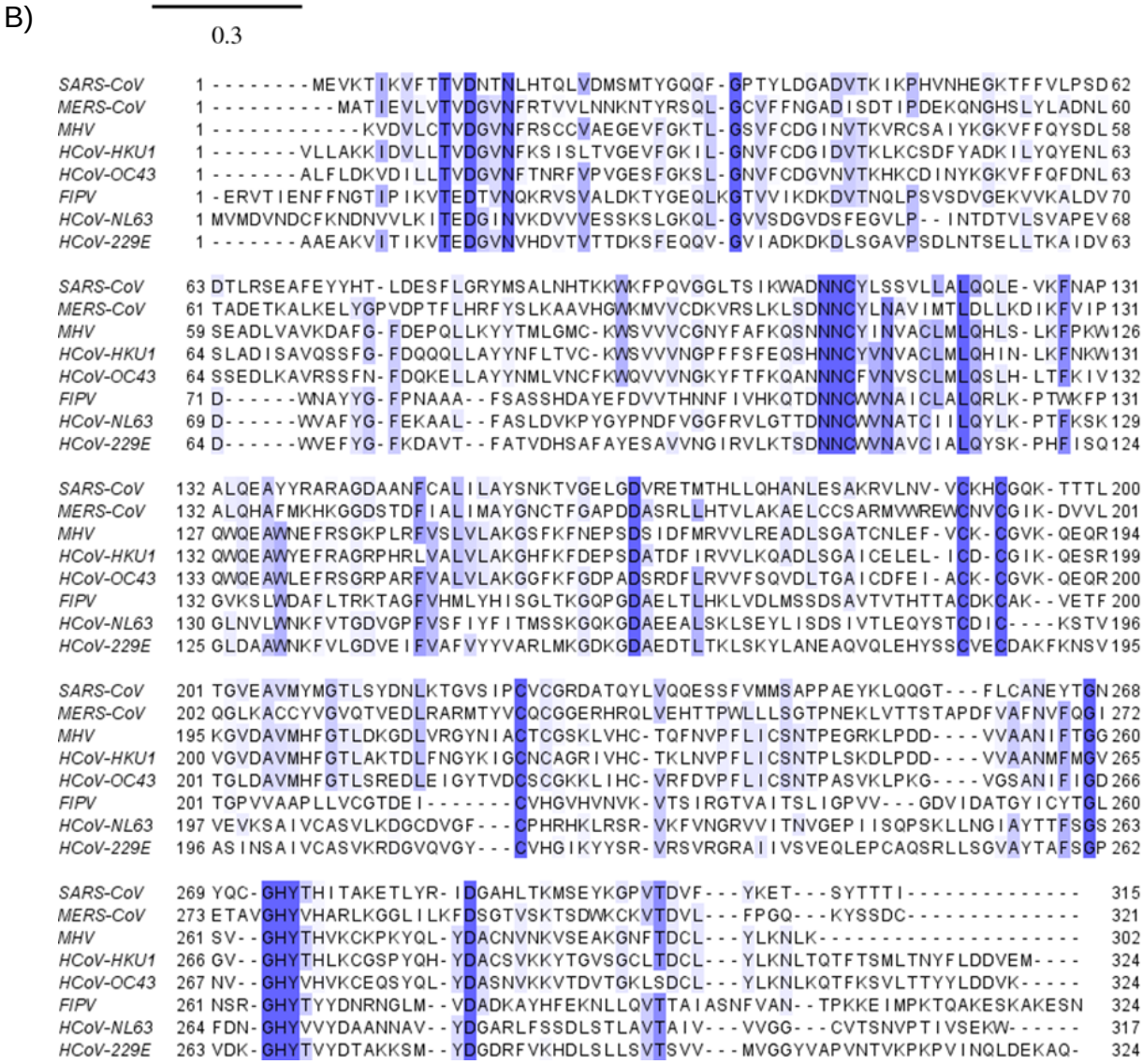

Figure 25. Alignment of the PLpro domains from selected alpha and beta coronaviruses. A) Phylogenetic tree based on the sequence similarities between the selected alpha and beta coronaviruses. Tree was generated using software and algorythms provided by phylogeny.fr (Dereeper et al., 2008). B) Alignments performed using ViPR software MUSCLE alignment algorithm; conserved residues highlighted in color with the darker color denoting more conservation.

activity at the PLP doses used in Figure 11. In addition to the levels of activity being different in each assay, the expression patterns were surprisingly varied, despite the predicted sizes to be similar (Figure 10). The differences in expression suggest that while there are probably conserved structural elements that account for the multifunctionality, there are regions of the papain-like protease that allow for structural flexibility, evolution driven by a particular host, etc. Infectious bronchitis virus (IBV) shows very high diversity among strains, with 20% sequence variance seen within the PLP2 domains and stretches of amino acids which have higher diversity than others (Mondal & Cardona, 2004). Codon adaptation occurs in coronaviruses within natural hosts, and the codon usage can influence rates of translation and how proteins fold within cells of specific hosts (Brandão, 2013). Each of these variances could create differences in levels of protein and the size and band characterizes seen using western blot. It is also possible that the PLP domains are not all the same size, and our 340aa constructs did not capture the full PLP domain. This could lead to parts which normally contribute to the correct conformation being excluded and thus leading to folding and expression changes.

Finally, I wanted to determine if these PLP constructs could activate the pGlo biosensor. This would create a platform to test if inhibitors identified against SARS-CoV or MERS-CoV PLpro would have broad spectrum inhibitory activity. All of the PLP constructs activated the biosensor (Figure 12) although the PLPs from HCoV-OC43 and HCoV-299E were not very high above background. Despite some low values, the ability to recognize and cleave the pGlo biosensor means this assay should be adaptable to screen for antiviral compounds that have effects across both alpha and beta coronavirus

groups. Candidate compounds can be screened for inhibitory activity against a number of coronavirus PLPs (and potentially any future emergent CoV PLPs) and inhibitory activity can be determined within cells before antivirals are tested against live virus in cell culture and animal models. The ability to test for inhibition directly on the protease is attractive, especially as cell culture work with some of the human coronaviruses is difficult, so any effect on the virus replication in cell culture could be hard to determine without previous demonstration of PLP inhibition (Pyrc et al., 2010).

These experiments, coupled with the SARS-CoV and MERS-CoV PLpro inhibitor work, demonstrate that coronavirus papain-like proteases have conserved functions beyond cleavage of the viral polyprotein during replication. However, while they have some structural similarity, there are regions within the PLPs that are not similar (such as the flexible inhibitor binding loop in SARS-CoV) and probably lead to differences in protein folding and stability. These differences might be important for affinity for host proteins like ubiquitin and ISG15, or for yet-to-be characterized interactions between PLPs and the host cell. With the knowledge that coronavirus PLPs have conserved multifunctionality and the ability to cleave host protein modifiers like ubiquitin came the question of the importance of these other functions of PLpro. To examine these other roles, they must be functionally separated from the protease activity of PLpro, which is difficult because the protease and isopeptidase activities of PLpro share the same catalytic residues. The next section will discuss work that separated the protease activity of PLpro from its deubiquitinating activity and the role that DUB activity plays in innate immune antagonism.

SEPARATING SARS-COV PLPRO PROTEASE AND DEUBIQUITINATING ACTIVITY AND A ROLE FOR PLPRO DUB ACTIVITY IN INNATE IMMUNE ANTAGONSIM

The papain-like protease of SARS-CoV is the best studied papain-like protease among coronaviruses because of its role in viral replication, its potential as an antiviral target, but also because it has multiple functions apart from viral polyprotein cleavage. These multiple functions are conserved among coronavirus PLPs (see above), and the challenge is to examine the role of PLpro multifunctionality during viral pathogenesis. To do this, the functions must be separated from one another, because the protease activity of PLpro needs to remain unchanged as any defect in protease activity will affect viral polyprotein cleavage and potentially replication and pathogenesis. This is especially difficult because for PLpro deubiquitinating and deISGylating activity, the catalytic residues needed for peptidase and isopeptidase activities are identical. To separate these functions, I used co-crystal structure data of PLpro bound to ubiquitin-aldehyde (Figure 3) and *in vitro* analysis of certain PLpro mutants to guide my mutagenesis of the SARS-CoV PLpro expression construct.

This approach has shown to be successful within the nidovirus order with equine arteritis virus (EAV) PLP2 (van Kasteren et al., 2013). Mutating residues distant from the active site that are still important for the interaction with ubiquitin of EAV PLP2 resulted in a retention of protease activity but a loss in deubiquitinating and interferon antagonism abilities. When reverse engineered into the virus, mutant EAV replicated

normally but induced more proinflammatory cytokines than WT in cell culture. This work suggested a role for DUB activity, but no mechanism was explored (however EAV PLP2 was previously shown to deubiquitinate RIG-I (van Kasteren et al., 2012). The structural basis of SARS-CoV PLpro deubiquitinating activity was also recently explored, however the authors mutations significantly reduced protease activity and the effect of loss of DUB activity was not explored within cells (Chi Yuan Chou et al., 2014). The goal of my research was to determine a mechanistic role for SARS-CoV PLpro deubiquitinating activity by creating mutants retaining WT levels of protease activity but losing affinity to ubiquitin and ubiquitin chains.

I first wanted to determine if PLpro antagonized innate immune pathways at steps that require K48-ubiquitination for their regulation. PLpro demonstrates a preference for K48-linked ubiquitin chains, so I hypothesized that K48-linked DUB activity would be a potent mechanism of innate immune antagonism. NFκB is a transcriptional regulator of many antiviral genes that can be activated by cytosolic sensors of viral replication like RIG-I and MDA5 (Figure 2). After the pathway is activated, IκBα becomes phosphorylated then poly K48-ubiquitinated. This targets IκBα for degradation by the proteasome and frees NFκB to translocate to the nucleus and activate transcription. Because of its importance in regulating host cell antiviral defenses, it's a logical target for antagonism by viral factors, including SARS-CoV PLpro (Clementz et al., 2010; Frieman et al., 2009; Le Negrate, 2012). While it is known that PLpro can block the activation of NFκB, the mechanism is unknown. The NFκB pathway has a very specific step

(ubiquitination of IκBα) which is regulated by K48-linked ubiquitin, so I examined whether PLpro inhibited NFκB at location within the pathway

If wild-type PLpro inhibited the NFκB pathway by removing K48-linked ubiquitin from IκBα, then IκBα will still be phosphorylated after activation of the pathway, but will not be efficiently degraded. In cells transfected with PLpro, the upstream events that lead to the phosphorylation of IκBα were not affected as IκBα was still phosphorylated (Figure 13), but the degradation was delayed. Some IκBα was still degraded in this experiment, but it is likely due to the fact that not all cells examined here in this lysate were transfected with WT PLpro. In cells transfected with WT PLpro (controlled for in an experiment using tagged IκBα (Figure 14)), IκBα does not get degraded after activation of the NFκB pathway. These data suggest deubiquitination as a mechanism for how SARS-CoV PLpro inhibits the NFκB pathway, but PLpro mutants that have low ubiquitin affinity will allow me to more definitively link PLpro DUB activity to innate immune antagonism.

The generation of mutants with decreased deubiquitinating activity is based on the co-crystal structure of SARS-CoV PLpro and ubiquitin aldehyde (Figure 4). By using the co-crystal structure to model how different ubiquitin chains would fit onto the PLpro structure, we identified a region within PLpro, distant from the active site that is potentially important for K48-linked ubiquitin interaction. This site was targeted for mutagenesis and determined *in vitro* by our collaborators that altering this proposed interacting "ridge" of PLpro affected its ability to cleave ubiquitin (Ratia et al., 2014).

The ridge of PLpro also likely contributes to the increased activity seen against K48-linked chains when compared to other ubiquitin linkages, like K63. When the modeling is compared, the interaction of the ridge of PLpro with the second ubiquitin molecule is important for K48, but the conformation of K63-linked chains does not allow for the second ubiquitin to contact the ridge residues. The residues F70, H74, and L76 were targeted for mutagenesis and analysis of their effects on NFκB antagonism, trans-cleavage activity, and global host protein deubiquitination.

To determine if PLpro ridge mutants lost the ability to antagonize the NFκB pathway, I first co-transfected mutant PLpros and an HA tagged IκBα. If PLpro prevents IκBα degradation through its DUB activity, then ridge mutants deficient in this should lose the ability to stabilize IκBα (Figure 14). Wild-type PLpro had a higher level of IκBα in transfected cells and prevented any degradation of IκBα after TNFα addition. F70S and the other ridge mutants lost the ability to stabilize IκBα after TNFα addition. These results could also be due to a general loss of protease activity by PLpro. To ensure that protease activity was not affected in the ridge mutants, I performed a trans-cleavage assay (Figure 15). All of the ridge mutants efficiently cleaved the synthetic nsp2-3 substrate, and these results support the separation of protease activity from deubiquitinating activity that was observed *in vitro* in addition to the IκBα assay.

If the loss of IκBα stabilization had any downstream effects on NFκB activation, then NFκB mediated transcription should be unaffected in the presence of PLpro ridge mutants. I utilized a luciferase reporter assay containing an NFκB response element and

examined the antagonism properties of SARS-CoV PLpro (Figure 16). As previously reported, wild-type PLpro prevents the activation of NFκB. The ridge mutants, which are deficient in deubiquitinating activity and IκBα stabilization, also lose the ability to block NFκB activation. All of these data point to the cleavage of K48-linked ubiquitin from IκBα as the mechanism of PLpro NFκB antagonism, however this was never directly tested. I never looked *in vitro* for PLpro ubiquitin cleavage from IκBα and was never able to immunoprecipitate IκBα with conjugated ubiquitin molecules. This is likely due to the rapid turnover of IκBα after the activation of the NFκB pathway. Despite not directly testing PLpro DUB activity on IκBα, the experiments I designed and executed elucidate the mechanism by which SARS-CoV PLpro blocks the NFκB pathway when transfected into cells.

These assays test a very specific role for PLpro deubiquitinating activity on innate immune pathways within host cells. It has been reported that PLpro broadly cleaves ubiquitin molecules from host cell substrates (Clementz et al., 2010). The ridge mutations were hypothesized to primarily effect interaction with K48-linked ubiquitin, but to determine if these mutants had an effect on the global DUB activity of SARS-CoV PLpro, mutants were co-transfected with a tagged ubiquitin construct. This allows for the visualization of host proteins that are conjugated to ubiquitin. Wild-type PLpro has broad DUB activity when transfected into host cells, and the PLpro ridge mutants F70S and F70A both are impaired in their global DUB activity (Figure 17). F70S has greater impairment than F70A, but the levels of ubiquitinated proteins in both mutant transfected cells approach the mock or catalytic mutant PLpro transfected cells. Either the majority

of cellular proteins conjugated to the tagged ubiquitin are K48-linked (or this linkage is the most abundant, thus the most likely to be seen by western blot), or mutations at residue F70 could affect PLpro's cleavage of different ubiquitin linkages in addition to K48.

van Kasteren et al were able to achieve protease and deubiquitinating activity separation in EAV PLP2 by simply making size changes to ubiquitin interacting residues (van Kasteren et al., 2013). To ensure that we had both more dramatic and more subtle changes made, mutations that changed both the polarity (nonpolar to polar F70S) and the size of the amino acid side chain (large to small F70A) were incorporated into SARS-CoV PLpro. With the knowledge that both these mutations affected the global deubiquitinating activity of PLpro, I examined the effects of F70A on NFκB antagonism and trans-cleavage activity. The F70A mutation had a similar phenotype to F70S with the loss of NFκB antagonism but retention of trans-cleavage activity (Figure 18). These data demonstrate the importance of the phenylalanine at position 70 of SARS-CoV PLpro and that changing the size or polarity of the side chain can disrupt PLpro-ubiquitin binding. The flexibility of mutations at key ubiquitin interacting residues might be important when determining how these mutations affect SARS-CoV replication when generating replication competent infectious clones.

With the goal of engineering these mutations into the infectious clone of SARS-CoV, assessing the replicative competency of viruses encoding these mutations is an important first step. This can be done at BSL2 using the SARS-CoV replicon system

developed by Almazan et al (Almazan et al., 2006). The F70S and F70A mutations were incorporated into nsp3 on the icSARS-CoV B clone (F1609S and F1609A of pp1a). The region containing these mutations was then engineered into the replicon using recombineering (methods). The levels of sub-genomic N gene RNA (can only be produced by working replication complexes formed from the replicon) were measured in cells transfected with WT, F1609A, and F1609S replicons at 24 and 48 hours post transfection (Figure 19). Compared to wild-type, F1609A replicated much more efficiently than F1609S, which barely replicated at all over the 48hrs.

The replication experiments create a lot of questions about the replication competency of an icSARS-CoV containing the F1609A or F1609S mutations. Many of these questions arise from the caveats of the experiments being done. There were no differences in the ability of F70A or F70S PLpro to cleave the nsp2-3 substrate during transfections (Figure 18). This is a qualitative endpoint assay so it is possible that differences in the rate of cleavage could occur over time that are indiscernible by western blot. The PLpro and nsp2-3-GFP expression constructs are both soluble proteins (when in the context of the virus they would be membrane and replication-transcription complex associated (Figure 1)) and highly overexpressed. These differences could lead to discrepancies between what happens during transfections and what happens during viral replication. Additionally, the replicon does not recapitulate all of the events during viral infection and replication so important replicative elements might be missing in the replicon system.

Even with the caveats of using transfections and replicons to predict what might happen during viral infection, it's possible the results do accurately portray what would happen to viral replication if these mutations were put into the icSARS-CoV system. There was no difference in NFκB antagonism between F70A and F70S, but there was a small difference in the DUB assay between F70A and F70S (F70S being more impaired for DUB activity). I limited the innate immune and host signaling pathways to the NFκB pathway as it is good model pathway and had a clear mechanism for the usage of K48-Ub to regulate signaling. Its known that PLpro influences other pathways important for the innate response to viral infection in addition to other host factors whose role in SARS-CoV infection is less clear (S. W. Li et al., 2011; S.-W. Li et al., 2012; Neuman et al., 2008).

When reviewing the DUB results, it is also possible that the small difference noted between F70A and F70S might be significant in the context of the virus. The deubiquitinating activity of SARS-CoV PLpro might play a critical role in viral replication, as recent work has implicated nsp3 in double membrane vesicle formation (Angelini et al., 2013). The role for nsp3 was not clearly defined in this work, but the availability of a system to test the influence of PLpro independent of viral replication presents the opportunity to determine if PLpro DUB activity is critical in the formation of replication complexes. This question could be very relevant when the role of ubiquitin modification is examined in the context of membrane rearrangements. Coronaviruses utilize the endoplasmic reticulum to form DMVs and convoluted membranes and these pathways are strongly regulated by ubiquitin and other ubiquitin-like modifiers

(Christianson & Ye, 2014; Reggiori et al., 2010; Reggiori, de Haan, & Molinari, 2011). The introduction of membrane-associated PLpro, especially if it is located on both the cytoplasmic and ER lumen sides, would have the ability to cleave ubiquitin on ER-associated factors that require ubiquitination to regulate ER membrane arrangement. nsp3 is also involved in interaction with coronavirus structural proteins that are ubiquitinated (nucleocapsid and envelope) and contains two ubiquitin-like domains (one within PLpro) (Alvarez et al., 2010; K R Hurst, Ye, Goebel, Jayaraman, & Masters, 2010; Kelley R Hurst, Koetzner, & Masters, 2013). Mutations within the ridge might affect interactions with these proteins or domains that interrupt the overall function of nsp3. A small difference in DUB impairment between F70A and F70S within nsp3 might manifest itself to greater consequence during viral replication.

Further complicating the interpretation is the uncertainty over where the papain-like protease and nsp3 are located during viral replication. The membrane structures necessary for coronavirus replication complex formation were previously described when discussing the inability of viral infection to activate the pGlo substrate. So far, PLpro in the context of nsp3 does not have the ability to cleave a soluble protein within the cytoplasm (pGlo). If PLpro is important for innate immune evasion, then it must be cleaving ubiquitin or ubiquitin-like molecules from host substrates activated due to the membrane rearrangement and vRNA replication that occurs during infection. The cleavage of host protein modifiers during infection would require the signaling complexes to be available to PLpro. Antiviral signaling complexes mediated by proteins like MAVS and STING are membrane associated (Barber, 2011; Horner, Liu, Park,

Briley, & Gale Jr, 2011), so it is logical that PLpro could modify host proteins located within these contexts. Supporting this hypothesis are the experiments done by Sun et al that demonstrate the ability of trans-membrane located PLpro to block STING mediated antiviral signaling (L. Sun et al., 2012).

PLpro as a domain within non-structural protein 3 also has the potential to influence other nsp3 domains. The ADP-ribose-1"-monophosphatase (ADRP) domain is located upstream from PLpro and the SARS unique domain (SUD) is located directly downstream of PLpro. Both have been hypothesized to influence viral pathogenesis. The ADRP domain was demonstrated to reduce the sensitivity of SARS-CoV to alpha interferon treatment (Kuri et al., 2011). The SUD binds to consecutive guanosine nucleotides that form RNA structures called G-quadruplexes, and this binding might be important for interaction with viral or host RNA present in the cytoplasm during infection (Tan et al., 2009). It's possible that the introduction of the F70S mutation affects the function of a domain separate from PLpro within nsp3 that is required for viral replication.

The ridge residues are important for ubiquitin chain interaction, but there are other regions within PLpro that were shown by co-crystal structure to directly interact with the single ubiquitin molecule. To affect not only K48 but also K63 and other ubiquitin linkage binding, these interaction faces were targeted next. Mutations of the hydrophobic pocket residues M209A and Q233E and combinations of M209A+Q233E and F70A+M209A+Q233E caused a loss of NFκB antagonism similar to the mutations

within the ridge of PLpro (Figure 20). There was no effect on trans-cleavage activity (Figure 21) but using the pGlo assay to quantitatively assess the protease activity of the mutants revealed differences (Figure 22). The single mutants were less active that the wild-type and the combination mutants were even less active. This was the first experiment to attempt to quantify the protease activity of PLpro mutants, so the impact of these results is unclear. It is possible that the protease activity of mutants is decreased, however with the more "authentic" nsp2-3 construct, no differences were detected. The mutations could affect how PLpro is translated or folds or how PLpro interacts with and cleaves the pGlo construct. It is difficult to determine, based on the conflicting results from the trans-cleavage and the pGlo biosensor assay alone, how the mutants might influence polyprotein cleavage in the context of the virus. However, all of the mutant constructs are active proteases at levels much greater than the catalytic mutant (C112A).

Further analysis of the mutant PLpros revealed that the combination mutants (M209A+Q233E and F70A+M209A+Q233E) were highly impaired in their ubiquitin cleavage ability (Figure 23). When compared to wild-type, these mutants were more impaired than the ridge mutants F70A and F70S alone (Figure 19). By mutating residues that interact with the single ubiquitin molecule, PLpro's affinity for all ubiquitin types and linkages is disrupted. Because of this, I next examined if these mutations had any effect on ISG15 cleavage by PLpro.

ISG15 is conformationally very similar to di-ubiquitin molecules, and plays a role in the innate defense against viral infection (Morales & Lenschow, 2013; Narasimhan et

al., 2005). SARS-CoV PLpro is a very efficient deISGylating enzyme, and has higher affinities towards ISG15 than the viral polyprotein cleavage peptide or ubiquitin (Ratia et al., 2014). As the residues important for ubiquitin interaction are likely also important for recognition of ISG15, we hypothesized that the ISG15 cleavage ability of PLpro would be decreased when M209A and Q233E mutations are incorporated. Surprisingly, the presence of M09A+Q233E or F70A+M209A+Q233E mutations had very little effect on the deISGylating activity of SARS-CoV PLpro (Figure 24). Because the cleavage rate of ISG15 by PLpro is so high, the transfected amounts of PLpro in this experiment are much lower than in the DUB assay. This could also be why the presence of only three mutations is not enough to separate the deISGylating activity of PLpro from its polyprotein cleavage. The separation of ISG15 cleavage ability from a host or viral protease has never been accomplished, so this remains an important aspect to explore, especially with the recent study that implicated ISG15 in MHV pathogenesis (Ma et al., 2014). When the conjugation of ISG15 in host cells was prevented by knocking out the E1 conjugation enzyme, MHV replicated more efficiently. Additionally, when an ISG15 specific deISGylating enzyme, USP18 was knocked out, mice had delayed courses of infection, with better pathology and lower titers. These results implicate ISG15 as an important molecule in host defense against coronaviruses, although not the only factor needed to control infection.

The continued discovery of host factors important for the detection and clearance of viral infections naturally leads to the discovery of viral gene products that combat these defenses. As the largest of the RNA viruses, coronaviruses have evolved to include

a number of innate immune antagonists. nsp1, while not directly an antagonist of innate immune pathways, inhibits host cell translation and promotes host-capped mRNA degradation (Kamitani, Huang, Narayanan, Lokugamage, & Makino, 2009; Lokugamage, Narayanan, Huang, & Makino, 2012). nsp3 encodes not only the papain-like protease, but also an ADP-ribose-1"-monophosphatase and "SARS-unique" domain that have been hypothesized to interact with host factors potentially involved in the antiviral response (Kuri et al., 2011; Putics, Filipowicz, Hall, Gorbalenya, & Ziebuhr, 2005; Tan et al., 2009). The methyltransferases encoded by nsp14 and nsp16 are important factors for innate immune evasion, as the 2′ O-methylation of viral RNA is important for evading innate immune detection of viral genomes and viral replication products (Yu Chen et al., 2011; Daffis et al., 2010; Zust et al., 2011).

In addition to these functions mediated by the non-structural proteins, coronavirus structural and accessory proteins also have the ability to block host responses. The nucleocapsid protein from coronaviruses blocks interferon production and ORF3b and ORF6 prevent interferon signaling from occurring (Kopecky-Bromberg, Martínez-Sobrido, Frieman, Baric, & Palese, 2007; Ye Ye, Hauns, Langland, Jacobs, & Hogue, 2007). MERS-CoV 4a was recently shown to inhibit PACT-mediated activation of RIG-I and MDA5 (Siu et al., 2014). ns2 from MHV is an antagonist of the OAS-RNase L pathway via 2',5'-phosphodiesterase activity that prevents the recognition of 2',5'-oligoadenylate by RNaseL, thus preventing the degradation of coronaviral RNA (L. Zhao et al., 2012). There is some overlap in the downstream effects of these innate immune antagonists, so the question remains, why do coronaviruses encode all of these

effectors and what does that say about the observed properties of the papain-like proteases? Coronaviruses have evolved to infect many cell types with the potential for zoonotic transmission into multiple hosts, including humans. In order to do this, coronaviruses must successfully evade the immune response that might be mounted against viral replication in any of these cell types and within any of the potential hosts. While the antagonists described here have overlapping functions, it is likely that different parts of different innate immune pathways contribute in unique ways depending on the cell type and host. The DUB and deISGylating functions (among other possible unknown functions of PLpro enzymatic activity) likely function to evade different antiviral defenses depending on where the virus is replicating. When this molecular dissection of the function of coronavirus nonstructural, structural, and accessory genes is combined with more bioinformatic approaches (Menachery et al., 2014) to evaluate virus-host interactions within infected cells, it opens the door to the discovery of further pathways influenced by the innate immune agtagonists encoded by coronaviruses.

The mutants I have identified within the ridge and hydrophobic pocket have effects on both the innate immune antagonism and the deubiquitinating activity of SARS-CoV PLpro. We have shown that these activities are conserved among coronavirus PLPs, so can the information and mutants generated for SARS-CoV PLpro be applicable to other PLPs? Based on amino acid conservation, the answer is no. The residues identified so far as being important for innate immune antagonism and deubiquitinating activity have no conservation among even more closely related coronaviruses (Figure 25). Because hydrophobic surfaces and the hydrophilic residues that help shape these

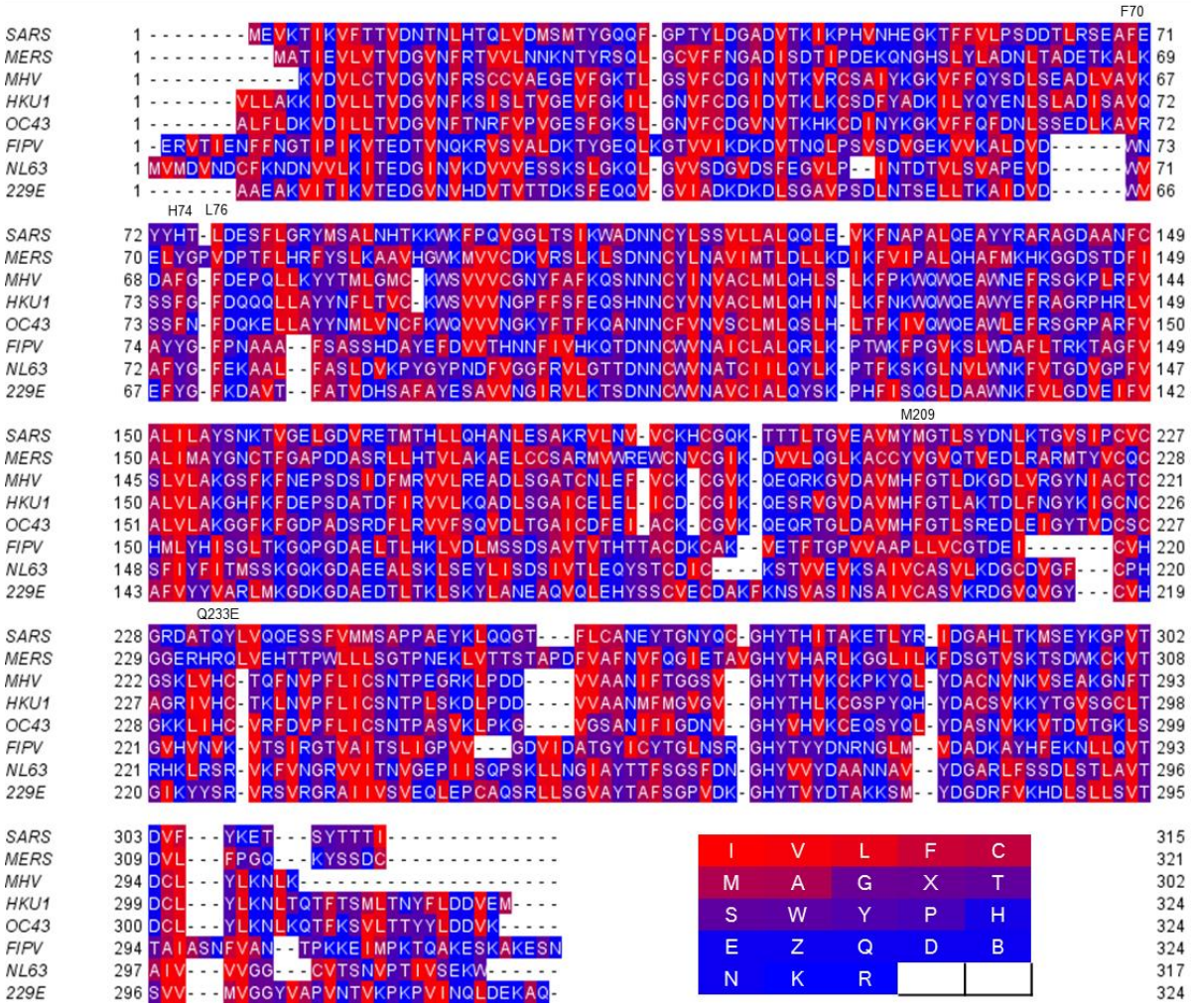

Figure 26. Alignment of coronavirus papain-like proteases and hydrophobicity characteristics of amino acid side chains. According to the hydrophobicity table of Kyte, J., and Doolittle, R.F., J. Mol. Biol. 1157, 105-132, 1982. The most hydrophobic residues according to this table are coloured red and the most hydrophilic ones are coloured blue.

surfaces are important for SARS-CoV PLpro interactions with ubiquitin, it might be more relevant to look at the conservation of hydrophobicity with coronavirus PLPs (Figure 26). It is evident that while at the primary sequence level there might not be much similarity between PLPs, when the hydrophobicity of each amino acid side chain is analyzed; there are definite regions that are conserved. Ridge region residues F70 and L76 are both highly conserved in their hydrophobicity while residues M209 and Q233 that help shape the hydrophobic pocket are conserved in their hydrophobicity and hydrophilicity, respectively. By analyzing the side chain characteristics of coronavirus PLPs, it might allow for the separation of multifunctionality without crystal structure information and a more thorough understanding of the role of PLpro deubiquitinating activity during pathogenesis.

SUMMARY

These studies resulted in the development of valuable tools for evaluating potential protease inhibitors while also making significant inroads towards the goal of separating the multifunctionality of coronavirus papain-like proteases. The luciferase biosensor will allow for the quantitative evaluation of antiviral inhibitors in the context of the cell, a method that has advantages over and can complement the traditional *in vitro* compound screening dogma. These assays are amenable to a broad range of coronavirus PLPs from the alpha and beta coronavirus groups and MERS-CoV and MHV 3CLpro (others have not been evaluated), and are useful in identifying broad spectrum inhibitors

to existing and potentially emergent coronaviruses. Evaluation of putative PLPs from alpha and beta coronaviruses revealed the extent of multifunctionality conservation and implicate deubiquitinating and deISGylating activities as being critical for the coronavirus life cycle. To determine a role for these activities, co-crystal structure of SARS-CoV PLpro bound to ubiquitin was used to guide mutagenesis of residues critical for ubiquitin interaction. The mutants retained protease activity but were deficient in deubiquitinating activity and lost their ability to act as NFκB antagonists in transfected cells. Mutations at F70 were analyzed in the context of viral replication using the SARS-CoV replicon system and it was determined that the F70S mutation caused a large defect in viral replication while the F70A mutation had little effect and replicated to wild-type levels. These mutants have led to the separation of PLpro's protease and deubiquitinating activity and give an excellent platform for incorporation into the infectious clone of SARS-CoV to determine if the deubiquitinating activity of PLpro is important for SARS-CoV replication and/or pathogenesis.

REFERENCES

(WHO), W. H. O. (2014). Middle East respiratory syndrome coronavirus (MERS-CoV) - update (Jan 20, 2014). *Global Alert and Response (GAR), 2014*(20 January 2014). Retrieved from http://www.who.int/csr/don/2013_07_21/en/index.html

Adedeji, A. O., Severson, W., Jonsson, C., Singh, K., Weiss, S. R., & Sarafianos, S. G. (2013). Novel inhibitors of severe acute respiratory syndrome coronavirus entry that act by three distinct mechanisms. *Journal of Virology*, *87*(14), 8017–8028. doi:10.1128/JVI.00998-13; 10.1128/JVI.00998-13

Adedeji, A. O., Singh, K., Calcaterra, N. E., DeDiego, M. L., Enjuanes, L., Weiss, S., & Sarafianos, S. G. (2012). Severe acute respiratory syndrome coronavirus replication inhibitor that interferes with the nucleic acid unwinding of the viral helicase. *Antimicrobial Agents and Chemotherapy*, *56*(9), 4718–4728. doi:10.1128/AAC.00957-12; 10.1128/AAC.00957-12

Ahn, D. G., Lee, W., Choi, J. K., Kim, S. J., Plant, E. P., Almazan, F., … Oh, J. W. (2011). Interference of ribosomal frameshifting by antisense peptide nucleic acids suppresses SARS coronavirus replication. *Antiviral Research*, *91*(1), 1–10. doi:10.1016/j.antiviral.2011.04.009; 10.1016/j.antiviral.2011.04.009

Akutsu, M., Ye, Y., Virdee, S., Chin, J. W., & Komander, D. (2011). Molecular basis for ubiquitin and ISG15 cross-reactivity in viral ovarian tumor domains. *Proceedings of the National Academy of Sciences of the United States of America*, *108*(6), 2228–2233. doi:10.1073/pnas.1015287108

Alagaili, A. N., Briese, T., Mishra, N., Kapoor, V., Sameroff, S. C., de Wit, E., … Lipkin, W. I. (2014). Middle East Respiratory Syndrome Coronavirus Infection in Dromedary Camels in Saudi Arabia. *mBio*, *5*(2), e00884–14–e00884–14. doi:10.1128/mBio.00884-14

Almazan, F., Dediego, M. L., Galan, C., Escors, D., Alvarez, E., Ortego, J., … Enjuanes, L. (2006). Construction of a severe acute respiratory syndrome coronavirus infectious cDNA clone and a replicon to study coronavirus RNA synthesis. *Journal of Virology*, *80*(21), 10900–10906. doi:10.1128/JVI.00385-06

Almazan, F., DeDiego, M. L., Sola, I., Zuniga, S., Nieto-Torres, J. L., Marquez-Jurado, S., … Enjuanes, L. (2013). Engineering a replication-competent, propagation-defective Middle East respiratory syndrome coronavirus as a vaccine candidate. *mBio*, *4*(5), e00650–13. doi:10.1128/mBio.00650-13; 10.1128/mBio.00650-13

Al-Tawfiq, J. A., & Memish, Z. A. (2014). What are our pharmacotherapeutic options for MERS-CoV? *Expert Review of Clinical Pharmacology*. doi:10.1586/17512433.2014.890515

Al-Tawfiq, J. A., Momattin, H., Dib, J., & Memish, Z. A. (2014). Ribavirin and interferon therapy in patients infected with the Middle East respiratory syndrome coronavirus: an observational study. *International Journal of Infectious Diseases : IJID : Official Publication of the International Society for Infectious Diseases*, *20*, 42–6. doi:10.1016/j.ijid.2013.12.003

Alvarez, E., DeDiego, M. L., Nieto-Torres, J. L., Jiménez-Guardeño, J. M., Marcos-Villar, L., & Enjuanes, L. (2010). The envelope protein of severe acute respiratory syndrome coronavirus interacts with the non-structural protein 3 and is ubiquitinated. *Virology*, *402*(2), 281–91. doi:10.1016/j.virol.2010.03.015

Anand, K., Palm, G. J., Mesters, J. R., Siddell, S. G., Ziebuhr, J., & Hilgenfeld, R. (2002). Structure of coronavirus main proteinase reveals combination of a chymotrypsin fold with an extra alpha-helical domain. *The EMBO Journal*, *21*(13), 3213–24. doi:10.1093/emboj/cdf327

Anand, K., Ziebuhr, J., Wadhwani, P., Mesters, J. R., & Hilgenfeld, R. (2003). Coronavirus main proteinase (3CLpro) structure: basis for design of anti-SARS drugs. *Science (New York, N.Y.)*, *300*(5626), 1763–1767. doi:10.1126/science.1085658

Angelini, M. M., Akhlaghpour, M., Neuman, B. W., & Buchmeier, M. J. (2013). Severe acute respiratory syndrome coronavirus nonstructural proteins 3, 4, and 6 induce double-membrane vesicles. *mBio*, *4*(4). doi:10.1128/mBio.00524-13

Baez-Santos, Y. M., Barraza, S. J., Wilson, M. W., Agius, M., Mielech, A. M., Davis, N. M., … Mesecar, A. D. (2014). X-Ray Structural and Biological Evaluation of a Series of Potent and Highly Selective Inhibitors of Human Coronavirus Papain-Like Proteases. *Journal of Medicinal Chemistry*. doi:10.1021/jm401712t

Balakirev, M. Y., Jaquinod, M., Haas, A. L., & Chroboczek, J. (2002). Deubiquitinating function of adenovirus proteinase. *Journal of Virology*, *76*(12), 6323–6331.

Barber, G. N. (2011). Innate immune DNA sensing pathways: STING, AIMII and the regulation of interferon production and inflammatory responses. *Current Opinion in Immunology*, *23*(1), 10–20. doi:10.1016/j.coi.2010.12.015

Barnard, D. L., & Kumaki, Y. (2011). Recent developments in anti-severe acute respiratory syndrome coronavirus chemotherapy. *Future Virology*, *6*(5), 615–631. doi:10.2217/fvl.11.33

Barretto, N., Jukneliene, D., Ratia, K., Chen, Z., Mesecar, A. D., & Baker, S. C. (2005). The papain-like protease of severe acute respiratory syndrome coronavirus has deubiquitinating activity. *Journal of Virology*, *79*(24), 15189–15198. doi:10.1128/JVI.79.24.15189-15198.2005

Binkowski, B. F., Butler, B. L., Stecha, P. F., Eggers, C. T., Otto, P., Zimmerman, K., … Wood, K. V. (2011). A luminescent biosensor with increased dynamic range for intracellular cAMP. *ACS Chemical Biology*, *6*(11), 1193–1197. doi:10.1021/cb200248h; 10.1021/cb200248h

Binkowski, B., Fan, F., & Wood, K. (2009). Engineered luciferases for molecular sensing in living cells. *Current Opinion in Biotechnology*, *20*(1), 14–18. doi:10.1016/j.copbio.2009.02.013; 10.1016/j.copbio.2009.02.013

Blanchard, J. E., Elowe, N. H., Huitema, C., Fortin, P. D., Cechetto, J. D., Eltis, L. D., & Brown, E. D. (2004). High-throughput screening identifies inhibitors of the SARS coronavirus main proteinase. *Chemistry & Biology*, *11*(10), 1445–1453. doi:10.1016/j.chembiol.2004.08.011

Bottcher, S., Maresch, C., Granzow, H., Klupp, B. G., Teifke, J. P., & Mettenleiter, T. C. (2008). Mutagenesis of the active-site cysteine in the ubiquitin-specific protease contained in large tegument protein pUL36 of pseudorabies virus impairs viral replication in vitro and neuroinvasion in vivo. *Journal of Virology*, *82*(12), 6009–6016. doi:10.1128/JVI.00280-08

Brandão, P. E. (2013). The evolution of codon usage in structural and non-structural viral genes: the case of Avian coronavirus and its natural host Gallus gallus. *Virus Research*, *178*(2), 264–71. doi:10.1016/j.virusres.2013.09.033

Bühler, S., & Bartenschlager, R. (2012). New targets for antiviral therapy of chronic hepatitis C. *Liver International : Official Journal of the International Association for the Study of the Liver*, *32 Suppl 1*, 9–16. doi:10.1111/j.1478-3231.2011.02701.x

Capodagli, G. C., McKercher, M. A., Baker, E. A., Masters, E. M., Brunzelle, J. S., & Pegan, S. D. (2011). Structural analysis of a viral ovarian tumor domain protease

from the Crimean-Congo hemorrhagic fever virus in complex with covalently bonded ubiquitin. *Journal of Virology*, *85*(7), 3621–3630. doi:10.1128/JVI.02496-10

Chen, Y., Rajashankar, K. R., Yang, Y., Agnihothram, S. S., Liu, C., Lin, Y. L., … Li, F. (2013). Crystal structure of the receptor-binding domain from newly emerged middle East respiratory syndrome coronavirus. *Journal of Virology*, *87*(19), 10777–10783. doi:10.1128/JVI.01756-13; 10.1128/JVI.01756-13

Chen, Y., Su, C., Ke, M., Jin, X., Xu, L., Zhang, Z., … Guo, D. (2011). Biochemical and structural insights into the mechanisms of SARS coronavirus RNA ribose 2'-O-methylation by nsp16/nsp10 protein complex. *PLoS Pathogens*, *7*(10), e1002294. doi:10.1371/journal.ppat.1002294

Chen, Z., Wang, Y., Ratia, K., Mesecar, A. D., Wilkinson, K. D., & Baker, S. C. (2007). Proteolytic processing and deubiquitinating activity of papain-like proteases of human coronavirus NL63. *Journal of Virology*, *81*(11), 6007–6018. doi:10.1128/JVI.02747-06

Chou, C. Y., Chien, C. H., Han, Y. S., Prebanda, M. T., Hsieh, H. P., Turk, B., … Chen, X. (2008). Thiopurine analogues inhibit papain-like protease of severe acute respiratory syndrome coronavirus. *Biochemical Pharmacology*, *75*(8), 1601–1609. doi:10.1016/j.bcp.2008.01.005; 10.1016/j.bcp.2008.01.005

Chou, C. Y., Lai, H. Y., Chen, H. Y., Cheng, S. C., Cheng, K. W., & Chou, Y. W. (2014). Structural basis for catalysis and ubiquitin recognition by the Severe acute respiratory syndrome coronavirus papain-like protease. *Acta Crystallographica. Section D, Biological Crystallography*, *70*(Pt 2), 572–81. doi:10.1107/S1399004713031040

Christianson, J. C., & Ye, Y. (2014). Cleaning up in the endoplasmic reticulum: ubiquitin in charge. *Nature Structural & Molecular Biology*, *21*(4), 325–35. doi:10.1038/nsmb.2793

Chuck, C. P., Chow, H. F., Wan, D. C., & Wong, K. B. (2011). Profiling of substrate specificities of 3C-like proteases from group 1, 2a, 2b, and 3 coronaviruses. *PloS One*, *6*(11), e27228. doi:10.1371/journal.pone.0027228; 10.1371/journal.pone.0027228

Clementz, M. A., Chen, Z., Banach, B. S., Wang, Y., Sun, L., Ratia, K., … Baker, S. C. (2010). Deubiquitinating and interferon antagonism activities of coronavirus papain-like proteases. *Journal of Virology*, *84*(9), 4619–29. doi:10.1128/JVI.02406-09; 10.1128/JVI.02406-09

Cotten, M., Watson, S. J., Zumla, A. I., Makhdoom, H. Q., Palser, A. L., Ong, S. H., … Memish, Z. A. (2014). Spread, circulation, and evolution of the middle East respiratory syndrome coronavirus. *mBio*, *5*(1). doi:10.1128/mBio.01062-13

Daffis, S., Szretter, K. J., Schriewer, J., Li, J., Youn, S., Errett, J., … Diamond, M. S. (2010). 2'-O methylation of the viral mRNA cap evades host restriction by IFIT family members. *Nature*, *468*(7322), 452–6. doi:10.1038/nature09489

De Wilde, A. H., Ray, V. S., Oudshoorn, D., Bestebroer, T. M., van Nieuwkoop, S., Limpens, R. W., … van den Hoogen, B. G. (2013). Human coronavirus-EMC replication induces severe in vitro cytopathology and is strongly inhibited by cyclosporin A or interferon-alpha treatment. *The Journal of General Virology*. doi:10.1099/vir.0.052910-0

De Wit, E., Prescott, J., Baseler, L., Bushmaker, T., Thomas, T., Lackemeyer, M. G., … Munster, V. J. (2013). The Middle East Respiratory Syndrome Coronavirus (MERS-CoV) Does Not Replicate in Syrian Hamsters. *PloS One*, *8*(7), e69127. doi:10.1371/journal.pone.0069127; 10.1371/journal.pone.0069127

De Wit, E., Rasmussen, A. L., Falzarano, D., Bushmaker, T., Feldmann, F., Brining, D. L., … Munster, V. J. (2013). Middle East respiratory syndrome coronavirus (MERS-CoV) causes transient lower respiratory tract infection in rhesus macaques. *Proceedings of the National Academy of Sciences*. doi:10.1073/pnas.1310744110

Dereeper, A., Guignon, V., Blanc, G., Audic, S., Buffet, S., Chevenet, F., … Gascuel, O. (2008). Phylogeny.fr: robust phylogenetic analysis for the non-specialist. *Nucleic Acids Research*, *36*(Web Server issue), W465–9. doi:10.1093/nar/gkn180

Devaraj, S. G., Wang, N., Chen, Z., Tseng, M., Barretto, N., Lin, R., … Li, K. (2007). Regulation of IRF-3-dependent innate immunity by the papain-like protease domain of the severe acute respiratory syndrome coronavirus. *The Journal of Biological Chemistry*, *282*(44), 32208–32221. doi:10.1074/jbc.M704870200

Dominguez, S. R., O'Shea, T. J., Oko, L. M., & Holmes, K. V. (2007). Detection of group 1 coronaviruses in bats in North America. *Emerging Infectious Diseases*, *13*(9), 1295–1300. doi:10.3201/eid1309.070491

Du, L., Zhao, G., Kou, Z., Ma, C., Sun, S., Poon, V. K., … Jiang, S. (2013). Identification of a receptor-binding domain in the s protein of the novel human coronavirus middle East respiratory syndrome coronavirus as an essential target for vaccine development. *Journal of Virology*, *87*(17), 9939–9942. doi:10.1128/JVI.01048-13; 10.1128/JVI.01048-13

Falzarano, D., de Wit, E., Rasmussen, A. L., Feldmann, F., Okumura, A., Scott, D. P., … Feldmann, H. (2013). Treatment with interferon-alpha2b and ribavirin improves outcome in MERS-CoV-infected rhesus macaques. *Nature Medicine*. doi:10.1038/nm.3362; 10.1038/nm.3362

Frieman, M., Basu, D., Matthews, K., Taylor, J., Jones, G., Pickles, R., … Engel, D. A. (2011). Yeast based small molecule screen for inhibitors of SARS-CoV. *PloS One*, *6*(12), e28479. doi:10.1371/journal.pone.0028479; 10.1371/journal.pone.0028479

Frieman, M., Ratia, K., Johnston, R. E., Mesecar, A. D., & Baric, R. S. (2009). Severe acute respiratory syndrome coronavirus papain-like protease ubiquitin-like domain and catalytic domain regulate antagonism of IRF3 and NF-kappaB signaling. *Journal of Virology*, *83*(13), 6689–6705. doi:10.1128/JVI.02220-08

Fukushi, S., Mizutani, T., Saijo, M., Matsuyama, S., Miyajima, N., Taguchi, F., … Morikawa, S. (2005). Vesicular stomatitis virus pseudotyped with severe acute respiratory syndrome coronavirus spike protein. *The Journal of General Virology*, *86*(Pt 8), 2269–2274. doi:10.1099/vir.0.80955-0

Galban, S., Jeon, Y. H., Bowman, B. M., Stevenson, J., Sebolt, K. A., Sharkey, L. M., … Rehemtulla, A. (2013). Imaging proteolytic activity in live cells and animal models. *PloS One*, *8*(6), e66248. doi:10.1371/journal.pone.0066248; 10.1371/journal.pone.0066248

Gao, J., Lu, G., Qi, J., Li, Y., Wu, Y., Deng, Y., … Gao, G. F. (2013). Structure of the fusion core and inhibition of fusion by a heptad-repeat peptide derived from the S protein of MERS-CoV. *Journal of Virology*. doi:10.1128/JVI.02433-13

Ge, F., Luo, Y., Liew, P. X., & Hung, E. (2007). Derivation of a novel SARS-coronavirus replicon cell line and its application for anti-SARS drug screening. *Virology*, *360*(1), 150–158. doi:10.1016/j.virol.2006.10.016

Ge, F., Xiong, S., Lin, F. S., Zhang, Z. P., & Zhang, X. E. (2008). High-throughput assay using a GFP-expressing replicon for SARS-CoV drug discovery. *Antiviral Research*, *80*(2), 107–113. doi:10.1016/j.antiviral.2008.05.005; 10.1016/j.antiviral.2008.05.005

Ghosh, A. K., Gong, G., Grum-Tokars, V., Mulhearn, D. C., Baker, S. C., Coughlin, M., … Mesecar, A. D. (2008). Design, synthesis and antiviral efficacy of a series of potent chloropyridyl ester-derived SARS-CoV 3CLpro inhibitors. *Bioorganic & Medicinal Chemistry Letters*, *18*(20), 5684–5688. doi:10.1016/j.bmcl.2008.08.082; 10.1016/j.bmcl.2008.08.082

Ghosh, A. K., Takayama, J., Aubin, Y., Ratia, K., Chaudhuri, R., Baez, Y., … Mesecar, A. D. (2009). Structure-based design, synthesis, and biological evaluation of a series of novel and reversible inhibitors for the severe acute respiratory syndrome-coronavirus papain-like protease. *Journal of Medicinal Chemistry*, *52*(16), 5228–5240. doi:10.1021/jm900611t; 10.1021/jm900611t

Ghosh, A. K., Takayama, J., Rao, K. V, Ratia, K., Chaudhuri, R., Mulhearn, D. C., … Mesecar, A. D. (2010). Severe acute respiratory syndrome coronavirus papain-like novel protease inhibitors: design, synthesis, protein-ligand X-ray structure and biological evaluation. *Journal of Medicinal Chemistry*, *53*(13), 4968–4979. doi:10.1021/jm1004489; 10.1021/jm1004489

Gierer, S., Bertram, S., Kaup, F., Wrensch, F., Heurich, A., Kramer-Kuhl, A., … Pohlmann, S. (2013). The Spike Protein of the Emerging Betacoronavirus EMC Uses a Novel Coronavirus Receptor for Entry, Can Be Activated by TMPRSS2, and Is Targeted by Neutralizing Antibodies. *Journal of Virology*, *87*(10), 5502–5511. doi:10.1128/JVI.00128-13; 10.1128/JVI.00128-13

Giroglou, T., Cinatl Jr, J., Rabenau, H., Drosten, C., Schwalbe, H., Doerr, H. W., & von Laer, D. (2004). Retroviral vectors pseudotyped with severe acute respiratory syndrome coronavirus S protein. *Journal of Virology*, *78*(17), 9007–9015. doi:10.1128/JVI.78.17.9007-9015.2004

Glowacka, I., Bertram, S., Muller, M. A., Allen, P., Soilleux, E., Pfefferle, S., … Pohlmann, S. (2011). Evidence that TMPRSS2 activates the severe acute respiratory syndrome coronavirus spike protein for membrane fusion and reduces viral control by the humoral immune response. *Journal of Virology*, *85*(9), 4122–4134. doi:10.1128/JVI.02232-10; 10.1128/JVI.02232-10

Gonzalez, C. M., Wang, L., & Damania, B. (2009). Kaposi's sarcoma-associated herpesvirus encodes a viral deubiquitinase. *Journal of Virology*, *83*(19), 10224–10233. doi:10.1128/JVI.00589-09

Gorbalenya, A. E., Koonin, E. V, Donchenko, A. P., & Blinov, V. M. (1989). Coronavirus genome: prediction of putative functional domains in the non-structural polyprotein by comparative amino acid sequence analysis. *Nucleic Acids Research*, *17*(12), 4847–61. Retrieved from http://www.pubmedcentral.nih.gov/articlerender.fcgi?artid=318036&tool=pmcentrez&rendertype=abstract

Gosert, R., Kanjanahaluethai, A., Egger, D., Bienz, K., & Baker, S. C. (2002). RNA replication of mouse hepatitis virus takes place at double-membrane vesicles. *Journal of Virology*, *76*(8), 3697–3708.

Gredmark, S., Schlieker, C., Quesada, V., Spooner, E., & Ploegh, H. L. (2007). A functional ubiquitin-specific protease embedded in the large tegument protein (ORF64) of murine gammaherpesvirus 68 is active during the course of infection. *Journal of Virology*, *81*(19), 10300–10309. doi:10.1128/JVI.01149-07

Hamre, D., Kindig, D. A., & Mann, J. (1967). Growth and intracellular development of a new respiratory virus. *Journal of Virology*, *1*(4), 810–6. Retrieved from http://www.pubmedcentral.nih.gov/articlerender.fcgi?artid=375356&tool=pmcentrez&rendertype=abstract

Han, D. P., Penn-Nicholson, A., & Cho, M. W. (2006). Identification of critical determinants on ACE2 for SARS-CoV entry and development of a potent entry inhibitor. *Virology*, *350*(1), 15–25. doi:10.1016/j.virol.2006.01.029

Han, Y.-S. S., Chang, G.-G. G., Juo, C.-G. G., Lee, H.-J. J., Yeh, S.-H. H., Hsu, J. T.-A., & Chen, X. (2005). Papain-like protease 2 (PLP2) from severe acute respiratory syndrome coronavirus (SARS-CoV): expression, purification, characterization, and inhibition. *Biochemistry*, *44*(30), 10349–10359. doi:10.1021/bi0504761

Harcourt, B. H., Jukneliene, D., Kanjanahaluethai, A., Bechill, J., Severson, K. M., Smith, C. M., … Baker, S. C. (2004). Identification of severe acute respiratory syndrome coronavirus replicase products and characterization of papain-like protease activity. *Journal of Virology*, *78*(24), 13600–13612. doi:10.1128/JVI.78.24.13600-13612.2004

Henrich, T. J., & Kuritzkes, D. R. (2013). HIV-1 entry inhibitors: recent development and clinical use. *Current Opinion in Virology*, *3*(1), 51–57. doi:10.1016/j.coviro.2012.12.002; 10.1016/j.coviro.2012.12.002

Hofmann, H., Hattermann, K., Marzi, A., Gramberg, T., Geier, M., Krumbiegel, M., … Pohlmann, S. (2004). S protein of severe acute respiratory syndrome-associated coronavirus mediates entry into hepatoma cell lines and is targeted by neutralizing antibodies in infected patients. *Journal of Virology*, *78*(12), 6134–6142. doi:10.1128/JVI.78.12.6134-6142.2004

Horner, S. M., Liu, H. M., Park, H. S., Briley, J., & Gale Jr, M. (2011). Mitochondrial-associated endoplasmic reticulum membranes (MAM) form innate immune synapses and are targeted by hepatitis C virus. *Proceedings of the National Academy of Sciences of the United States of America*, *108*(35), 14590–14595. doi:10.1073/pnas.1110133108

Hou, F., Sun, L., Zheng, H., Skaug, B., Jiang, Q. X., & Chen, Z. J. (2011). MAVS forms functional prion-like aggregates to activate and propagate antiviral innate immune response. *Cell*, *146*(3), 448–461. doi:10.1016/j.cell.2011.06.041

Hurst, K. R., Koetzner, C. A., & Masters, P. S. (2013). Characterization of a critical interaction between the coronavirus nucleocapsid protein and nonstructural protein 3 of the viral replicase-transcriptase complex. *Journal of Virology*, *87*(16), 9159–72. doi:10.1128/JVI.01275-13

Hurst, K. R., Ye, R., Goebel, S. J., Jayaraman, P., & Masters, P. S. (2010). An interaction between the nucleocapsid protein and a component of the replicase-transcriptase complex is crucial for the infectivity of coronavirus genomic RNA. *Journal of Virology*, *84*(19), 10276–10288. doi:10.1128/JVI.01287-10

Inn, K. S., Lee, S. H., Rathbun, J. Y., Wong, L. Y., Toth, Z., Machida, K., … Jung, J. U. (2011). Inhibition of RIG-I-mediated signaling by Kaposi's sarcoma-associated herpesvirus-encoded deubiquitinase ORF64. *Journal of Virology*, *85*(20), 10899–10904. doi:10.1128/JVI.00690-11

James, T. W., Frias-Staheli, N., Bacik, J. P., Levingston Macleod, J. M., Khajehpour, M., Garcia-Sastre, A., & Mark, B. L. (2011). Structural basis for the removal of ubiquitin and interferon-stimulated gene 15 by a viral ovarian tumor domain-containing protease. *Proceedings of the National Academy of Sciences of the United States of America*, *108*(6), 2222–2227. doi:10.1073/pnas.1013388108

Jiang, X., Kinch, L. N., Brautigam, C. A., Chen, X., Du, F., Grishin, N. V, & Chen, Z. J. (2012). Ubiquitin-induced oligomerization of the RNA sensors RIG-I and MDA5 activates antiviral innate immune response. *Immunity*, *36*(6), 959–973. doi:10.1016/j.immuni.2012.03.022

Josset, L., Menachery, V. D., Gralinski, L. E., Agnihothram, S., Sova, P., Carter, V. S., … Katze, M. G. (2013). Cell host response to infection with novel human coronavirus EMC predicts potential antivirals and important differences with SARS coronavirus. *mBio*, *4*(3), e00165–13. doi:10.1128/mBio.00165-13; 10.1128/mBio.00165-13

Kamitani, W., Huang, C., Narayanan, K., Lokugamage, K. G., & Makino, S. (2009). A two-pronged strategy to suppress host protein synthesis by SARS coronavirus Nsp1 protein. *Nature Structural & Molecular Biology*, *16*(11), 1134–40. doi:10.1038/nsmb.1680

Kanjanahaluethai, A., Jukneliene, D., & Baker, S. C. (2003). Identification of the murine coronavirus MP1 cleavage site recognized by papain-like proteinase 2. *Journal of*

Virology, *77*(13), 7376–7382. Retrieved from http://www.pubmedcentral.nih.gov/articlerender.fcgi?artid=164800&tool=pmcentrez&rendertype=abstract

Kao, R. Y., Tsui, W. H., Lee, T. S., Tanner, J. A., Watt, R. M., Huang, J. D., … Yuen, K. Y. (2004). Identification of novel small-molecule inhibitors of severe acute respiratory syndrome-associated coronavirus by chemical genetics. *Chemistry & Biology*, *11*(9), 1293–1299. doi:10.1016/j.chembiol.2004.07.013

Karpe, Y. A., & Lole, K. S. (2011). Deubiquitination activity associated with hepatitis E virus putative papain-like cysteine protease. *The Journal of General Virology*, *92*(Pt 9), 2088–2092. doi:10.1099/vir.0.033738-0

Kawase, M., Shirato, K., van der Hoek, L., Taguchi, F., & Matsuyama, S. (2012). Simultaneous treatment of human bronchial epithelial cells with serine and cysteine protease inhibitors prevents severe acute respiratory syndrome coronavirus entry. *Journal of Virology*, *86*(12), 6537–6545. doi:10.1128/JVI.00094-12; 10.1128/JVI.00094-12

Ke, M., Chen, Y., Wu, A., Sun, Y., Su, C., Wu, H., … Guo, D. (2012). Short peptides derived from the interaction domain of SARS coronavirus nonstructural protein nsp10 can suppress the 2'-O-methyltransferase activity of nsp10/nsp16 complex. *Virus Research*, *167*(2), 322–328. doi:10.1016/j.virusres.2012.05.017; 10.1016/j.virusres.2012.05.017

Kilianski, A., & Baker, S. C. (2014). Cell-based antiviral screening against coronaviruses: Developing virus-specific and broad-spectrum inhibitors. *Antiviral Research*, *101*(0), 105–112. doi:http://dx.doi.org/10.1016/j.antiviral.2013.11.004

Kilianski, A., Mielech, A. M., Deng, X., & Baker, S. C. (2013). Assessing activity and inhibition of Middle East respiratory syndrome coronavirus papain-like and 3C-like proteases using luciferase-based biosensors. *Journal of Virology*, *87*(21), 11955–62. doi:10.1128/JVI.02105-13

Knoops, K., Bárcena, M., Limpens, R. W. A. L., Koster, A. J., Mommaas, A. M., & Snijder, E. J. (2012). Ultrastructural characterization of arterivirus replication structures: reshaping the endoplasmic reticulum to accommodate viral RNA synthesis. *Journal of Virology*, *86*(5), 2474–87. doi:10.1128/JVI.06677-11

Knoops, K., Kikkert, M., Worm, S. H. E. van den, Zevenhoven-Dobbe, J. C., van der Meer, Y., Koster, A. J., … Snijder, E. J. (2008). SARS-coronavirus replication is supported by a reticulovesicular network of modified endoplasmic reticulum. *PLoS Biology*, *6*(9), e226. doi:10.1371/journal.pbio.0060226

Konstantinidis, A. K., Richardson, P. L., Kurtz, K. A., Tripathi, R., Chen, C.-M., Huang, P., … Kati, W. M. (2007). Longer wavelength fluorescence resonance energy transfer depsipeptide substrates for hepatitis C virus NS3 protease. *Analytical Biochemistry*, *368*(2), 156–67. doi:10.1016/j.ab.2007.06.020

Kopecky-Bromberg, S. A., Martínez-Sobrido, L., Frieman, M., Baric, R. A., & Palese, P. (2007). Severe acute respiratory syndrome coronavirus open reading frame (ORF) 3b, ORF 6, and nucleocapsid proteins function as interferon antagonists. *Journal of Virology*, *81*(2), 548–57. doi:10.1128/JVI.01782-06

Kuri, T., Eriksson, K. K., Putics, A., Züst, R., Snijder, E. J., Davidson, A. D., … Weber, F. (2011). The ADP-ribose-1''-monophosphatase domains of severe acute respiratory syndrome coronavirus and human coronavirus 229E mediate resistance to antiviral interferon responses. *The Journal of General Virology*, *92*(Pt 8), 1899–905. doi:10.1099/vir.0.031856-0

Lau, S. K., Woo, P. C., Li, K. S., Huang, Y., Tsoi, H. W., Wong, B. H., … Yuen, K. Y. (2005). Severe acute respiratory syndrome coronavirus-like virus in Chinese horseshoe bats. *Proceedings of the National Academy of Sciences of the United States of America*, *102*(39), 14040–14045. doi:10.1073/pnas.0506735102

Le Negrate, G. (2012). Viral interference with innate immunity by preventing NF-κB activity. *Cellular Microbiology*, *14*(2), 168–81. doi:10.1111/j.1462-5822.2011.01720.x

Lee, J. I., Sollars, P. J., Baver, S. B., Pickard, G. E., Leelawong, M., & Smith, G. A. (2009). A herpesvirus encoded deubiquitinase is a novel neuroinvasive determinant. *PLoS Pathogens*, *5*(4), e1000387. doi:10.1371/journal.ppat.1000387; 10.1371/journal.ppat.1000387

Lenschow, D. J. (2010). Antiviral Properties of ISG15. *Viruses*, *2*(10), 2154–2168. doi:10.3390/v2102154

Lenschow, D. J., Giannakopoulos, N. V, Gunn, L. J., Johnston, C., O'Guin, A. K., Schmidt, R. E., … Virgin 4th, H. W. (2005). Identification of interferon-stimulated gene 15 as an antiviral molecule during Sindbis virus infection in vivo. *Journal of Virology*, *79*(22), 13974–13983. doi:10.1128/JVI.79.22.13974-13983.2005

Lenschow, D. J., Lai, C., Frias-Staheli, N., Giannakopoulos, N. V, Lutz, A., Wolff, T., … Virgin 4th, H. W. (2007). IFN-stimulated gene 15 functions as a critical antiviral molecule against influenza, herpes, and Sindbis viruses. *Proceedings of the National Academy of Sciences of the United States of America*, *104*(4), 1371–1376. doi:10.1073/pnas.0607038104

Li, F. (2013). Receptor recognition and cross-species infections of SARS coronavirus. *Antiviral Research*, *100*(1), 246–254. doi:10.1016/j.antiviral.2013.08.014; 10.1016/j.antiviral.2013.08.014

Li, S. W., Lai, C. C., Ping, J. F., Tsai, F. J., Wan, L., Lin, Y. J., … Lin, C. W. (2011). Severe acute respiratory syndrome coronavirus papain-like protease suppressed alpha interferon-induced responses through downregulation of extracellular signal-regulated kinase 1-mediated signalling pathways. *The Journal of General Virology*, *92*(Pt 5), 1127–1140. doi:10.1099/vir.0.028936-0

Li, S.-W., Yang, T.-C., Wan, L., Lin, Y.-J., Tsai, F.-J., Lai, C.-C., & Lin, C.-W. (2012). Correlation between TGF-β1 expression and proteomic profiling induced by severe acute respiratory syndrome coronavirus papain-like protease. *Proteomics*, *12*(21), 3193–205. doi:10.1002/pmic.201200225

Lin, C. W., Tsai, C. H., Tsai, F. J., Chen, P. J., Lai, C. C., Wan, L., … Lin, K. H. (2004). Characterization of trans- and cis-cleavage activity of the SARS coronavirus 3CLpro protease: basis for the in vitro screening of anti-SARS drugs. *FEBS Letters*, *574*(1-3), 131–137. doi:10.1016/j.febslet.2004.08.017

Lindner, H. A., Fotouhi-Ardakani, N., Lytvyn, V., Lachance, P., Sulea, T., & Menard, R. (2005). The papain-like protease from the severe acute respiratory syndrome coronavirus is a deubiquitinating enzyme. *Journal of Virology*, *79*(24), 15199–15208. doi:10.1128/JVI.79.24.15199-15208.2005

Lindner, H. A., Lytvyn, V., Qi, H., Lachance, P., Ziomek, E., & Menard, R. (2007). Selectivity in ISG15 and ubiquitin recognition by the SARS coronavirus papain-like protease. *Archives of Biochemistry and Biophysics*, *466*(1), 8–14. doi:10.1016/j.abb.2007.07.006

Liu, I. J., Kao, C. L., Hsieh, S. C., Wey, M. T., Kan, L. S., & Wang, W. K. (2009). Identification of a minimal peptide derived from heptad repeat (HR) 2 of spike protein of SARS-CoV and combination of HR1-derived peptides as fusion inhibitors. *Antiviral Research*, *81*(1), 82–87. doi:10.1016/j.antiviral.2008.10.001; 10.1016/j.antiviral.2008.10.001

Lokugamage, K. G., Narayanan, K., Huang, C., & Makino, S. (2012). Severe acute respiratory syndrome coronavirus protein nsp1 is a novel eukaryotic translation inhibitor that represses multiple steps of translation initiation. *Journal of Virology*, *86*(24), 13598–608. doi:10.1128/JVI.01958-12

Lu, G., Hu, Y., Wang, Q., Qi, J., Gao, F., Li, Y., … Gao, G. F. (2013). Molecular basis of binding between novel human coronavirus MERS-CoV and its receptor CD26. *Nature*, *500*(7461), 227–231. doi:10.1038/nature12328; 10.1038/nature12328

Ma, X.-Z., Bartczak, A., Zhang, J., He, W., Shalev, I., Smil, D., … McGilvray, I. (2014). Protein ISGylation delays but does not overcome coronavirus proliferation in a model of fulminant hepatitis. *Journal of Virology*. doi:10.1128/JVI.03801-13

Matsuyama, S., Nagata, N., Shirato, K., Kawase, M., Takeda, M., & Taguchi, F. (2010). Efficient activation of the severe acute respiratory syndrome coronavirus spike protein by the transmembrane protease TMPRSS2. *Journal of Virology*, *84*(24), 12658–12664. doi:10.1128/JVI.01542-10; 10.1128/JVI.01542-10

Memish ZA Olival KJ, Fagbo SF, Kapoor V, Epstein JH, et al., M. N. (2013). Middle East Respiratory Syndrome Coronavirus in Bats, Saudi Arabia. *Emerg Infect Dis [Internet]*. doi:0.3201/eid1911.131172

Menachery, V. D., Eisfeld, A. J., Schäfer, A., Josset, L., Sims, A. C., Proll, S., … Baric, R. S. (2014). Pathogenic influenza viruses and coronaviruses utilize similar and contrasting approaches to control interferon-stimulated gene responses. *mBio*, *5*(3), e01174–14. doi:10.1128/mBio.01174-14

Mielech, A. M., Chen, Y., Mesecar, A. D., & Baker, S. C. (2014). Nidovirus papain-like proteases: Multifunctional enzymes with protease, deubiquitinating and deISGylating activities. *Virus Research*. doi:10.1016/j.virusres.2014.01.025

Mielech, A. M., Kilianski, A., Baez-Santos, Y. M., Mesecar, A. D., & Baker, S. C. (2014). MERS-CoV papain-like protease has deISGylating and deubiquitinating activities. *Virology*, *450-451*, 64–70. doi:10.1016/j.virol.2013.11.040

Mondal, S. P., & Cardona, C. J. (2004). Comparison of four regions in the replicase gene of heterologous infectious bronchitis virus strains. *Virology*, *324*(1), 238–48. doi:10.1016/j.virol.2004.03.032

Moore, M. J., Dorfman, T., Li, W., Wong, S. K., Li, Y., Kuhn, J. H., … Choe, H. (2004). Retroviruses pseudotyped with the severe acute respiratory syndrome coronavirus spike protein efficiently infect cells expressing angiotensin-converting enzyme 2. *Journal of Virology*, *78*(19), 10628–10635. doi:10.1128/JVI.78.19.10628-10635.2004

Morales, D. J., & Lenschow, D. J. (2013). The antiviral activities of ISG15. *Journal of Molecular Biology*, *425*(24), 4995–5008. doi:10.1016/j.jmb.2013.09.041

Mou, H., Raj, V. S., van Kuppeveld, F. J., Rottier, P. J., Haagmans, B. L., & Bosch, B. J. (2013). The receptor binding domain of the new MERS coronavirus maps to a 231-residue region in the spike protein that efficiently elicits neutralizing antibodies. *Journal of Virology*, *87*(16), 9379–9383. doi:10.1128/JVI.01277-13; 10.1128/JVI.01277-13

Muller, M. A., Raj, V. S., Muth, D., Meyer, B., Kallies, S., Smits, S. L., … Drosten, C. (2012). Human coronavirus EMC does not require the SARS-coronavirus receptor and maintains broad replicative capability in mammalian cell lines. *mBio*, *3*(6), 10.1128/mBio.00515–12. doi:10.1128/mBio.00515-12; 10.1128/mBio.00515-12

Munster, V. J., de Wit, E., & Feldmann, H. (2013). Pneumonia from human coronavirus in a macaque model. *The New England Journal of Medicine*, *368*(16), 1560–1562. doi:10.1056/NEJMc1215691; 10.1056/NEJMc1215691

Narasimhan, J., Wang, M., Fu, Z., Klein, J. M., Haas, A. L., & Kim, J. J. (2005). Crystal structure of the interferon-induced ubiquitin-like protein ISG15. *J Biol Chem*, *280*(29), 27356–27365. doi:M502814200 [pii] 10.1074/jbc.M502814200

Neuman, B. W., Joseph, J. S., Saikatendu, K. S., Serrano, P., Chatterjee, A., Johnson, M. A., … Kuhn, P. (2008). Proteomics analysis unravels the functional repertoire of coronavirus nonstructural protein 3. *Journal of Virology*, *82*(11), 5279–94. doi:10.1128/JVI.02631-07

Ni, L., Zhu, J., Zhang, J., Yan, M., Gao, G. F., & Tien, P. (2005). Design of recombinant protein-based SARS-CoV entry inhibitors targeting the heptad-repeat regions of the spike protein S2 domain. *Biochemical and Biophysical Research Communications*, *330*(1), 39–45. doi:10.1016/j.bbrc.2005.02.117

Ohnuma, K., Haagmans, B. L., Hatano, R., Raj, V. S., Mou, H., Iwata, S., … Morimoto, C. (2013). Inhibition of Middle East Respiratory Syndrome Coronavirus (MERS-CoV) Infection by Anti-CD26 Monoclonal Antibody. *Journal of Virology*. doi:10.1128/JVI.02448-13

Oka, T., Takagi, H., Tohya, Y., Murakami, K., Takeda, N., Wakita, T., & Katayama, K. (2011). Bioluminescence technologies to detect calicivirus protease activity in cell-free system and in infected cells. *Antiviral Research*, *90*(1), 9–16. doi:10.1016/j.antiviral.2011.02.002; 10.1016/j.antiviral.2011.02.002

Paul, D., & Bartenschlager, R. (2013). Architecture and biogenesis of plus-strand RNA virus replication factories. *World Journal of Virology*, *2*(2), 32–48. doi:10.5501/wjv.v2.i2.32

Perera, R., Wang, P., Gomaa, M., El-Shesheny, R., Kandeil, A., Bagato, O., … Kayali, G. (2013). Seroepidemiology for MERS coronavirus using microneutralisation and pseudoparticle virus neutralisation assays reveal a high prevalence of antibody in dromedary camels in Egypt, June 2013. *Euro Surveillance : Bulletin Europeen Sur Les Maladies Transmissibles = European Communicable Disease Bulletin*, *18*(36), 20574.

Perlman, S., & Netland, J. (2009). Coronaviruses post-SARS: update on replication and pathogenesis. *Nature reviews.Microbiology*, *7*(6), 439–450. doi:10.1038/nrmicro2147

Pfefferle, S., Schopf, J., Kogl, M., Friedel, C. C., Muller, M. A., Carbajo-Lozoya, J., … von Brunn, A. (2011). The SARS-coronavirus-host interactome: identification of cyclophilins as target for pan-coronavirus inhibitors. *PLoS Pathogens*, *7*(10), e1002331. doi:10.1371/journal.ppat.1002331; 10.1371/journal.ppat.1002331

Poon, L. L., Chu, D. K., Chan, K. H., Wong, O. K., Ellis, T. M., Leung, Y. H., … Peiris, J. S. (2005). Identification of a novel coronavirus in bats. *Journal of Virology*, *79*(4), 2001–2009. doi:10.1128/JVI.79.4.2001-2009.2005

Putics, A., Filipowicz, W., Hall, J., Gorbalenya, A. E., & Ziebuhr, J. (2005). ADP-ribose-1"-monophosphatase: a conserved coronavirus enzyme that is dispensable for viral replication in tissue culture. *Journal of Virology*, *79*(20), 12721–31. doi:10.1128/JVI.79.20.12721-12731.2005

Pyrc, K., Sims, A. C., Dijkman, R., Jebbink, M., Long, C., Deming, D., … Pickles, R. (2010). Culturing the unculturable: human coronavirus HKU1 infects, replicates, and produces progeny virions in human ciliated airway epithelial cell cultures. *Journal of Virology*, *84*(21), 11255–63. doi:10.1128/JVI.00947-10

Raj, V. S., Mou, H., Smits, S. L., Dekkers, D. H., Muller, M. A., Dijkman, R., … Haagmans, B. L. (2013). Dipeptidyl peptidase 4 is a functional receptor for the emerging human coronavirus-EMC. *Nature*, *495*(7440), 251–254. doi:10.1038/nature12005; 10.1038/nature12005

Ratia, K., Kilianski, A., Baez-Santos, Y. M., Baker, S. C., & Mesecar, A. D. (2014). Structural basis for the ubiquitin-linkage specificity and deISGylating activity of SARS-CoV papain-like protease. *PLoS Pathogens*, *In Press*.

Ratia, K., Pegan, S., Takayama, J., Sleeman, K., Coughlin, M., Baliji, S., … Mesecar, A. D. (2008). A noncovalent class of papain-like protease/deubiquitinase inhibitors blocks SARS virus replication. *Proceedings of the National Academy of Sciences of*

the United States of America, *105*(42), 16119–16124. doi:10.1073/pnas.0805240105; 10.1073/pnas.0805240105

Ratia, K., Saikatendu, K. S., Santarsiero, B. D., Barretto, N., Baker, S. C., Stevens, R. C., & Mesecar, A. D. (2006). Severe acute respiratory syndrome coronavirus papain-like protease: structure of a viral deubiquitinating enzyme. *Proceedings of the National Academy of Sciences of the United States of America*, *103*(15), 5717–5722. doi:10.1073/pnas.0510851103

Reggiori, F., de Haan, C. A., & Molinari, M. (2011). Unconventional use of LC3 by coronaviruses through the alleged subversion of the ERAD tuning pathway. *Viruses*, *3*(9), 1610–1623. doi:10.3390/v3091610

Reggiori, F., Monastyrska, I., Verheije, M. H., Cali, T., Ulasli, M., Bianchi, S., … Molinari, M. (2010). Coronaviruses Hijack the LC3-I-positive EDEMosomes, ER-derived vesicles exporting short-lived ERAD regulators, for replication. *Cell Host & Microbe*, *7*(6), 500–508. doi:10.1016/j.chom.2010.05.013

Ren, Z., Yan, L., Zhang, N., Guo, Y., Yang, C., Lou, Z., & Rao, Z. (2013). The newly emerged SARS-like coronavirus HCoV-EMC also has an "Achilles' heel": current effective inhibitor targeting a 3C-like protease. *Protein & Cell*, *4*(4), 248–250. doi:10.1007/s13238-013-2841-3; 10.1007/s13238-013-2841-3

Reusken, C. B. E. M., Haagmans, B. L., Müller, Gutierrez, C., Godeke, G.-J. J., Meyer, B., … Koopmans, M. P. (2013). Middle East respiratory syndrome coronavirus neutralising serum antibodies in dromedary camels: a comparative serological study. *The Lancet Infectious Diseases*. doi:10.1016/S1473-3099(13)70164-6; 10.1016/S1473-3099(13)70164-6

Romero-Brey, I., Merz, A., Chiramel, A., Lee, J.-Y., Chlanda, P., Haselman, U., … Bartenschlager, R. (2012). Three-dimensional architecture and biogenesis of membrane structures associated with hepatitis C virus replication. *PLoS Pathogens*, *8*(12), e1003056. doi:10.1371/journal.ppat.1003056

Scobey, T., Yount, B. L., Sims, A. C., Donaldson, E. F., Agnihothram, S. S., Menachery, V. D., … Baric, R. S. (2013). Reverse genetics with a full-length infectious cDNA of the Middle East respiratory syndrome coronavirus. *Proceedings of the National Academy of Sciences of the United States of America*, *110*(40), 16157–16162. doi:10.1073/pnas.1311542110; 10.1073/pnas.1311542110

Shah, P. P., Wang, T., Kaletsky, R. L., Myers, M. C., Purvis, J. E., Jing, H., … Diamond, S. L. (2010). A small-molecule oxocarbazate inhibitor of human cathepsin L blocks severe acute respiratory syndrome and ebola pseudotype virus infection into human

embryonic kidney 293T cells. *Molecular Pharmacology*, *78*(2), 319–324. doi:10.1124/mol.110.064261; 10.1124/mol.110.064261

Shirato, K., Kawase, M., & Matsuyama, S. (2013). Middle East Respiratory Syndrome Coronavirus (MERS-CoV) Infection Mediated by the Transmembrane Serine Protease TMPRSS2. *Journal of Virology*. doi:10.1128/JVI.01890-13

Shulla, A., Heald-Sargent, T., Subramanya, G., Zhao, J., Perlman, S., & Gallagher, T. (2011). A transmembrane serine protease is linked to the severe acute respiratory syndrome coronavirus receptor and activates virus entry. *Journal of Virology*, *85*(2), 873–882. doi:10.1128/JVI.02062-10; 10.1128/JVI.02062-10

Siddell, S., Wege, H., & Ter Meulen, V. (1983). The biology of coronaviruses. *The Journal of General Virology*, *64 (Pt 4)*, 761–76. Retrieved from http://www.ncbi.nlm.nih.gov/pubmed/6300299

Simmons, G., Gosalia, D. N., Rennekamp, A. J., Reeves, J. D., Diamond, S. L., & Bates, P. (2005). Inhibitors of cathepsin L prevent severe acute respiratory syndrome coronavirus entry. *Proceedings of the National Academy of Sciences of the United States of America*, *102*(33), 11876–11881. doi:10.1073/pnas.0505577102

Simmons, G., Zmora, P., Gierer, S., Heurich, A., & Pohlmann, S. (2013). Proteolytic activation of the SARS-coronavirus spike protein: Cutting enzymes at the cutting edge of antiviral research. *Antiviral Research*. doi:10.1016/j.antiviral.2013.09.028; 10.1016/j.antiviral.2013.09.028

Siu, K.-L., Yeung, M. L., Kok, K.-H., Yuen, K.-S., Kew, C., Lui, P.-Y., … Jin, D.-Y. (2014). Middle east respiratory syndrome coronavirus 4a protein is a double-stranded RNA-binding protein that suppresses PACT-induced activation of RIG-I and MDA5 in the innate antiviral response. *Journal of Virology*, *88*(9), 4866–76. doi:10.1128/JVI.03649-13

Snijder, E. J., van der Meer, Y., Zevenhoven-Dobbe, J., Onderwater, J. J., van der Meulen, J., Koerten, H. K., & Mommaas, A. M. (2006). Ultrastructure and origin of membrane vesicles associated with the severe acute respiratory syndrome coronavirus replication complex. *Journal of Virology*, *80*(12), 5927–5940. doi:10.1128/JVI.02501-05

Stockman, L. J., Haynes, L. M., Miao, C., Harcourt, J. L., Rupprecht, C. E., Ksiazek, T. G., … Anderson, L. J. (2008). Coronavirus antibodies in bat biologists. *Emerging Infectious Diseases*, *14*(6), 999–1000. doi:10.3201/eid1406.070964

Struck, A. W., Axmann, M., Pfefferle, S., Drosten, C., & Meyer, B. (2012). A hexapeptide of the receptor-binding domain of SARS corona virus spike protein blocks viral entry into host cells via the human receptor ACE2. *Antiviral Research*, *94*(3), 288–296. doi:10.1016/j.antiviral.2011.12.012; 10.1016/j.antiviral.2011.12.012

Sulea, T., Lindner, H. A., Purisima, E. O., Menard, R., & Ménard, R. (2005). Deubiquitination, a new function of the severe acute respiratory syndrome coronavirus papain-like protease? *J Virol*, *79*(7), 4550–4551. doi:10.1128/JVI.79.7.4550-4551.2005

Sun, L., Xing, Y., Chen, X., Zheng, Y., Yang, Y., Nichols, D. B., … Chen, Z. (2012). Coronavirus papain-like proteases negatively regulate antiviral innate immune response through disruption of STING-mediated signaling. *PloS One*, *7*(2), e30802. doi:10.1371/journal.pone.0030802; 10.1371/journal.pone.0030802

Sun, S., Elwood, J., & Greene, W. C. (1996). Both amino- and carboxyl-terminal sequences within I kappa B alpha regulate its inducible degradation. *Molecular and Cellular Biology*, *16*(3), 1058–1065.

Sun, Z., Li, Y., Ransburgh, R., Snijder, E. J., & Fang, Y. (2012). Nonstructural protein 2 of porcine reproductive and respiratory syndrome virus inhibits the antiviral function of interferon-stimulated gene 15. *Journal of Virology*, *86*(7), 3839–3850. doi:10.1128/JVI.06466-11

Tan, J., Vonrhein, C., Smart, O. S., Bricogne, G., Bollati, M., Kusov, Y., … Hilgenfeld, R. (2009). The SARS-unique domain (SUD) of SARS coronavirus contains two macrodomains that bind G-quadruplexes. *PLoS Pathogens*, *5*(5), e1000428. doi:10.1371/journal.ppat.1000428

Tanner, J. A., Zheng, B. J., Zhou, J., Watt, R. M., Jiang, J. Q., Wong, K. L., … Huang, J. D. (2005). The adamantane-derived bananins are potent inhibitors of the helicase activities and replication of SARS coronavirus. *Chemistry & Biology*, *12*(3), 303–311. doi:10.1016/j.chembiol.2005.01.006

Te Velthuis, A. J., van den Worm, S. H., Sims, A. C., Baric, R. S., Snijder, E. J., & van Hemert, M. J. (2010). Zn(2+) inhibits coronavirus and arterivirus RNA polymerase activity in vitro and zinc ionophores block the replication of these viruses in cell culture. *PLoS Pathogens*, *6*(11), e1001176. doi:10.1371/journal.ppat.1001176; 10.1371/journal.ppat.1001176

Totura, A. L., & Baric, R. S. (2012). SARS coronavirus pathogenesis: host innate immune responses and viral antagonism of interferon. *Current Opinion in Virology*, *2*(3), 264–275. doi:10.1016/j.coviro.2012.04.004

Tsang, K. W., Ho, P. L., Ooi, G. C., Yee, W. K., Wang, T., Chan-Yeung, M., … Lai, K. N. (2003). A cluster of cases of severe acute respiratory syndrome in Hong Kong. *The New England Journal of Medicine*, *348*(20), 1977–1985. doi:10.1056/NEJMoa030666

Ujike, M., Nishikawa, H., Otaka, A., Yamamoto, N., Matsuoka, M., Kodama, E., … Taguchi, F. (2008). Heptad repeat-derived peptides block protease-mediated direct entry from the cell surface of severe acute respiratory syndrome coronavirus but not entry via the endosomal pathway. *Journal of Virology*, *82*(1), 588–592. doi:10.1128/JVI.01697-07

Van Hemert, M. J., van den Worm, S. H. E., Knoops, K., Mommaas, A. M., Gorbalenya, A. E., & Snijder, E. J. (2008). SARS-coronavirus replication/transcription complexes are membrane-protected and need a host factor for activity in vitro. *PLoS Pathogens*, *4*(5), e1000054. doi:10.1371/journal.ppat.1000054

Van Kasteren, P. B., Bailey-Elkin, B. A., James, T. W., Ninaber, D. K., Beugeling, C., Khajehpour, M., … Kikkert, M. (2013). Deubiquitinase function of arterivirus papain-like protease 2 suppresses the innate immune response in infected host cells. *Proceedings of the National Academy of Sciences of the United States of America*, *110*(9), E838–47. Retrieved from http://archer.luhs.org/login?url=http://tb2lc4tl2v.search.serialssolutions.com/?url_ver=Z39.88-2004&rft_val_fmt=info:ofi/fmt:kev:mtx:journal&rfr_id=info:sid/Ovid:medc&rft.genre=article&rft_id=info:doi/10.1073/pnas.1218464110&rft_id=info:pmid/23401522&rft.issn=0027-8424&rft.volume=110&rft.issue=9&rft.spage=E838&rft.pages=E838-47&rft.date=2013&rft.jtitle=Proceedings+of+the+National+Academy+of+Sciences+of+the+United+States+of+America&rft.atitle=Deubiquitinase+function+of+arterivirus+papain-like+p

Van Kasteren, P. B., Beugeling, C., Ninaber, D. K., Frias-Staheli, N., van Boheemen, S., Garcia-Sastre, A., … Kikkert, M. (2012). Arterivirus and nairovirus ovarian tumor domain-containing Deubiquitinases target activated RIG-I to control innate immune signaling. *Journal of Virology*, *86*(2), 773–785. doi:10.1128/JVI.06277-11

Verschueren, K. H., Pumpor, K., Anemuller, S., Chen, S., Mesters, J. R., & Hilgenfeld, R. (2008). A structural view of the inactivation of the SARS coronavirus main

proteinase by benzotriazole esters. *Chemistry & Biology*, *15*(6), 597–606. doi:10.1016/j.chembiol.2008.04.011; 10.1016/j.chembiol.2008.04.011

Viswanathan, K., Fruh, K., & DeFilippis, V. (2010). Viral hijacking of the host ubiquitin system to evade interferon responses. *Current Opinion in Microbiology*, *13*(4), 517–523. doi:10.1016/j.mib.2010.05.012

Wang, D., Fang, L., Li, P., Sun, L., Fan, J., Zhang, Q., … Xiao, S. (2011). The leader proteinase of foot-and-mouth disease virus negatively regulates the type I interferon pathway by acting as a viral deubiquitinase. *Journal of Virology*, *85*(8), 3758–3766. doi:10.1128/JVI.02589-10

Wang, G., Chen, G., Zheng, D., Cheng, G., & Tang, H. (2011). PLP2 of mouse hepatitis virus A59 (MHV-A59) targets TBK1 to negatively regulate cellular type I interferon signaling pathway. *PloS One*, *6*(2), e17192. doi:10.1371/journal.pone.0017192

Wang, N., Shi, X., Jiang, L., Zhang, S., Wang, D., Tong, P., … Wang, X. (2013). Structure of MERS-CoV spike receptor-binding domain complexed with human receptor DPP4. *Cell Research*, *23*(8), 986–993. doi:10.1038/cr.2013.92; 10.1038/cr.2013.92

Warming, S., Costantino, N., Court, D. L., Jenkins, N. A., & Copeland, N. G. (2005). Simple and highly efficient BAC recombineering using galK selection. *Nucleic Acids Research*, *33*(4), e36. doi:10.1093/nar/gni035

Whitehurst, C. B., Ning, S., Bentz, G. L., Dufour, F., Gershburg, E., Shackelford, J., … Pagano, J. S. (2009). The Epstein-Barr virus (EBV) deubiquitinating enzyme BPLF1 reduces EBV ribonucleotide reductase activity. *Journal of Virology*, *83*(9), 4345–4353. doi:10.1128/JVI.02195-08

Wilkins, C., & Gale Jr, M. (2010). Recognition of viruses by cytoplasmic sensors. *Current Opinion in Immunology*, *22*(1), 41–47. doi:10.1016/j.coi.2009.12.003

Wojdyla, J. A., Manolaridis, I., van Kasteren, P. B., Kikkert, M., Snijder, E. J., Gorbalenya, A. E., & Tucker, P. A. (2010). Papain-like protease 1 from transmissible gastroenteritis virus: crystal structure and enzymatic activity toward viral and cellular substrates. *Journal of Virology*, *84*(19), 10063–10073. doi:10.1128/JVI.00898-10

Woo, P. C., Lau, S. K., Huang, Y., & Yuen, K. Y. (2009). Coronavirus diversity, phylogeny and interspecies jumping. *Experimental Biology and Medicine (Maywood, N.J.)*, *234*(10), 1117–1127. doi:10.3181/0903-MR-94

Wu, C. Y., Jan, J. T., Ma, S. H., Kuo, C. J., Juan, H. F., Cheng, Y. S., … Wong, C. H. (2004). Small molecules targeting severe acute respiratory syndrome human coronavirus. *Proceedings of the National Academy of Sciences of the United States of America*, *101*(27), 10012–10017. doi:10.1073/pnas.0403596101

Xing, Y., Chen, J., Tu, J., Zhang, B., Chen, X., Shi, H., … Chen, Z. (2013). The papain-like protease of porcine epidemic diarrhea virus negatively regulates type I interferon pathway by acting as a viral deubiquitinase. *The Journal of General Virology*, *94*(Pt 7), 1554–67. doi:10.1099/vir.0.051169-0

Yang, H., Yang, M., Ding, Y., Liu, Y., Lou, Z., Zhou, Z., … Rao, Z. (2003). The crystal structures of severe acute respiratory syndrome virus main protease and its complex with an inhibitor. *Proceedings of the National Academy of Sciences of the United States of America*, *100*(23), 13190–13195. doi:10.1073/pnas.1835675100

Yang, X., Chen, X., Bian, G., Tu, J., Xing, Y., Wang, Y., & Chen, Z. (2013). Proteolytic processing, deubiquitinase and interferon antagonist activities of Middle East respiratory syndrome coronavirus papain-like protease. *The Journal of General Virology*, *95*(Pt 3), 614–26. doi:10.1099/vir.0.059014-0

Ye, Y., Akutsu, M., Reyes-Turcu, F., Enchev, R. I., Wilkinson, K. D., & Komander, D. (2011). Polyubiquitin binding and cross-reactivity in the USP domain deubiquitinase USP21. *EMBO Reports*, *12*(4), 350–357. doi:10.1038/embor.2011.17

Ye, Y., Hauns, K., Langland, J. O., Jacobs, B. L., & Hogue, B. G. (2007). Mouse hepatitis coronavirus A59 nucleocapsid protein is a type I interferon antagonist. *Journal of Virology*, *81*(6), 2554–63. doi:10.1128/JVI.01634-06

Yi, L., Li, Z., Yuan, K., Qu, X., Chen, J., Wang, G., … Xu, X. (2004). Small molecules blocking the entry of severe acute respiratory syndrome coronavirus into host cells. *Journal of Virology*, *78*(20), 11334–11339. doi:10.1128/JVI.78.20.11334-11339.2004

Yu, M. S., Lee, J., Lee, J. M., Kim, Y., Chin, Y. W., Jee, J. G., … Jeong, Y. J. (2012). Identification of myricetin and scutellarein as novel chemical inhibitors of the SARS coronavirus helicase, nsP13. *Bioorganic & Medicinal Chemistry Letters*, *22*(12), 4049–4054. doi:10.1016/j.bmcl.2012.04.081; 10.1016/j.bmcl.2012.04.081

Yuan, K., Yi, L., Chen, J., Qu, X., Qing, T., Rao, X., … Deng, H. (2004). Suppression of SARS-CoV entry by peptides corresponding to heptad regions on spike glycoprotein. *Biochemical and Biophysical Research Communications*, *319*(3), 746–752. doi:10.1016/j.bbrc.2004.05.046

Zaki, A. M., van Boheemen, S., Bestebroer, T. M., Osterhaus, A. D., & Fouchier, R. A. (2012). Isolation of a novel coronavirus from a man with pneumonia in Saudi Arabia. *The New England Journal of Medicine*, *367*(19), 1814–1820. doi:10.1056/NEJMoa1211721; 10.1056/NEJMoa1211721

Zeng, W., Sun, L., Jiang, X., Chen, X., Hou, F., Adhikari, A., … Chen, Z. J. (2010). Reconstitution of the RIG-I pathway reveals a signaling role of unanchored polyubiquitin chains in innate immunity. *Cell*, *141*(2), 315–330. doi:10.1016/j.cell.2010.03.029

Zhao, G., Du, L., Ma, C., Li, Y., Li, L., Poon, V., … Zhou, Y. (2013). A safe and convenient pseudovirus-based inhibition assay to detect neutralizing antibodies and screen for viral entry inhibitors against the novel human coronavirus MERS-CoV. *Virology Journal*, *10*(1), 266. Retrieved from http://www.virologyj.com/content/10/1/266

Zhao, J., Li, K., Wohlford-Lenane, C., Agnihothram, S. S., Fett, C., Zhao, J., … Perlman, S. (2014). Rapid generation of a mouse model for Middle East respiratory syndrome. *Proceedings of the National Academy of Sciences of the United States of America*. doi:10.1073/pnas.1323279111

Zhao, L., Jha, B. K., Wu, A., Elliott, R., Ziebuhr, J., Gorbalenya, A. E., … Weiss, S. R. (2012). Antagonism of the interferon-induced OAS-RNase L pathway by murine coronavirus ns2 protein is required for virus replication and liver pathology. *Cell Host & Microbe*, *11*(6), 607–16. doi:10.1016/j.chom.2012.04.011

Zheng, B. J., Guan, Y., Hez, M. L., Sun, H., Du, L., Zheng, Y., … Huang, J. D. (2005). Synthetic peptides outside the spike protein heptad repeat regions as potent inhibitors of SARS-associated coronavirus. *Antiviral Therapy*, *10*(3), 393–403.

Zhu, J., Xiao, G., Xu, Y., Yuan, F., Zheng, C., Liu, Y., … Gao, G. F. (2004). Following the rule: formation of the 6-helix bundle of the fusion core from severe acute respiratory syndrome coronavirus spike protein and identification of potent peptide inhibitors. *Biochemical and Biophysical Research Communications*, *319*(1), 283–288. doi:10.1016/j.bbrc.2004.04.141

Zust, R., Cervantes-Barragan, L., Habjan, M., Maier, R., Neuman, B. W., Ziebuhr, J., … Thiel, V. (2011). Ribose 2'-O-methylation provides a molecular signature for the distinction of self and non-self mRNA dependent on the RNA sensor Mda5. *Nature Immunology*, *12*(2), 137–143. doi:10.1038/ni.1979

VITA

The author, Andy Kilianski, was born on July 30, 1987 in Westwood, NJ to Thomas and Carol Kilianski. He graduated from Centerville High School (Centerville, OH) in 2005 and received a Bachelor of Arts degree in Microbiology in 2009 from Miami University (Oxford, OH). While at Miami, Andy received two intramural research grants to work on highly variable regions within ascovirus genomes in the laboratory of Dr. Xiao-Wen Cheng. He graduated in 2009 and joined the Department of Microbiology and Immunology at Loyola University Chicago in July of 2009.

Andy joined the laboratory of Dr. Susan C. Baker in 2010 where he developed biosensor assays for the evaluation of antiviral compounds against coronavirus proteases while also dissecting the multifunctionality of the papain-like protease of SARS-CoV. Andy received multiple travel awards and received the Research Mentoring Program award for mentoring undergraduate summer students. He has also been active in the public health field, working closely with the Cook County Department of Public Health to evaluate their response to infectious disease emergencies, and will be graduating with honors in Science Leadership for this work. Andy will be joining the BioSciences division at Edgewood Chemical and Biological Center in Edgewood, MD as a National Research Council postdoctoral fellow in June.